

UNIVERSITY OF CALGARY

Spatial Synchrony of Predator-Prey Dynamics in Response to Cyclic Temperature Fluctuations

By

Kaitlin B. Osterlund

A THESIS

SUBMITTED TO THE FACULTY OF GRADUATE STUDIES
IN PARTIAL FULFILMENT OF THE REQUIREMENTS FOR THE
DEGREE OF MASTER OF SCIENCE

BIOLOGICAL SCIENCES

CALGARY, ALBERTA

JULY, 2021

© Kaitlin B. Osterlund 2021

ABSTRACT

Spatial synchrony occurs for many species, but is most apparent for species with populations that experience cyclic fluctuations. Population cycles can enhance the strength of synchrony-producing mechanisms by phase-locking cycles through dispersal events, or by entraining cycles to local cyclic environmental perturbations. Comparative evidence shows that density-dependent population regulation can differ spatially based on local environmental fluctuations that drive synchrony, but there is a lack of empirical evidence to further support this mechanism. This study looked to determine whether population cycles and cyclic environmental fluctuations impact the occurrence and persistence of spatial synchrony. A literature review was conducted to support the relation between spatial synchrony and population cycles. A Rosenzweig-MacArthur model with oscillating density dependence was produced to establish expected results for empirical tests. Patches of microcosm jars were then cycled between different temperatures to create environmental perturbations on model protist species *Tetrahymena pyriformis* and *Euplotes patella* which generate predator-prey cycles. The population cycles were manipulated by varying media enrichment and temperature cycle period length to establish a threshold synchrony range. Model results show that spatial synchrony occurs at high amplitude cyclic environmental fluctuations with cycle periods that closely match to the cycle period of the populations that are being synchronized. Due to COVID-19 restrictions, the experiment could not be carried out as initially intended, and results reflect the limitations imposed. Results suggested by the model could not be replicated experimentally. Future directions are suggested for studies with no pandemic-related restrictions.

PREFACE

This thesis is the original, unpublished, independent work by the author, Kaitlin Osterlund.

ACKNOWLEDGEMENTS

I would like to thank my supervisor Dr. Jeremy Fox for all his guidance and support amidst the struggles we all faced in the rise of the COVID-19 pandemic. I would like to thank Dr. Mary Reid and Dr. Paul Galpern for their feedback and support as trusted members of my committee. I would also like to thank Ross Conner and Laura Costello, for their encouragement and support in the lab. Finally, while slightly unconventional, I would like to thank close members of my family for their tireless support as I built my DIY home lab during the pandemic. I want to specifically thank my mother, Brenda Osterlund, for all her help with putting together my laboratory setup and lending me part of her house for the four months that I conducted my experiment. I also want to specifically thank my brother Colton Osterlund, and my partner Matthew Bell, for their inspirational ideas and technical support in building and running the incubators necessary for my experiment. Funding for this project was provided by the NSERC Discovery Grant and personal support came from the University of Calgary Department of Biological Sciences.

TABLE OF CONTENTS

PREFACE	i
ACKNOWLEDGEMENTS	ii
TABLE OF CONTENTS	iii
LIST OF TABLES	v
LIST OF FIGURES	vi
CHAPTER 1: Spatial Synchrony and Predator-Prey Population Cycles	1
1.1 Defining Spatial Synchrony	1
1.2 Spatial Synchrony and Population Cycles	4
1.3 Literature Review of Cycles and Synchrony	6
1.4 Investigating Spatial Synchrony and Cyclic Environmental Fluctuations	9
CHAPTER 2: Spatial Synchrony and Predator-Prey Population Cycles	12
2.1 Building a Synchronous Model with Simulated External Cycle Perturbations	12
Phase locking cycles into synchrony through cyclic entrainment	12
Rosenzweig-MacArthur predator-prey model with cyclic parameter for simulated entrainment	15
2.2 Establishing Model Parameters	16
2.3 Simulation Results	21
2.4 Discussion	28
CHAPTER 3: Empirically Testing Spatial Synchrony and Population Cycles Under Cyclic Temperature Fluctuations	31
3.1 Introduction to Microcosm Experiment	31

3.2 Experimental Methods	32
COVID-19 and the Home Laboratory	32
Study Species	34
Experimental Design	35
Data Processing and Statistical Analysis	40
3.3 Experiment Results	50
Time Series Visualization	50
Wavelet Analysis	57
Time Series Cross Correlation and Permutation	77
Clustering Analysis	88
PERMANOVA	90
3.4 Discussion	99
CHAPTER 4: Conclusions and Future Directions	102
4.1 Can cyclic environmental fluctuations synchronize population cycles?	102
4.2 Future Directions	103
REFERENCES	105
APPENDIX A: Spatial Synchrony and Population Cycles Literature Review	112
APPENDIX B: Homemade Incubator Building Setup and Software	126
APPENDIX C: Microcosm Heat Tolerance Pilot Experiment	128

LIST OF TABLES

Table 1.1: Spatial synchrony and population cycles literature review summary	8
Table 2.1: Rosenzweig-MacArthur model parameters	20
Table 2.2: Model simulation starting abundances	20
Table 3.1: Experiment study design	47
Table 3.2: Experiment microcosm jar setup	48
Table 3.3: Experiment temperature cycle schedule	49
Table 3.4: Approximative K-sample Fisher-Pitman permutation tests	85
Table 3.5: PERMANOVA results for <i>T. pyriformis</i> without predation	93
Table 3.6: Post-hoc pairwise comparisons by temperature cycle for <i>T. pyriformis</i> without predation	93
Table 3.7: Post-hoc pairwise comparisons by temperature cycle and enrichment level for <i>T. pyriformis</i> without predation	94
Table 3.8: PERMANOVA results for <i>T. pyriformis</i>	96
Table 3.9: PERMANOVA results for <i>E. patella</i>	97
Table 3.10: Post-hoc pairwise comparisons by temperature cycle and enrichment level for <i>E. patella</i>	98
Table A: Spatial synchrony and population cycles literature review	112
Table B: Pilot experiment design	129

LIST OF FIGURES

Figure 2.1: Model control plots	24
Figure 2.2: Model simulations for asynchronously mismatched starting densities	25
Figure 2.3: Model simulations for large mismatched starting densities	26
Figure 2.4: Model simulations for small mismatched starting densities	27
Figure 3.1: COVID-19 laboratory setup	45
Figure 3.2: COVID-19 incubator setup	46
Figure 3.3: <i>T. pyriformis</i> without predation time series	53
Figure 3.4: Low enrichment time series by temperature cycle	54
Figure 3.5: High enrichment time series by temperature cycle	55
Figure 3.6: Temperature cycle time series by enrichment level and patch number	56
Figure 3.7: Low enrichment 16-day temperature cycle wavelet power spectra	65
Figure 3.8: High enrichment 16-day temperature cycle wavelet power spectra	66
Figure 3.9: Low enrichment 20-day temperature cycle wavelet power spectra	67
Figure 3.10: High enrichment 20-day temperature cycle wavelet power spectra	68
Figure 3.11: Low enrichment 24-day temperature cycle wavelet power spectra	69
Figure 3.12: High enrichment 24-day temperature cycle wavelet power spectra	70
Figure 3.13: Low enrichment 28-day temperature cycle wavelet power spectra	71
Figure 3.14: High enrichment 28-day temperature cycle wavelet power spectra	72
Figure 3.15: Low enrichment 32-day temperature cycle wavelet power spectra	73
Figure 3.16: High enrichment 32-day temperature cycle wavelet power spectra	74
Figure 3.17: Low enrichment 36-day temperature cycle wavelet power spectra	75

Figure 3.18: High enrichment 36-day temperature cycle wavelet power spectra	76
Figure 3.19: Correlogram for <i>T. pyriformis</i>	83
Figure 3.20: Correlogram for <i>E. patella</i>	84
Figure 3.21: Boxplots of cross correlation values for <i>T. pyriformis</i> density time series	86
Figure 3.22: Boxplots of cross correlation values for <i>E. patella</i> density time series	87
Figure 3.23: Clustering NMDS by temperature cycles and enrichment levels	89
Figure B.1: Pilot experiment results under no predation	130
Figure B.2: Pilot experiment results under predation	131

CHAPTER 1: Spatial Synchrony and Predator-Prey Population Cycles

Life is full of patterns, and as scientists, we strive to understand patterns that describe the natural world around us. Whether it is patterns in behaviour, visible regularities of form and function, or some other natural phenomenon thereof, there is an inherent beauty in the way nature conducts itself. Understanding these patterns can lead to a better understanding of nature as a whole and allow us to make better-informed decisions on the preservation of Earth's ecology. One such natural pattern worth exploring is spatial synchrony.

1.1 Defining Spatial Synchrony

The term "synchrony" is derived from the Greek words "syn" meaning same and "chronos" meaning time, and "synchronization" is an adjustment of rhythms of oscillating objects due to their weak interaction (Pikovsky et al. 2001). The term "spatial synchrony" is defined as an ecological phenomenon where changes in population abundance occur synchronously over time across multiple populations that are geographically disjunct from one another (Liebhold et al. 2004a). When the abundance of one population rises or falls, synchronous populations will rise and fall in abundance to the same degree. An example of spatial synchrony can be seen in outbreaks of spruce budworm, *Choristoneura fumiferana*, that experience synchronized outbreaks between multiple patches within large regions of Eastern North America (Williams & Liebhold 2000). Another example of spatial synchrony can be found in synchronized population cycles of greater sage-grouse, *Centrocercus urophasianus*, spread across the Great Basin and Wyoming Basin in North America (Row & Fedy 2017). There are three currently known primary mechanisms that drive spatial synchrony which includes;

dispersal among populations, synchronous stochastic environmental effects (known as the Moran effect), and trophic interactions among populations of species that are mobile or are also spatially synchronous (Liebhold et al. 2004a, Korpimaki et al. 2004).

Dispersal produces synchrony when individuals disperse between populations that are governed by the same density-dependent processes that produce population fluctuations (Liebhold et al. 2004a). Dispersal will reduce the difference in the abundances between the populations since individuals from larger populations often disperse to smaller populations (Liebhold et al. 2004a). However, constraints exist on dispersal rates through predators capable of causing local prey extinctions, which ensures the persistence of region-wide abundance fluctuations (Liebhold et al. 2004b). This dispersal may synchronize populations that only differ slightly in their driving processes of fluctuation in abundance (Liebhold et al. 2004a), making it a significant contributing factor to synchronizing effects on populations. It is possible that local dispersal alone can induce region-wide synchrony (Bjornstad 2001) where populations become more similar in abundance to one another as dispersal events occur over time and balance the number of individuals across populations.

The second primary mechanism, synchronous stochastic environmental effects, is commonly known as the Moran effect which is attributed to the work of Australian statistician Patrick Moran (Moran 1953). Moran demonstrated that populations governed by linear dynamics can correlate with synchronous stochasticity in the environment (Moran 1953, Bjornstad 2001, Liebhold et al. 2004a). A widely used example of a Moran effect on a natural population is synchronous weather fluctuations (i.e. seasonal temperature and precipitation) (Bjornstad 2001, Liebhold et al. 2004a). For instance, imagine a region-wide drought that causes widespread mortality of many plants, generating a synchronous decline in all local herbivore

populations in the region. The Moran effect can influence population growth dynamics across a wide geographic range by driving synchrony across all populations experiencing the same stochastic environmental fluctuations (Bjornstad 2001, Liebhold et al. 2004a). Regardless of whether or not the populations fluctuate in abundance in a constant environment, the Moran effect may still precipitate spatial synchrony of population fluctuations (Liebhold et al. 2004a). The distance range of synchronized populations can vary to a wide degree across their geography, as long as the synchronized populations experience the same synchronous environmental stochasticity in order for the Moran effect to function (Bjornstad 2001, Liebhold et al. 2004a).

The third mechanism is trophic interactions between populations of species that are spatially synchronous or mobile (Liebhold et al. 2004a). In some systems, synchrony can occur between prey populations due to synchronizing effects from a shared predator population due to time-lagged trophic interactions (Koenig 2001, Liebhold et al. 2004a, Jones et al. 2003). Often referred to as “apparent competition”, predator functional responses force oscillations in prey population abundance to synchronize (Liebhold et al. 2004a). This occurs because of highly mobile predators rapidly moving from areas of low prey abundance to areas of high prey abundance, and rapidly depleting these areas of prey to the same extent which brings the prey populations into synchrony (Liebhold et al. 2004a). Similar synchronizing effects can take place among predators that share a fluctuating prey, where numerical tracking of the prey by predator populations can lead to synchrony (Curran and Webb 2000, Schauber et al. 2002, Satake et al. 2004).

While these mechanisms describe generally how synchrony arises, there are still areas of investigation within these mechanisms that need to be explored to paint a full picture of how and

why we see spatial synchrony occurring in natural populations. It is important to determine how all the mechanistic puzzle pieces work individually so that we can better understand how they might all fit together. Gathering a deeper understanding of spatial synchrony is important since synchronous metapopulations are subject to higher risks of global extinction (Liebhold et al. 2004a). The expected persistence of a metapopulation becomes drastically reduced with respect to its degree of spatial synchrony since strong synchronous fluctuations in abundance can easily lead to synchronous population collapse (Liebhold et al. 2004a). Conversely, large-scale outbreaks of dangerous diseases and pests can persist when populations undergo synchronous surges in abundance (Bjornstad 2001, Liebhold et al. 2004a). A heightened understanding of the mechanisms that drive spatial synchrony can lead to improved strategies for conservation and for management of disease and pest outbreaks (Liebhold et al. 2004a, Earn et al. 2000).

1.2 Spatial Synchrony and Population Cycles

Spatial synchrony has been observed across a wide range of taxa over varying spatial and temporal scales, spanning multiple decades and across ranges of hundreds of kilometres in some cases. There are many small mammals that are known to experience spatial synchrony, including a wide range of voles, lemmings, hares, and other rodents (Bjornstad 2001, Korpimaki et al. 2004, Ims et al. 2008, Brommer et al. 2010). Similarly, spatial synchrony has been observed across a wide range of bird species, including guillemots and many species of grouse (Fedy & Doherty 2011, Kvasnes et al. 2014, Pomara & Zuckerberg 2017, Row & Fedy 2017). Another very common study system for spatial synchrony includes insect outbreaks, notably in outbreaks of spruce budworm, spruce and mountain pine beetles, gypsy moth, and larch budmoth (Williams & Liebhold 2000, Ims et al. 2004, Koenig & Liebhold 2005, Buntgen et al. 2009,

Haynes et al. 2009 & 2017, DeRose & Long 2012, Allstadt et al. 2015, Kahilainen et al. 2018).

A comparable study system to insect outbreaks includes spatially synchronous disease outbreaks of measles, whooping cough, and dengue (Bjornstad 2001, Van Panhuis et al. 2015).

Interestingly, there are many shared commonalities between all these study systems. All of these systems experience cyclic population dynamics or are located in environments with strong seasonal or between-year variation (Bjornstad 2001, Korpimaki et al. 2004). This lends credence to the idea that spatial synchrony among populations is not due to the species-specific biology of any particular system, but rather is due to some common principle involving cyclic population dynamics.

Spatial synchrony is common, but not universal. There are populations of many species that are not spatially synchronized, so what explains variation in the occurrence of spatial synchrony? It may be variation in the occurrence or strength of the mechanisms producing synchrony, or it could also be variation in other factors that mediate the strength of synchrony-producing mechanisms. One factor in particular could be population cycles. There are two particular cases I will discuss where this link with population cycles is more apparent. First, Bjornstad (2001) reviewed the dynamics of measles and whooping cough measured over multiple decades for pre-and-post vaccination phases. During the pre-vaccination phase, multi-annual cycles were observed in measles population outbreaks while whooping cough displayed more erratic and non-cyclic population dynamics. Measles populations during this phase were spatially synchronous while whooping cough populations were not. In the post-vaccination phase, measles populations experienced a loss of cyclicity and, subsequently, a loss of spatial synchrony. On the other hand, post-vaccination whooping cough dynamics bifurcated into multi-annual cycles and populations also became spatially synchronized. A

second example involves vole population dynamics in similar studies performed at different times by Ims et al. (2008) and Brommer et al. (2010). Both studies observed cyclic dynamics and spatial synchrony in vole abundance over time, and also witnessed a temporary loss of cyclicity closely followed by an associated temporary loss of spatial synchrony. What all these cases highlight is an apparent link between spatial synchrony and cyclic population dynamics, where synchrony occurs when populations cycle, and vice versa. Next, I will review the lines of evidence suggesting that population cycles may promote spatial synchrony before I review hypotheses to explain this association between cycles and synchrony.

1.3 Literature Review of Cycles and Synchrony

While the cases previously mentioned provide some objective evidence supporting the association between cyclic population dynamics and the occurrence of spatial synchrony, there is limited evidence in other studies of a similar nature. It is unclear if the few well-known cases where synchrony is linked with cyclic dynamics are an exception to the rules. To attempt to determine if this is the case or not, I conducted a literature review of 140 journal articles to better understand the association between population cycles and synchrony. I specifically searched for empirical journal articles on synchrony and cyclic population dynamics within the last 20 years (from the years 2000 to 2020) using “spatial synchrony”, “cycle”, “oscillation” and “fluctuation” search terms. I discovered that the majority of studies involving spatially synchronous populations also display cyclical population dynamics (Table 1). In approximately 16% of the articles that observe both cycles and synchrony, variation over space and time in synchrony and variation in cycles are explicitly linked wherein the article examines spatial synchrony in conjunction with population cycles and noticing that one may not persist without the other, and

when cycling is lost, synchrony is also lost. While not all the articles I reviewed directly linked cycles and synchrony, there is some mention of the occurrence of fluctuations in population abundances over time. I noticed that many of these articles displayed more limited efforts in measuring population dynamics over time, or the studies did not span an adequate length of time to produce a time series that could deduce the presence or absence of population cycles. Therefore, if there were more data provided, it is possible that more studies would provide support for an association between population cycles and spatial synchrony.

Of all the articles I reviewed, there were only two that disputed the association between cyclic population dynamics and the occurrence of spatial synchrony (Table 1). The first article was written by Duncan et al. (2015) and illustrates how parasites can generate dispersal-driven synchrony in noncyclic declining populations. The second article was written by Paradis et al. (2000) and focuses on a large number of noncyclic British bird species. Paradis et al. (2000) mention that spatial synchrony can occur for all fluctuating populations and that population cycles are not necessary for synchrony to occur, but then later suggests that synchrony may be weaker when there is less cyclical in the population fluctuations. Duncan et al. (2015) supports this claim in stating that predator-prey systems often show cyclical population dynamics, which are more conducive to dispersal-induced synchrony. Interestingly, both articles agree that synchrony appears to be most intense during population decline, and since populations that cycle experience a higher frequency of declines over time, they would then experience higher synchrony (Paradis et al. 2000, Duncan et al. 2015). From my review of the literature, it becomes more clear that cyclic population dynamics have a vital role to play in the occurrence of spatial synchrony.

Table 1.1: Spatial synchrony and population cycles literature review summary

Article Parameter	Number of Articles	Summary of Study Systems
Cycles and synchrony are directly linked	22	Birds (British birds, ptarmigan, grouse) Disease outbreaks (measles, whooping cough) Insect outbreaks (larch budmoth, gypsy moth) Protist microcosms (<i>Tetrahymena pyriformis</i> and <i>Euplates patella</i>) Large mammals (Canadian lynx) Small mammals (rodents, muskrat, mink, voles, lemmings, snowshoe hares)
Cycles and synchrony present but not directly linked	68	Salmonids Marine phytoplankton Birds (grouse, wintering birds, ptarmigan, guillemot, raptors, cuckoos, woodpeckers, jays, grackles, cowbirds, titmice, thrashers, thrushes, mockingbirds, sparrows) Disease outbreaks (dengue, measles) Plants (green algae, oaks)
No cycles but a mention of population fluctuations with synchrony	34	Mussels Atlantic salmon Yellow perch Birds (seabirds, swifts, swallows) Harvest crops Insect outbreaks (mountain pine beetle, butterflies, soil mites) Microorganisms (phytoplankton, zooplankton)
Synchrony present but cycles not measured	14	Atlantic weakfish Mussels Amphipods Birds (guillemots, great tits and blue tits) Bacterioplankton Disease outbreaks (influenza) Insect outbreaks (ants, moths) Plants (oaks, algae, giant kelp, algae) Small mammals (voles)
Synchrony present without cycles	2	British birds Parasites

NOTE: Total of 140 articles reviewed. A full table of all articles reviewed is in Appendix A.

1.4 Investigating Spatial Synchrony and Cyclic Environmental Fluctuations

Previous research has proposed two ways in which cyclic population fluctuations can enhance the strength of a synchrony-producing mechanism. The first mechanism involves a single cyclic population that may have the ability to “phase-lock” other nearby cyclic populations (Liebhold et al. 2004a). The second mechanism involves two or more fluctuating populations which can become synchronized by an external source of some particular cyclic perturbation that can simultaneously “entrain” both populations to phase-lock with the perturbation cycles (Liebhold et al. 2004a).

The first proposed mechanism specifically involves short-distance dispersal which can synchronize close-range populations but cannot synchronize non-cyclic fluctuations (Bjornstad 2001, Vasseur & Fox 2009). Local populations can become near-perfectly synchronized when their cyclic dynamics become “phase-locked” (i.e. coupled, where there is no phase difference between two oscillators) (Bjornstad 2001, Liebhold et al. 2004a, Vasseur & Fox 2009). Dispersal acts to equalize populations, where individuals from larger populations tend to migrate to smaller populations (Vasseur & Fox 2009, Becks & Arndt 2013). This action of dispersal shifts the phases of the population cycles so that they become more closely coupled and eventually phase-lock and begin to produce synchronous population cycles (Vasseur & Fox 2009). Vasseur and Fox (2009) looked to see how dispersal influenced the occurrence of synchrony both in the presence and absence of cycles. They found that there was a large effect of dispersal on prey synchrony when population cycles were present, and there was no detectable effect when cycles were absent. Depending on the system, it may not take a large degree of dispersal both in terms of its relative strength and distance to produce synchrony, as long as the populations

experiencing dispersal are cycling with an adequate cycle amplitude and period to allow for the necessary phase-locking to occur (Fox et al. 2013, Hopson & Fox 2018).

The second mechanism specifically involves environmental fluctuations that drive spatio-temporal variation in population demographic rates that interferes with natural population cycles and has the ability to force population cycles into spatial synchrony (Ims et al. 2008, Brommer et al. 2010, Pomara & Zuckerberg 2017). The incidence of cycles can become reliant on density-dependent demographic rates in populations that have “entrained” (i.e. modified to a phase or a period) the periodicity of their cycles with periodic stochastic environmental fluctuations (e.g. seasonal temperatures and precipitation) (Bjornstad 2001, Haynes et al. 2017). Populations may become entrained to cyclic environmental fluctuations when those cycles have a similar period to the intrinsically-generated population cycles and shift the phases of the population cycles (Fedy & Doherty 2011, Allstadt et al. 2015, Kahilainen et al. 2018). The occurrence of spatial synchrony becomes limited when there are limited incidences of cycling unless populations are entrained by specific periodic environmental conditions (Bjornstad 2001). Comparative evidence suggests that density-dependent population regulation may differ across spatial locations based on how local environmental fluctuations drive synchrony dynamics (Walters et al. 2017). Variation in density dependence may result from heterogeneity in the environment, and synchrony is reduced between sites where density-dependent dynamics differ (Walters et al. 2017).

Despite the small extent of comparative evidence for this mechanism, there is a lack of empirical evidence. This thesis focused on empirically investigating the second mechanism discussed above to determine if periodic environmental fluctuations act as a driver for spatial synchrony. The central question being answered is; when can cyclic environmental fluctuations

synchronize population cycles? I hypothesize that spatial synchrony is driven by high amplitude cyclic environmental fluctuations that closely match the cycle period of the populations that are being synchronized. Synchrony should occur when population cycles become entrained to the cyclic environmental fluctuations in temperature, and will, in turn, become entrained to one another. I predict that synchrony will not occur when temperature fluctuations deviate from 28 days because the cycle period of the protist populations will be unable to match their cycles to the differing temperature periods and will not be able to adequately entrain their cycles. I predict that synchrony will not occur when low resource enrichment causes low-amplitude population cycles, even when the temperature period is at 28 days because the cycles will be too weak to entrain one another. I also predict that high amplitude temperature cycles with a period of 28 days will increase population cycling, even when resource enrichment is low, and therefore should produce a higher occurrence of spatial synchrony.

The goal of this thesis is to reveal whether population cycles and cyclic environmental fluctuations have a significant impact on the occurrence and persistence of spatial synchrony, and to establish if a threshold exists that determines what cyclic environmental parameters promote the occurrence of spatial synchrony. The above hypothesis will be explored over two chapters, a modelling chapter and an experiment chapter. In the modelling chapter, I will explore and discuss the results from model simulations conducted on cyclic predator-prey population dynamics subjected to extrinsic cycles. In the experiment chapter, the hypothesis will be explored using a microcosm experiment subjecting predator and prey protist populations to temperature cycles. In all, these chapters aim to provide more significant information that may aid in better understanding the occurrence and persistence of spatial synchrony in population dynamics under cyclic environmental fluctuations.

CHAPTER 2: Modelling Spatial Synchrony and Population Cycles

2.1 Building a Synchrony Model with Simulated External Cyclic Perturbations

While it would theoretically be possible to measure synchrony through entrainment by cyclic environmental perturbations with field studies, it is oftentimes a very difficult and laborious project to undertake due to the large spatial and temporal scale necessary for an effective study. An alternative approach to understand synchrony is the use of population model simulations that can provide insight into dynamics that might take decades to observe in the field. While model simulations are not a perfect reflection of systems behaving in natural settings, they do provide supplemental insight into patterns that can be drawn from these natural systems through time. I used model simulations in this study to establish expected dynamics from my study system of interest. Before I continue to discuss how the model was constructed for this study, I will first discuss the general theory of synchrony and cycle entrainment that the model is used to describe through its simulations.

Phase locking cycles into synchrony through cyclic entrainment

Pikovsky et al. (2001) used a great example of defining synchrony with a series of swinging pendulum clocks, and I will make use of this same example here. Imagine that there are two pendulum clocks sitting on a table, with the pendulums actively oscillating back and forth. The oscillatory movement of the clocks is generated through their own autonomous internal source of energy, defined by parameters of the clock's system, and maintains a constant rhythm through time. The rhythm of the oscillating clocks could take on any wave form or shape, but for our purposes, the pendulum swings follow a simple sine-wave form. The natural sine-wave

frequency of these pendulum oscillations remain autonomous for each clock, but the frequency can be changed through external action from interactions with the system of the clocks.

To simulate this, imagine the table that the clocks are sitting on is able to move. Maybe the table legs are on wheels, or the table is strung from the ceiling, and motion created by the pendulums can transfer motion into the table. Now suppose that the clocks are set to slightly different times, with the pendulums swinging in slightly different positions from one another. Since both clocks are sitting on the same free-moving table, it can be assumed that the clocks are not independent, and they interact weakly through the shared motion experienced on the table. Even if the table motion is small, it can still potentially alter the rhythms of pendulum swings of both clocks, and so the interaction through the table couples the oscillations of the pendulum swings. When coupled, the clocks with different pendulum oscillation periods will adjust and begin to oscillate with a common period, a phenomenon known as frequency entrainment that can lead to synchrony of the pendulum oscillations.

Pikovsky et al. (2001) describe two factors that determine whether synchrony will occur in the system described above. The first being “coupling strength”, and the second being “frequency detuning” or “mismatch”. The coupling strength of the system describes the strength of the interaction between the oscillators. In our example, if the table was set on wheels that experienced a lot of friction that restricted movement, less motion would be experienced by both clocks on the table and the clocks would then have a weaker coupling strength. The weaker the coupling strength, the less likely synchrony is to occur, and coupling strength becomes zero when there is no motion in the table and the clocks do not interact. Next, frequency detuning, also known as mismatch, describes how different the two oscillators are, or how far out of phase the oscillations are. When the mismatch between oscillations of clock pendulums is not very

large, it is easier for synchronization to take place since the phases between oscillations are not spaced too far apart for entrainment to couple them. These two factors described function dependently on one another, where the width of the region of synchronization between phases of the oscillators increases with increased coupling strength. Also, higher degrees of mismatch between oscillators require either higher coupling strength or greater external force to synchronize the pendulum swings.

For this study, we will be subjecting the oscillators in the system to varying degrees of mismatch and coupling strength through cyclic environmental perturbations. Continuing with our clock example, imagine that there is a person with a metronome standing next to the free-moving table, and this person is able to move the table by hand using their own external force. This person moves the table in side-to-side oscillations in perfect time with the metronome that is set to a specific frequency. It is predicted that the oscillating clocks should become entrained to the cyclic movement induced by the person moving the table, and the pendulums should phase lock and the clocks would synchronize with one another as they become entrained to these environmental cycles. Synchrony should only occur when the environmental cycles induced by moving the table are close to the natural oscillations of the pendulums (i.e., the metronome frequency the person follows to move the table is similar to the frequency of the pendulum oscillations of the clocks), where the amount of mismatch is reduced to be within the range of synchronization and allows for the entrainment of the clocks to the cycles in table motion. The person moving the table also has the ability to alter the coupling strength depending on how much movement they generate in swinging the table, where more force applied to the movement of the table alters the drive of the trajectory for the pendulum cycles. The more aggressively they swing the table side-to-side, the higher the amplitude of the environmental cycles, and the higher

the coupling strength. Even if the pendulums are swinging with a higher degree of mismatch, or if the person is swinging the table back and forth at a frequency that appears to be outside the range of synchronization for the clocks, high coupling strength will entrain the oscillating pendulums to the swinging table cycles, and the clocks will then become synchronized with one another.

Rosenzweig-MacArthur predator-prey model with cyclic parameter for simulated entrainment

This clock example of synchrony induced by cyclic environmental perturbations can also be applied to natural population dynamics. For this study, the clocks are the population patches, the swinging pendulums are the predator-prey population cycles, the table is the local environment that the patches occupy, and the person moving the table is cyclic environmental perturbation (e.g. cyclic temperatures or cyclic precipitation). The model built for this study examines the effects of these cyclic environmental perturbations on the occurrence of spatial synchrony in cyclic predator-prey population dynamics. This model will then be used to establish expected dynamics from a natural predator-prey system that will be experimentally subjected to varying cyclic environmental perturbations.

The particular model being used is based on the classic Rosenzweig-MacArthur model (Rosenzweig & MacArthur 1963) of density dependent predator-prey interactions. This model was chosen as it best fits the natural dynamics of the protist species of interest for this study, and the parameters were set to closely match these natural dynamics. To model the cyclic environmental perturbations, one of the model parameters was made to cycle as a sine wave oscillator. For this study, it is assumed that the environmental cyclic forcing can act on parameters of the model. The prey carrying capacity was chosen as the oscillating parameter, as

it has been mentioned in the literature that temperature has a significant effect on carrying capacity (Beveridge et al. 2010) and in the experiment discussed in the next chapter, we will be cycling temperature as the cyclic environmental perturbation on the system.

2.2 Establishing Model Parameters

The model was built in R Studio (Core R Team 2020) and was adapted from a simple Rosenzweig-MacArthur model R script provided by Dr. John Post from the Ecology of Populations course at the University of Calgary. The equations for the Rosenzweig-MacArthur model are described as;

Prey abundance at time t ;

$$\frac{dH}{dt} = bH\left(1 - H\left(\frac{1}{K}\right)\right) - \frac{wPH}{(D+H)}$$

And predator abundance at time t ;

$$\frac{dP}{dt} = \frac{ewPH}{(D+H)} - sP$$

Where H is the abundance of prey and P is the predator abundance for a single population patch. Both differential equations also make use of varying parameters including; the per capita birth rate of prey (b), the prey carrying capacity (K), the maximum capture rate of prey by predators or capture efficiency (w), the half saturation rate of prey density that gives rise to half the maximum capture rate (D), the per capita birth rate (e), and the per capita death rate of the predator (s). Table 2.1 displays the parameter values that were chosen to match as closely as possible to the natural predator-prey cycle of *Euplotes patella* and *Tetrahymena pyriformis* based on observed predator-prey dynamics from past experiments (Fox et al. 2011, Hopson & Fox 2018, Laan & Fox 2019). These protist species are the respective predator and prey chosen for the experiment described in the next chapter.

To model the cyclic environmental perturbations, a sine wave function was used to manipulate one of the parameters of the Rosenzweig-MacArthur model to replicate the interaction with the predator-prey cycles. For this model, I decided to use the sine wave function on the carrying capacity of the prey. I chose this density-dependent parameter because it is suggested in past literature that the carrying capacity is significantly influenced by temperature (Beveridge et al. 2010) which is the parameter that was cycled for the main experiment of this study that will be discussed in the next chapter. While Beveridge et al. (2010) also state that other parameters such as predator birth rates are significantly impacted by temperature, I decided to focus on cycling only one parameter with the first run of this model for the sake of simplicity when interpreting the simulation outputs, and to ensure that the cycling parameter yields the desired effect on predator and prey abundance. The general equation for a sine wave is;

$$y(t) = A \sin(2\pi f t + \phi)$$

Where A is the cycle amplitude, f is the frequency, and ϕ is the phase shift of the cycle. The first derivative of this equation was used to determine the carrying capacity (K) at time t to create a series of cyclic carrying capacity abundances that prey would follow through time, which has the following equation;

$$\frac{dK_c}{dt} = \cos(K_0 \cdot 2\pi \cdot f) \cdot A$$

K_c denotes the cycling carrying capacity while K_0 depicts the natural static carrying capacity of the prey. The phase shift (ϕ) was excluded from this first derivative equation as it was not necessary for the purposes of this model and the phase shift would remain equal to zero. This cyclic carrying capacity was then integrated into the Rosenzweig-MacArthur model, replacing the original static carrying capacity in the equation for prey abundance.

This Rosenzweig-MacArthur model was repeated twice to create a two-patch system, where patch population abundances could be compared to determine any instances of spatial synchrony between the two patches. Synchrony was denoted as any portion of time where the abundances between patches perfectly overlapped, indicating phase locking of predator-prey cycles into synchrony. The simulations that were run were selected based on different starting abundances between the two patches, as well as different cycle periods and cycle amplitudes of the cyclic perturbations on carrying capacity. All simulations were run for 600 time points, or “days”, to ensure there was enough time given for any late instances of synchrony in the time series. Three different starting abundances were chosen; in complete asynchronous mismatch, in a large amount of mismatch, and in a small amount of mismatch (Table 2.2). Larger mismatched cycles had cycle phases that were farther apart between patches than smaller mismatched cycles. Asynchronous mismatched cycles had patches with cycle phases that were shifted to where the cycle trough of one patch would be aligned with the cycle peak of the other patch. There were three cycle amplitudes chosen for the cyclic carrying capacity, with a low amplitude of 50 prey individuals, a medium amplitude of 150 prey individuals, and a high amplitude of 300 prey individuals. The amplitude here is a measure of how many prey individuals will oscillate above and below the starting carrying capacity of 4000 individuals. There were also six cycle periods chosen for the cyclic carrying capacity, with a 16-day cycle, a 20-day cycle, a 24-day cycle, a 28-day cycle, a 32-day cycle, and a 36-day cycle. These period lengths were chosen based on the natural predator-prey cycle of *T. pyriformis* and *E. patella* (Fox et al. 2011, Hopson & Fox 2018, Laan & Fox 2019), which was the central cycle period chosen. The longer and shorter cycle period lengths were chosen to explore whether synchrony would occur at periods that deviate above and below the 28-day cycle period. In the sine equation above, the period is the inverse

measure of frequency (f), therefore the inverse of each period was used to provide the frequency necessary for the sine equation. In all, 54 simulations were run to investigate the effects of cyclic environmental perturbations on predator-prey cycles, and whether any synchrony arises and persists as a result.

Table 2.1: Rosenzweig-MacArthur model parameters simulating natural predator-prey cycles of *T. pyriformis* and *E. patella*.

Parameter	Value
Per capita prey birth rate (b)	0.9
Per capita predator birth rate (e)	0.07
Per capita predator death rate (s)	0.2
Predator capture rate of prey (w)	6
Half saturation rate (D)	1200
Prey carrying capacity (K)	4000

Table 2.2: Starting abundances for spatial synchrony simulations.

Starting Point	Patch	Prey (H) Abundance	Predator (P) Abundance
Asynchronous Mismatch	Patch 1	4000	20
	Patch 2	4000	100
Large Mismatch	Patch 1	4000	50
	Patch 2	4000	100
Small Mismatch	Patch 1	4000	80
	Patch 2	4000	100

2.3 Simulation Results

Overall, the simulations run with the model created behaved as predicted, and set up a clear picture of how synchrony may occur through cycle entrainment via cyclic environmental perturbations. All simulations displayed unique predator-prey dynamics, and some instances of spatial synchrony between patches were observed. Before exploring the simulation outputs, I first ran some control simulations to ensure the model was producing the proper expected base outputs, which can be seen in Figure 2.1.

First, looking at simulations with asynchronous starting conditions between the two patches (Figure 2.2), a telling narrative was displayed. There were quite a few instances of spatial synchrony that appeared, and all instances of spatial synchrony appeared where it was expected. First, spatial synchrony occurred at the 28-day environmental cycle period for all environmental cycle amplitudes, and the occurrence of synchrony decayed as environmental cycle periods deviated above and below 28 days. As amplitude increased, there were more instances of synchrony across all environmental cycle periods and cycles would also phase lock earlier in the time series with increasing amplitude. Therefore, synchrony appeared more frequently with higher amplitude environmental cycles, and with environmental cycles with closely matched periods to the predator-prey cycles of the patches. This allowed for easier entrainment of predator-prey cycles to the environmental cycles, and in turn more synchrony between the patches.

There were also some other interesting patterns observed in the simulations from Figure 2.2. In some cases, it appeared that some patches were close to synchrony, but would have cycle phases that would drift close together and then drift further apart without ever perfectly phase locking. This pattern was most notable in the low amplitude and 32-day period simulation. The

dynamics in the medium amplitude and 36-day simulation are also unique in that the predator-prey cycles of both patches appear to be highly disrupted compared to all other simulations. There were other instances where it appeared that there were larger scale cycles integrated with the predator-prey cycles, most notably in the medium amplitude and 16-day period simulation. It appeared that the amplitude of the predator-prey cycles would cycle with respect to the cyclic carrying capacity, where amplitudes would be low when the carrying capacity was low, and vice versa. This observed pattern was considered to be a resonance effect (Pikovsky et al. 2001), which describes an external oscillatory pattern that is separate from any patterns of synchronization.

Next, looking at simulations with large mismatched starting conditions between the two patches (Figure 2.3), the overall patterns of synchrony were the same as what was observed in Figure 2.2, except that instances synchrony occurred sooner in time. Since there was a smaller mismatch between the patches, the environmental cycles didn't have as large of a distance between cycle phases to entrain, and so phase locking could occur sooner. The medium amplitude and 36-day period simulation had similarly unique dynamics as before, except in this case the phase between both patches was closer. Also, there were more instances of patches with cycle phases that would drift in and out without ever perfectly phase locking. There is also a strong case of a resonance effect (Pikovsky et al. 2001) in the high amplitude/16-day period simulation, as well as some resonance in the low amplitude/24-day period simulation and the low amplitude/32-day period simulation..

Finally, looking at simulations with small mismatched starting conditions between the two patches (Figure 2.4), the overall patterns of synchrony were the same as what was observed in Figures 2.2 and 2.3, except that instances of synchrony occurred at the earliest points in time

compared to all other simulations. Once again, this was due to a smaller amount mismatch between patches creating smaller distances between phases to be entrained into synchrony. Once again, the medium amplitude/36-day period simulation had similarly unique dynamics as before in Figures 2.2 and 2.3. However, there were fewer instances of patches with cycle phases that would drift in and out of phase, and instead there were many cycles that had phases that were very nearly overlapping, but never perfectly phase locked. There was also a higher amount of resonance (Pikovsky et al. 2004) amongst many simulations in Figure 2.4, most notably in the low amplitude/24-day period simulation and in the low amplitude/32-day simulation.

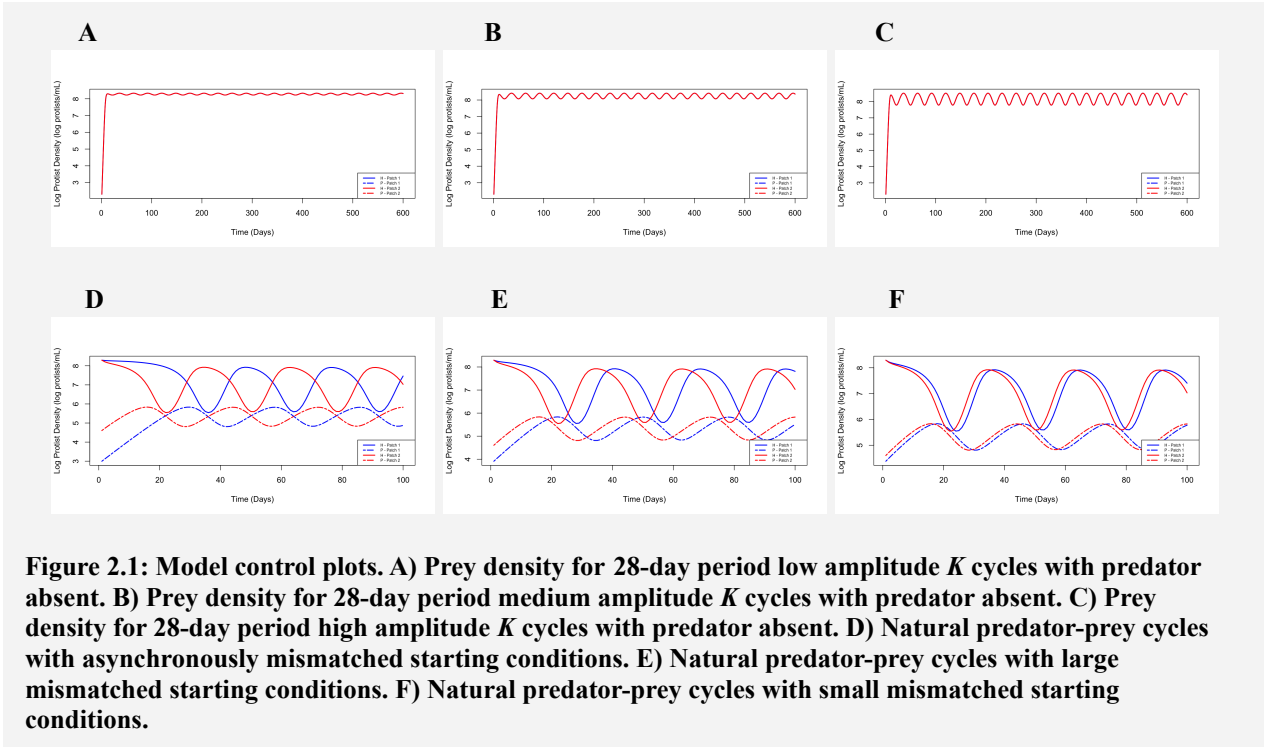


Figure 2.1: Model control plots. A) Prey density for 28-day period low amplitude K cycles with predator absent. B) Prey density for 28-day period medium amplitude K cycles with predator absent. C) Prey density for 28-day period high amplitude K cycles with predator absent. D) Natural predator-prey cycles with asynchronously mismatched starting conditions. E) Natural predator-prey cycles with large mismatched starting conditions. F) Natural predator-prey cycles with small mismatched starting conditions.

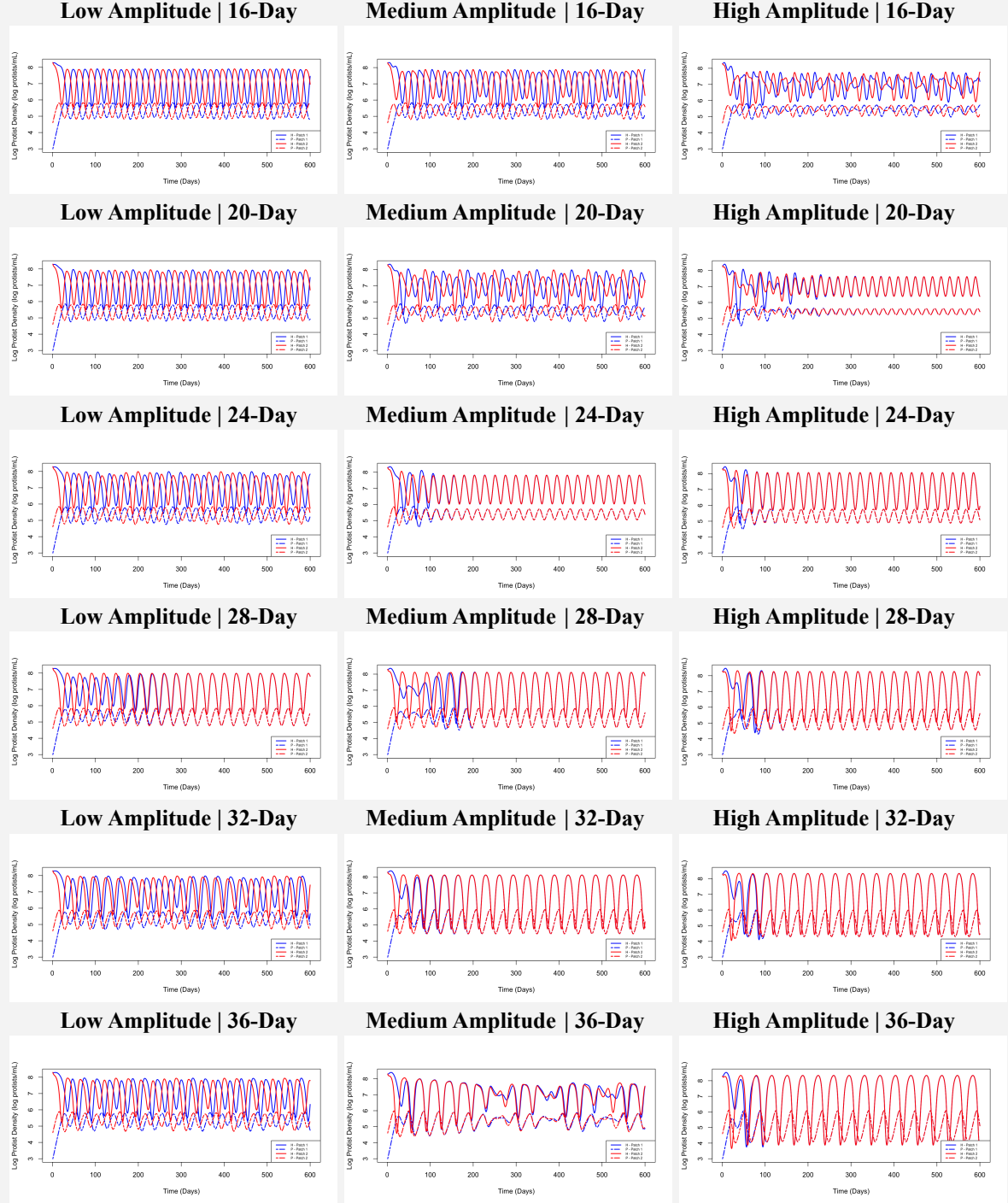


Figure 2.2: Model simulations for asynchronously mismatched starting densities.

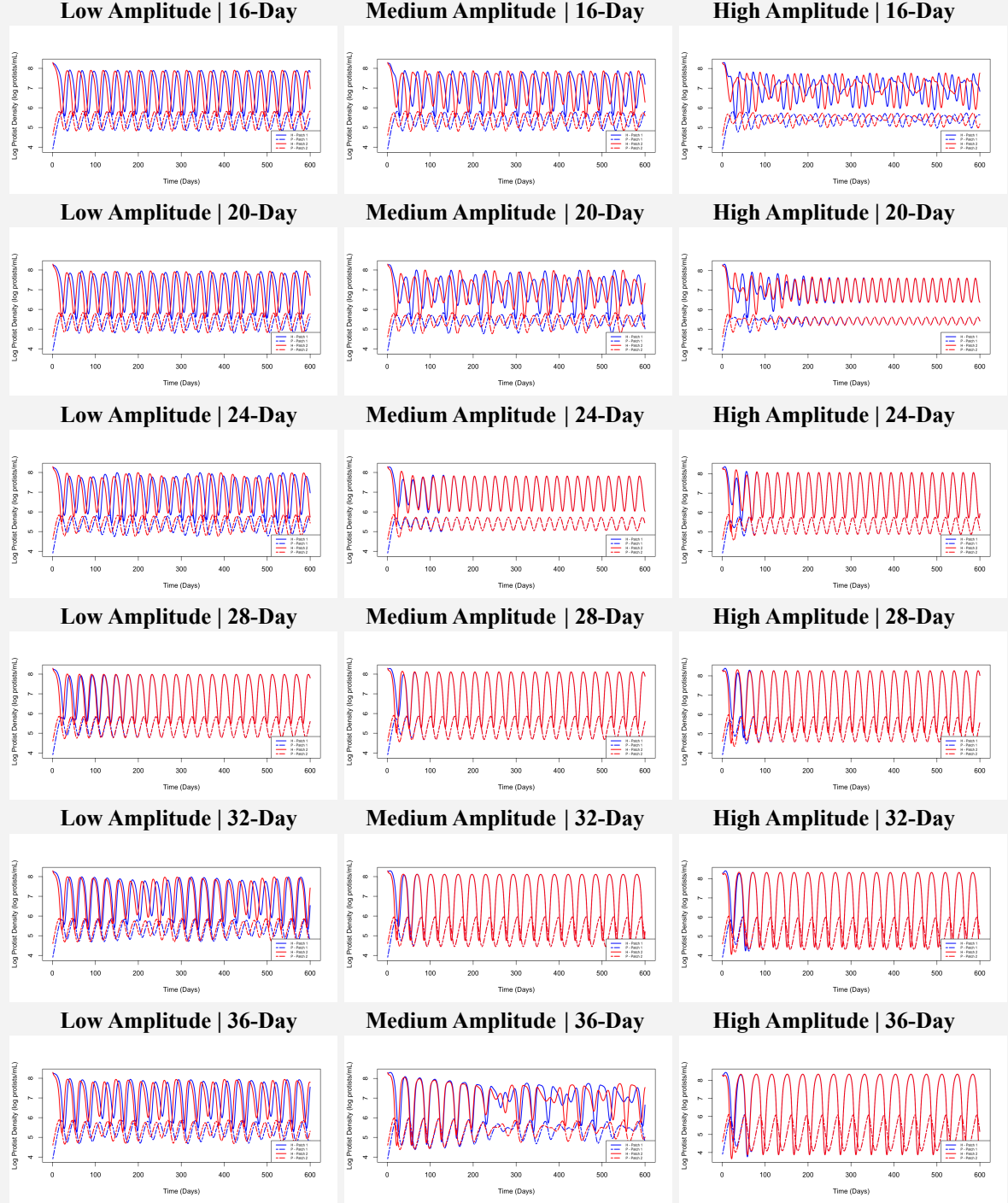


Figure 2.3: Model simulations for large mismatched starting densities.

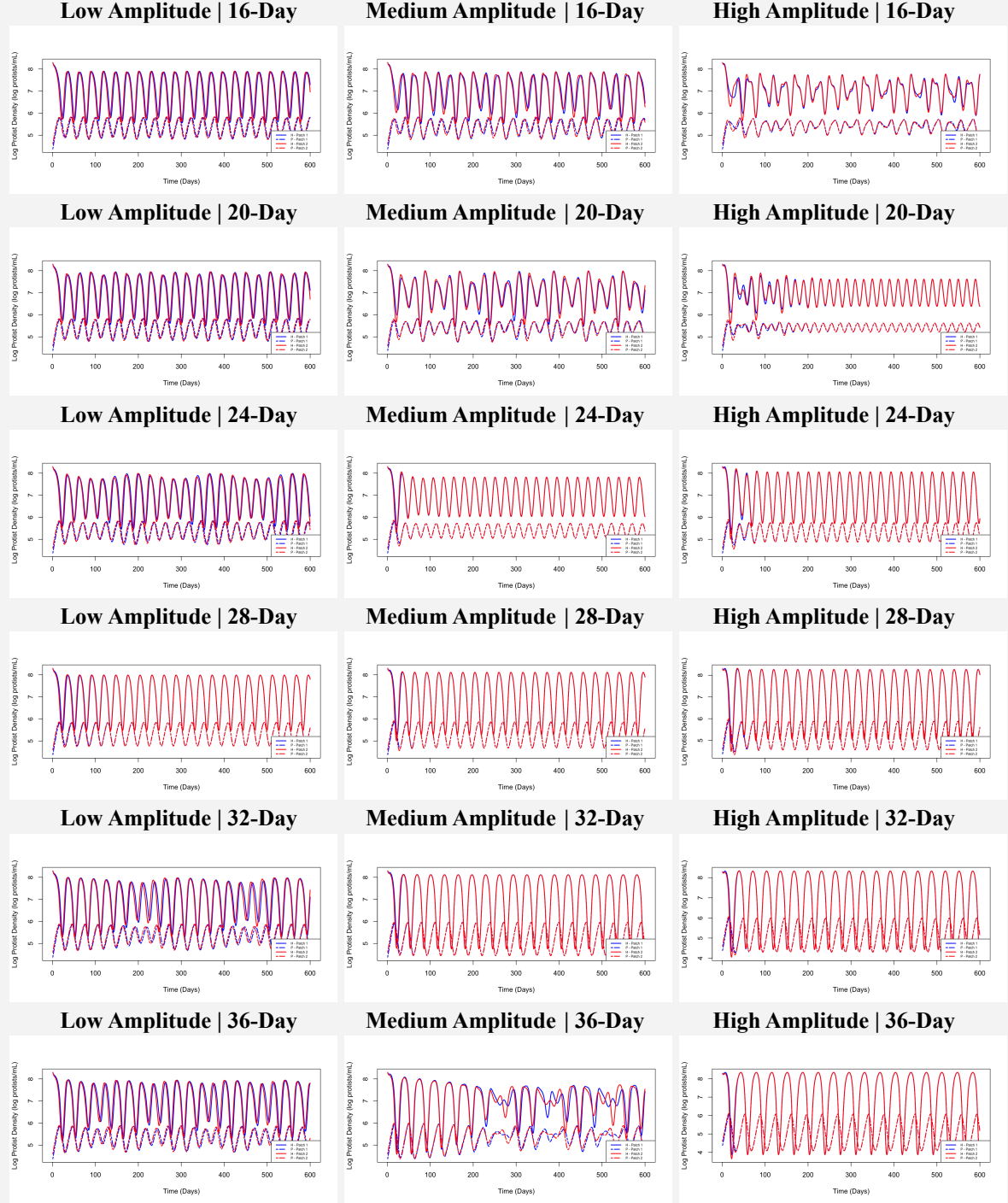


Figure 2.4: Model simulations for small mismatched starting densities.

2.4 Discussion

The results of this model provided a clear picture of what one might expect with regards to spatial synchrony of a two-patch predator-prey system experiencing varying cyclic environmental perturbations. Simulations showed that synchrony would occur when population cycles became entrained to the cyclic environmental perturbations, which then entrained the patches to one another through phase-locked cycles. Synchrony decayed when environmental cycles deviated from the natural 28-day predator-prey cycles of interest (Fox et al. 2011, Hopson & Fox 2018, Laan & Fox 2019). As the environmental cycle period deviated from 28-days, the cyclic predator-prey dynamics were unable to align with the period of the environmental cycles, and therefore could not be entrained. Synchrony also occurred more frequently with increasing environmental cycle amplitude, occurring even at most environmental cycle periods when the amplitude was at its highest.

Essentially, the environmental cycles are acting as an external force that drives the trajectory of the predator-prey cycles in the patches and can drive the phase of the cycle so it entrains to the environmental cycle (Pikovsky et al. 2001). This external force is only able to influence a given synchronization region around the patch cycles, where deviations outside of this region do not lead to synchrony through cycle entrainment (Pikovsky et al. 2001) as displayed through the decay in synchrony around the 28-day cycle period. Outside this synchronization region, the environmental cycles oscillate at a frequency that is generally quasiperiodic to the predator-prey cycles of the patches and is unable to exert enough force on the predator-prey cycles long enough for entrainment to occur (Pikovsky et al. 2001). Though as the environmental cycle amplitude increases, the external force becomes strong enough to where the large amount of coupling strength drives the entrainment of cycles regardless of cycle period

or phase alignment (Pikovsky et al. 2001). Pikovsky et al. (2001) also note that this external force significantly influences the phase of the predator-prey cycles, but only has a small effect on the amplitude of the cycles. This can be seen in all simulations of Figures 2.2, 2.3, and 2.4 where there are often major deviations in the cycle phase, but less substantial changes in amplitude between all the simulations.

In some simulations, there were interesting cases of a resonance effect that developed. The peak-to-peak height of the cycles varied with respect to the changing carrying capacity. When the carrying capacity was high, the cycle amplitudes for both predator and prey would increase as well. Similarly, when the carrying capacity was low, the cycle amplitudes of both predator and prey would decrease. While this resonance effect is an interesting dynamic to observe, it is important to note that there is a difference between resonance and synchrony and that this resonance effect is not a driver of synchrony between the two patches (Pikovsky et al. 2001).

While this model has created a general scaffold for what to expect in a two-patch predator-prey system experiencing varying cyclic environmental perturbations, there is much more that can be explored with it. With limited time, I was not able to expand on this model, and instead, I will suggest other areas of this model that should be explored in future work. It was assumed in this model that the carrying capacity alone for protist species would be impacted by environmental perturbations, but Bevelridge et al. (2010) also found that predator birth rates are also significantly affected by temperature. This model should be expanded upon to look at how a cyclic predator per capita birth rate (e) or a cyclic per capita death rate (s) would affect spatial synchrony between the patches. This could be done independently of cycling carrying capacity, or multiple parameters could be set to cycle with the environment. If cycling with multiple

parameters, I would suggest also varying the cycle periods, amplitude, and phases of the cycles between the parameters to see how it might impact synchrony. Also, investigating cycles of these birth and death rates without cycling carrying capacity would further be able to identify the effects of cycles in density-independent versus density-dependent parameters. I would also suggest testing wider ranges of environmental cycle periods and amplitudes to see if there is a distinct outline for a synchronization region for this two-patch system. Finally, I would also suggest changing the base Rosenzweig-MacArthur model parameters to produce intrinsically generated dampening predator-prey cycles, and then test the effects of cyclic environmental perturbations on this system. In natural populations, there is often some intrinsically-generated dampening of predator-prey cycle dynamics (Hastings 2019), and this could create simulation outcomes that are even more reflective of natural predator-prey systems.

CHAPTER 3: Empirically Testing Spatial Synchrony and Population Cycles Under Cyclic Temperature Fluctuations

3.1 Introduction to Microcosm Experiment

With the model simulation results establishing the predicted effects on synchrony, we will now explore and see if these results hold true in a model system. This chapter will explore the experimental methods and results of a microcosm experiment using a protist predator-prey system to determine if temperature cycles can synchronize population cycles.

Microcosms are very useful for empirically studying general theories in population dynamics. Microcosms might not precisely mimic any one particular natural system, but often that is not the goal of microcosm studies. Microcosms work well for testing general principles that many natural systems are thought to obey (Benton et al. 2007). In field studies on natural systems, results are often suggestive from observational data, and there is often a lack of empirical data from studies being limited to short time series and small geographic study ranges which can also give rise to ambiguity (Benton et al. 2007). Observational field data on spatial synchrony is ideally complemented with manipulative experiments where the known mechanisms of synchrony and of cycling can be manipulated, but this is a rare occurrence in current literature. The use of protist microcosms in this experiment should establish their efficacy as a complementary empirical tool to support field-based observational evidence of spatial synchrony.

Protist microcosm experiments are also an ideal means for reproducing modelled population simulations where specific parameters of the system can be manipulated and controlled, just as they are in a computed model simulation. Microcosms provide a real-world

system that can be studied and easily replicated. To experimentally test the model in the previous chapter, I will be making use of laboratory microcosms to replicate populations of cyclic predator-prey dynamics.

3.2 Experimental Methods

COVID-19 and the Home Laboratory

The microcosm experiment for this Masters thesis was scheduled to begin in May of 2020. However, these plans were changed when the global COVID-19 pandemic arrived in Canada two months earlier in March and brought about lots of uncertainty as the world shut down in quarantine. The initial plan to run an experiment in the Fox laboratory on the university campus was no longer feasible, and I could no longer work alongside my supervisor and colleagues unless it was in a virtual setting. After much discussion about the best course of action, it was decided that I would continue with my intended research, just in a slightly unconventional way. If I could not go to the lab to do my experiment, I would bring the lab to me.

Thanks to the nature of the protist microcosms I was working with, it made it safe and feasible to conduct the same research that I would have done in the laboratory in my family home. All the necessary equipment required for the experiment was packed up, and the laboratory was moved into my family's dining room (Figure 3.1). The dining room table was covered with a sheet of vinyl fabric to protect the wood table. The vinyl fabric also created a surface that could be properly sanitized to minimize the risk of contamination during the experiment. There are no doors to the dining room, so to maintain a steady room temperature, a shower curtain was installed in the doorway, and a thermometer was installed to monitor room

temperature. This shower curtain not only helped keep out any drafts that could shift the ambient room temperature, but it also limited any potential contaminants coming from other places in the house.

Moving the lab into my family home allowed me to run my planned experiment, however there were still a wide variety of hurdles to overcome to make it run as intended. I was initially going to work with a research assistant to complete the necessary daily sampling of the microcosms, but quarantine would not allow for that. Due to this, I was required to cut my sample size in half to accommodate for the lack of assistance in sampling effort. This inherently forced me to reconsider my study design to accommodate the limited number of jars I would be able to sample on my own. In addition to this, I would also be responsible for all laboratory equipment and media sterilization. Instead of using traditional autoclaves, I boiled all equipment on the stove for 20 minutes at a rolling boil and left glassware to dry face-down on a clean paper towel. To sterilize media, I used my knowledge of canning (learned from making jams and pickles) to boil and seal media in varying sizes of mason jars (Bernardin, subsidiary of Newell Brands Canada ULC). The rubber ring of the mason jar lids ensured an airtight seal, and media was used immediately once a mason jar was opened. Over the duration of the experiment, there were no visual signs of contamination in any mason jars, microcosm jars, or protist samples.

The most significant hurdle to overcome was determining how I would incorporate the temperature treatment into my experiment. The incubators I intended on using for my experiment could not be moved to my house since they were both the size of a refrigerator. Without the incubators, I would not be able to create the temperature cycles necessary for the central question of my thesis. I was not ready to abandon my study, and with no other available options, I began considering building my own small-scale incubators at home. I viewed a video on YouTube

where an incubator was built using a beer cooler and a reptile heating pad (The Thought Emporium 2018), and it inspired me to recreate a similar incubator design for my experiment. With the help of my brother, a software engineering undergraduate student at the University of Calgary, I was able to build the incubators I needed for only \$200. They were built with temperature sensors and a custom program to collect and print temperature readings every hour to ensure the incubators were working effectively. The incubators worked very effectively and were very reliable over the duration of the experiment, and they are currently still in use in the Fox Lab. For a full description of how the incubators were designed and built, see Appendix B.

Study Species

The microcosms used in this experiment were host to ciliate protists *Euplotes patella* and *Tetrahymena pyriformis*, a well-established model predator-prey system that has been used for a wide array of spatial synchrony research (Vasseur & Fox 2009, Fox et al. 2011, 2013, 2017, Hopson & Fox 2018, Laan & Fox 2019). *T. pyriformis* measures 20 to 50 um long and primarily feeds on bacteria (Laan & Fox 2019). *E. patella* is the natural predator of *T. pyriformis*, and both of these protists will be used as the predator and prey, respectively, in the microcosm system for this experiment. *E. patella* measures 80 to 200 um long, making it a substantially larger predator that is able to consume *T. pyriformis* (Laan & Fox 2019). Although *E. patella* is a natural predator of *T. pyriformis*, this ciliate may also feed on bacteria, but *E. patella* cannot persist on a bacteria-only diet (Laan & Fox 2019). Both species reproduce through binary fission and *E. patella* has a longer generation time (~24-48 hours) than *T. pyriformis* (~4-6 hours) under optimal conditions (Laan & Fox 2019). Both species will exhibit consistent predator-prey cycles with a period of approximately 28 days in stable, non-fluctuating environments (Fox et al. 2011,

Hopson & Fox 2018, Laan & Fox 2019) and cycle amplitudes increase with resource enrichment (Laan & Fox 2019).

Experimental Design

For this experiment, *T. pyriformis* and *E. patella* populations were established in 100 mL glass culture jars each filled with 40 mL media that were loosely capped to avoid contamination but still allow for gas exchange. A total of 108 jars were established, which utilized all available incubator space, while also ensuring there were not too many jars to be counted in a single day. The microcosm culture jars were filled with solution media of sterilized spring water from a local freshwater spring in Big Hill Spring Provincial Park, located northwest of the city of Calgary in the foothills of Alberta, Canada. Following standard microcosm setups from previously run experiments (Vasseur & Fox 2009, Fox et al. 2013, Hopson & Fox 2018, Laan & Fox 2019), the spring water media was first sterilized and enriched with weighted crushed pellets (standard Protozoan Pellets) made of dried plant material serving as an organic carbon and nutrient source (Carolina Biological Supply, Burlington, NC, USA). A sterile wheat seed was also added, serving as a nutrient source for bacteria (Laan & Fox 2019). Microcosm jars were assigned one of two resource enrichment level treatments, either a low enrichment of 0.1 g PP/L or a high enrichment of 0.4 g PP/L. These enrichment levels were chosen based on enrichment levels tested by Laan and Fox (2019) and pilot experiments that provide different degrees of cycling (Appendix C). The lower enrichment treatment of 0.1 g PP/L provides enough nutrients for populations to persist with stable dynamics over time with little-to-no cycles, but not enough for higher amplitude cycles to persist. The higher enrichment treatment of 0.4 g PP/L provided enough nutrients for high amplitude predator-prey cycles to persist but did not provide an

abundance of nutrients to create cycles with large enough amplitudes that could potentially lead to the extinction of either predator or prey.

Once the enriched media was prepared, the jars were established trophically from the bottom up. First, jar media was inoculated with 1.0 mL media containing isogenic strains of bacteria and were left to rest for 24 hours to allow the bacteria to establish. The bacteria for this experiment could not be customarily sourced from plates grown in the lab. Instead, it was sourced from 0.3 mL *T. pyriformis* stock culture media containing no protists and placed in two jars of 80 mL sterile stock media that was given 24 hours for bacteria to establish and proliferate. Jars were then inoculated with 1.0 mL *T. pyriformis* culture stock and were left to rest for 72 hours to allow the protist prey to establish and grow to carrying capacity.

The jars were then randomly crossed with a temperature cycle treatment. Six sequences of temperature cycles were chosen to reflect the predator-prey cycles of both species in the system. This was done by setting one sequence centred on a 28-day cycle, reflective of the natural predator-prey cycles of *T. pyriformis* and *E. patella* (Fox et al. 2011, Hopson & Fox 2018, Laan & Fox 2019), and other sequences falling at a defined scale above and below the central 28-day cycle period. Three sequences were set shorter at 24-day, 20-day, and 16-day temperature cycle lengths. Another two sequences were set longer at 32-day and 36-day temperature cycle lengths. In scaling the temperature cycle lengths above and below the natural predator-prey cycle of 28 days, we could determine if cycles were easily entrained when the cycle lengths of the environment and the predator-prey system are closely matched. Conversely, if cycles were more easily entrained with periods that were longer or shorter than the natural predator-prey cycle period length, the sequences set at incrementally longer and shorter periods should be able to detect for cycle entrainment at a given threshold of varying period lengths. Jars

were assigned one of the six temperature cycle period sequences carried out on a prescribed schedule over the course of the experiment by moving specifically labelled jars between high and low temperatures to create a cyclic effect.

Temperature cycle amplitudes ranged between 22°C (room temperature) and 27°C. The upper-temperature limit was chosen based on the thermal tolerance of *E. patella* since the thermal tolerance of *T. pyriformis* is much higher at up to 39°C (Slater 1954). The upper 27°C temperature limit was established based on pilot experiments (Appendix C) and past microcosm experiments (Vasseur & Fox 2009, Fox et al. 2011). The lower temperature limit was constrained to room temperature since the incubators that were built could only heat and could not produce colder temperatures. The jars themselves experienced two-point limit cycles between these two temperatures as they were moved from one incubator at room temperature to another incubator heated to 27°C to create the cyclic effect. Jars would be switched between incubators every morning at 9:00 am, and jars that were being moved from a high-temperature incubator would be left on the lab bench for 8 hours before being placed in the room temperature incubator to ensure the room-temperature incubator was not being unintentionally heated by the warmer jars. While it may appear that the two-point limit cycle produced by these switches between incubators does not align with the sine wave predator-prey cycles, the protists themselves would experience more of a gradual sine wave in temperature gradient as the specific heat of water heats and cools at a slower rate than the air temperature.

Before completing the final setup step and adding *E. patella*, jars were randomly grouped into replicate metapopulation crosses according to specified enrichment level treatments and temperature cycle length treatments (Table 3.1). The metapopulation and treatment crosses were designed in this experiment based on a similar unreplicated factorial design conducted by

Vasseur and Fox (2009). This design was the ideal choice to optimize power without needing to reduce the number of jars or treatments sampled. Within each temperature cycle and enrichment level cross, four jar patch replicates are set aside to form a predation-free control. In these jars, *T. pyriformis* was allowed to persist for the duration of the experiment in the absence of the predator, and therefore in the absence of predator-prey cycles. Another five jars were grouped into replicate metapopulations that will experience predation with both *T. pyriformis* and *E. patella* present.

Once *T. pyriformis* was well established and all jars were grouped in their respective metapopulation crosses, the jars experiencing predation were sequentially inoculated with *E. patella* based on the randomly assigned patch replicate number of the jars, with one day spaced between each sequential addition (Table 3.2). By sequentially adding the predator within treatment patches, microcosm jars began their predator-prey cycles at disparate times so the jars did not begin the experiment in perfect synchrony. It also allowed for certain patches to have cycles closer in phase compared to other patches depending on how close the protist additions were to one another. The closer the addition of *E. patella* to another jar replicate, the closer the predator-prey cycle phases align, and vice versa. This allowed us to see whether the distance between cycle phases of the jars plays a role in which jars would synchronize if synchrony occurs. Jars were left at room temperature on the lab bench during the period of sequential additions of *E. patella* to the microcosm jars. After the fifth sequential *E. patella* addition, all jars were placed in the room temperature incubator and the experiment began at Day 0.

Sampling began on Day 1 of the experiment, and the abundance of *T. pyriformis* and *E. patella* were sampled daily for a total of 80 days. Since it was not feasible to sample all 108 jars in a single day, metapopulations were assigned to one of two temporal sampling blocks that

alternated the days that jars were sampled. Each metapopulation would be sampled on Monday, Wednesday, and Friday one week, and then would be sampled on Tuesday, Thursday, and Saturday the next week, and this alternating pattern would repeat until the 80 days were reached. There was no sampling on Sundays, and each jar was sampled 35 times over the 80-day span of the experiment.

To sample, each jar was gently swirled to agitate the contents settled on the bottom before 0.3 mL of media was removed and dropped on a plate. Under a binocular light microscope, the abundance of both *E. patella* and *T. pyriformis* was counted and recorded. The drawn samples were not returned to the jars and were discarded. In the often likely case that the abundance of either predator or prey (or both) were too abundant to count, the sample would be diluted with a known volume of sterile media and a sub-sample of 0.3 mL of media is re-drawn, dropped onto a new plate, and the abundance is counted and recorded. Based on the abundance from the small sample volume or diluted sub-sample volume the total abundance for the jar for *T. pyriformis* and *E. patella* was estimated.

Starting on Day -4 and on every Friday after sampling thereafter, 10% of the jar media is replaced and the volume spent sampling for the week (0.9 mL) is replenished. To replace the media, each jar was gently swirled to agitate the contents, and then 4 mL (10%) media was removed and discarded. Then, 4.9 mL fresh sterile media of the same enrichment level the jar is assigned as its treatment was added to each jar. Some weeks when either *T. pyriformis* abundance or *E. patella* abundance was too low to be detected by the above sampling methods, the media removed from those jars during media replacement is visually scanned for protist presence or absence before it is discarded. This weekly replacement of media ensured that the microcosm would not age too quickly and that the protists would be provided with enough fresh nutrients to

persist for the duration of the experiment. While this media replacement could be considered a small synchronous perturbation that could increase synchrony across metapopulations, it has previously been found to have no effect on the protist system (Laan & Fox 2019).

In all, the short-period temperature cycle experienced 6 cycles and the long-period temperature cycle experienced two cycles, with all other temperature cycle periods experiencing some number of cycles in between (Table 3.3). While it may seem like only two complete cycles does not seem like a sufficient number of cycles to observe any spatial synchrony, there has been synchrony that occurs within less than one cycle for previous microcosm studies undergoing similar methods (Vasseur & Fox 2009). Extending the experiment any longer than 80 days runs the risk of the jar contents naturally decaying, despite the weekly media replacements.

Data Processing and Statistical Analysis

The densities of both *T. pyriformis* and *E. patella* were calculated for each microcosm jar from the sampled abundance and the sample or subsample volume and the densities were then log transformed ($\log_{10}(n/ml + 1)$). All analyses used these densities from all jars and analyses were conducted in R Studio (R Core Team 2020) and data was organized within R using the “tidyverse” R package (Wickham et al. 2019). First, the log protist densities were plotted over experiment days using the “ggplot2” R package for visual analysis of the time series (Wickham 2016). Patches within treatments were plotted together to look for instances of visual overlap where densities are the same through time, indicating potential instances of synchrony between jars.

Wavelet analysis was conducted next to detect for significant instances of predator-prey cycles within the time series of the jars. This analysis was only conducted on jars where both *E.*

patella and *T. pyriformis* were present, since the intention was to look for predator-prey cycles, and there are no cycles expected in jars with only *T. pyriformis*. A Morlet wavelet transform was performed twice on each jar, once for *T. pyriformis* density over time and once for *E. patella* density over time. Analysis of *T. pyriformis* densities for the first patch jars at low enrichment/16-day temperature cycle, low enrichment/20-day temperature cycle, and high enrichment/32-day temperature cycle treatments were excluded since these jars had densities that remained below the detectable sampling density threshold for the entire duration of the time series. (It is important to note that these instances of long strings of zero density were possible, since these jars were all first patch jars which had *E. patella* added at the very start of the sequential predator addition to patches. Therefore, the density of *T. pyriformis* could have been depleted to very low density by *E. patella* before sampling began.) For all remaining jars that could be analyzed, the Morlet wavelet transforms were used to produce power spectra for each jar, utilizing the “stats” and “utils” R packages (R Core Team 2020), as well as the “dplR” package (Bunn et al. 2020). Within the power spectra produced for each jar, 5% significance contours helped to determine the presence or absence of cycles, as well as to determine cycle period if cycles were present.

Next, cross correlation between time series were calculated as a measure of synchrony between jars. When jars are synchronized, their densities track together through time and are therefore highly correlated, which makes correlation a strong indicator of spatial synchrony between jars. The cross correlation values for all pairwise crosses between jars under predation were calculated using the “magrittr” (Bache & Wickham 2020), “reshape2” (Wickham 2007), and “Hmisc” (Harrell 2020) R packages. The cross correlation values that were calculated were then plotted in a correlogram matrix using the “ggcorrplot” R package (Kassambara 2019) to

visualize any patterns in correlation both between and within treatments. Boxplots of cross correlation values within enrichment level and temperature cycle treatments were also produced to visually analyze patterns in correlation between jars. These boxplots were created using the “ggplot2” R package (Wickham 2016). Jars with only *T. pyriformis* were excluded from this analysis as these jars function as a control for understanding treatment effects in the absence of predation. These jars were not expected to yield meaningful results on spatial synchrony patterns as there were no mechanisms in which spatial synchrony could affect population persistence in these jars.

To formally test for differences in cross correlation values between temperature cycle and enrichment level treatments, permutation tests were used. In permuting the time series of log densities amongst treatments, it could be determined if certain treatments were more highly correlated than others and potentially indicating treatments where there were more instances of spatial synchrony. Three separate permutation tests were run. The first test randomized time series correlation values across temperature cycles, the second randomized the same correlation values across enrichment levels, and the third test randomized them across both temperature cycles and enrichment levels. The “coin” R package (Hothorn et al. 2006) was used to perform these permutation tests.

The next steps in the analysis sought to understand treatment level effects on the time series without looking specifically for instances of spatial synchrony or population cycles. First, clustering analysis was performed to determine if the dynamics seen in *T. pyriformis* and *E. patella* densities were a direct result of their assigned treatments, and if they can be accurately clustered based on these treatment groups. Euclidean distance matrices and k-means clustering was specifically used, and all jars (jars with *T. pyriformis* and *E. patella*, and control jars with

only *T. pyriformis*) were included in this analysis. Clustering analysis for the temperature cycle treatment was conducted using a k-means set at six since there are six total temperature cycles being tested. Similarly, clustering analysis for the enrichment level treatment was conducted using a k-means set at two since there are two enrichment levels being tested. This analysis was repeated three times in all; once for time series of *T. pyriformis* density under no predation, once for time series of *T. pyriformis* density under predation, and once for time series of *E. patella* density. The “vegan” R package (Oksanen et al. 2020) was used to conduct the clustering analysis and the “ggplot2” R package (Wickham 2016) was used to create NMDS plots for visualizing the k-means clustering.

The last portion analysis also looked at treatment level effects, but instead of searching for treatment-level clusters, I wanted to see if I could statistically impose treatment-level groupings based on the protist densities. To do this, a PERMANOVA was used. Initially I wanted to run a MANOVA (multivariate analysis of variance), but the assumption that there are more samples than there are variables was violated. To run this analysis, densities are grouped based on their sampling day (a total 35 sampling observations per time series), and this was then crossed with experimental treatment (enrichment level, temperature cycle, or both). Within each temperature cycle, there were 10 density samples, and there were 30 density samples, which are both less than the 35 sampling days being used as a grouping variable. Therefore, PERMANOVA (permutational multivariate analysis of variance) was used instead, which geometrically partitions variance in multivariate space while being defined by a chosen dissimilarity measure (Euclidean distance used in this case) in response to multiple factors in an ANOVA design (Anderson 2017). Standard measures for this analysis were used by running 999 permutations and sequentially adding terms. PERMANOVA was conducted three times on the

log density of *T. pyriformis* under no predation, *T. pyriformis* under predation, and *E. patella* like before for clustering analysis. One analysis was run for temperature cycles crossed with sampling days, the second was run for enrichment levels crossed with sampling days, and the third was run for temperature cycles and enrichment levels crossed with sampling days. Significant results were followed up with post-hoc multivariate pairwise comparisons to determine specific pairwise significance between treatment groups. The “vegan” R package (Oksanen et al. 2020) and “devtools” R package (Wickham et al. 2020) were necessary for running the PERMANOVA, and the “pairwiseAdonis” R package (Arbizu 2017) was used to conduct the post-hoc multivariate pairwise comparisons.



Figure 3.1: COVID-19 laboratory setup. Photo by Kaitlin Osterlund.



Figure 3.2 COVID-19 incubator setup. A) Full incubator setup with Arduino board delivering temperature readouts to a computer. B) Incubator interior top-shelf supporting microcosm jars. C) Incubator interior bottom-shelf supporting reptile heating pad and temperature sensor. All photos by Kaitlin Osterlund.

Table 3.1: Experiment study design, total 108 microcosm jars.

Temperature Cycle	Enrichment			
	High (0.4 g PP/L)		Low (0.1 g PP/L)	
	No Predation	Predation	No Predation	Predation
A 16-day cycle (8 days at 27°C, 8 days at 22°C)	4 jars	5 jars	4 jars	5 jars
B 20-day cycle (10 days at 27°C, 10 days at 22°C)	4 jars	5 jars	4 jars	5 jars
C 24-day cycle (12 days at 27°C, 12 days at 22°C)	4 jars	5 jars	4 jars	5 jars
D 28-day cycle (14 days at 27°C, 14 days at 22°C)	4 jars	5 jars	4 jars	5 jars
E 32-day cycle (16 days at 27°C, 16 days at 22°C)	4 jars	5 jars	4 jars	5 jars
F 36-day cycle (18 days at 27°C, 18 days at 22°C)	4 jars	5 jars	4 jars	5 jars

Table 3.2: Experiment microcosm jar setup.

Date	Experiment Day	Jar Processing
May 27, 2020	-13	All jars sterilized and enriched media added.
May 28, 2020	-12	All jars inoculated with bacteria, and allowed to grow for 24 hours.
May 29, 2020	-11	<i>Tetrahymena pyriformis</i> added to all jars and allowed 72 hours to grow.
May 30, 2020	-10	<i>T. pyriformis</i> allowed to grow for 72 hours.
May 31, 2020	-9	<i>T. pyriformis</i> allowed to grow for 72 hours.
June 1, 2020	-8	<i>Euploites patella</i> added to patches 1 out of 5.
June 2, 2020	-7	N/A
June 3, 2020	-6	<i>E. patella</i> added to patches 2 out of 5.
June 4, 2020	-5	N/A
June 5, 2020	-4	<i>E. patella</i> added to patches 3 out of 5.
June 6, 2020	-3	N/A
June 7, 2020	-2	<i>E. patella</i> added to patches 4 out of 5.
June 8, 2020	-1	N/A
June 9, 2020	0	<i>E. patella</i> added to patches 5 out of 5. All jars placed into incubator 3 (22°C).
June 10, 2020	1	Sampling begins.

Table 3.3: Experiment temperature cycle schedule.

Cycle Number	Temperature (°C)	Experiment Days Spent per Temperature Cycle Period					
		A (16 days)	B (20 days)	C (24 days)	D (28 days)	E (32 days)	F (36 days)
1	22	0-7	0-9	0-11	0-13	0-15	0-17
	27	8-15	10-19	12-23	14-27	16-31	18-35
2	22	16-23	20-29	24-35	28-41	32-47	36-53
	27	24-31	30-39	36-47	42-55	48-63	54-71
3	22	32-39	40-49	48-59	56-69	64-79	72-81
	27	40-47	50-59	60-71	70-10	80-81	
4	22	48-55	60-69	72-80	81		
	27	56-63	70-79				
5	22	64-71	80-81				
	27	72-79					
6	22	80-81					

3.3 Experiment Results

The results for this experiment showed no significant patterns of spatial synchrony and cycles in both *T. pyriformis* and *E. patella* population densities over time. Both visual analysis and statistical analysis displayed no significant spatial synchrony between jar patches, as well as no significant cycling over the duration of the experiment in the jars. Since the outcome of this experiment is dependent on the occurrence of population cycles over time, the analysis of spatial synchrony becomes limited only to jar replicates that display distinct cycles. Therefore, analyzing the correlation between jars may not yield any meaningful results to describe spatial synchrony in the absence of population cycles. The results of this analysis are discussed in detail below.

Time Series Visualization

First looking at the control jars of *T. pyriformis* under no predation (Figure 3.3), the protists at high enrichment maintained a higher carrying capacity than the protists at low enrichment, and this difference in density remained relatively constant across all temperature cycle treatments until the jars were moved to 27°C. After the first rise in temperature for all temperature cycle treatments, *T. pyriformis* density increased in both low and high enrichment treatments. After this rapid rise in density, the high enrichment jar densities converged with the low enrichment jar densities. Both high and low enrichment jars then slowly declined towards the end of the time series. While it is expected that populations will decline over time (due to potential carbon respiration out of the jars and accumulation of metabolic waste products), the densities at high enrichment were not expected to converge with the densities at low enrichment. Rather, it was expected that high enrichment jars would maintain a higher carrying capacity than

low enrichment jars, and all jars would gradually decline while maintaining this separation in density with respect to the difference in media enrichment of the treatments.

In low enrichment jars with predation (Figure 3.4), there visually appeared to be some synchrony occurring within the first 10 to 20 days of the experiment where protist densities within jars closely followed similar dynamics to one another over time. It also appeared as if this initial synchrony persisted longer with increasing temperature cycle length. However, this synchrony was not long-lasting across all temperature cycle treatments and was lost after the first sharp decline in *T. pyriformis* density and first rise in temperature. Once *T. pyriformis* returned from low density if they did so at all (which they didn't do in all jars), *T. pyriformis* did not continue cycling as expected, but rather fluctuated irregularly over time or eventually declined to extinction. *E. patella* would follow a similar pattern to its prey: either stochastic fluctuations or declines to extinction. No two jars exhibited visually obvious synchrony with one another for the remainder of the experiment. The first and third patches in the 32 day temperature cycle, and the third patch in the 36 day temperature cycle displayed early extinctions of *E. patella* which allowed *T. pyriformis* to grow and persist at carrying capacity.

T. pyriformis was absent from some samples from most jars. Some of these zero densities may represent extinctions; others may represent failure to detect small *T. pyriformis* populations. If protist density remained below the detectable sampling threshold for a substantial amount of time, it could then be assumed that the protist has gone extinct. Checking discarded media during the weekly media replacements of the jars further helped in determining protist extinction.

Patterns from the low enrichment time series were similarly observed for the high enrichment time series (Figure 3.5). The initial appearance of synchrony at the start of the experiment was especially apparent for the longer 24 day, 28 day, 32 day, and 36 day temperature

cycles. This initial appearance of synchrony was more clearly defined for high enrichment than for low enrichment with population densities overlapping to a stronger degree. As in the low enrichment treatment, jar densities lost the initial synchrony once the jars were placed at 27°C and *T. pyriformis* fell to low density. The population dynamics that followed for both predator and prey were similarly stochastic in nature, resulting in either random fluctuations over time or extinction. Unlike the low enrichment jars, there were more jars that experienced extinction of the predator that allowed *T. pyriformis* to grow and persist at carrying capacity, and predator extinctions occurred in every temperature cycle treatment.

In Figure 3.6, the same time series discussed above were plotted with respect to their patch replicate number rather than their temperature cycle, with the goal of observing jars diverge away from initial synchrony at different intervals with respect to their temperature cycle. Since all patches were numbered based on when *E. patella* was added, all patches share the same initial abundances and in theory will begin the experiment in near-perfect synchrony. Across all patches at both high and low enrichment, this appears to be the case where population densities are visually correlated in the first 10 to 20 days of the experiment. In all of Figures 3.4, 3.5, and 3.6, the initial cycles that appeared close in phase fell out of phase once *T. pyriformis* declined at 27°C, and cycles were then lost. Since these cycles were lost, any patterns in the population dynamics relative to temperature cycles could not be visually discerned from the stochastic fluctuations of both *T. pyriformis* and *E. patella*.

With no visual evidence of spatial synchrony over the length of the experiment, further statistical approaches are necessary to detect the presence of cycles or synchrony in the populations of *T. pyriformis* and *E. patella*. First, we will examine if predator-prey cycles were

present during the experiment that could not be easily distinguished by visually inspecting the time series of both *T. pyriformis* and *E. patella*.

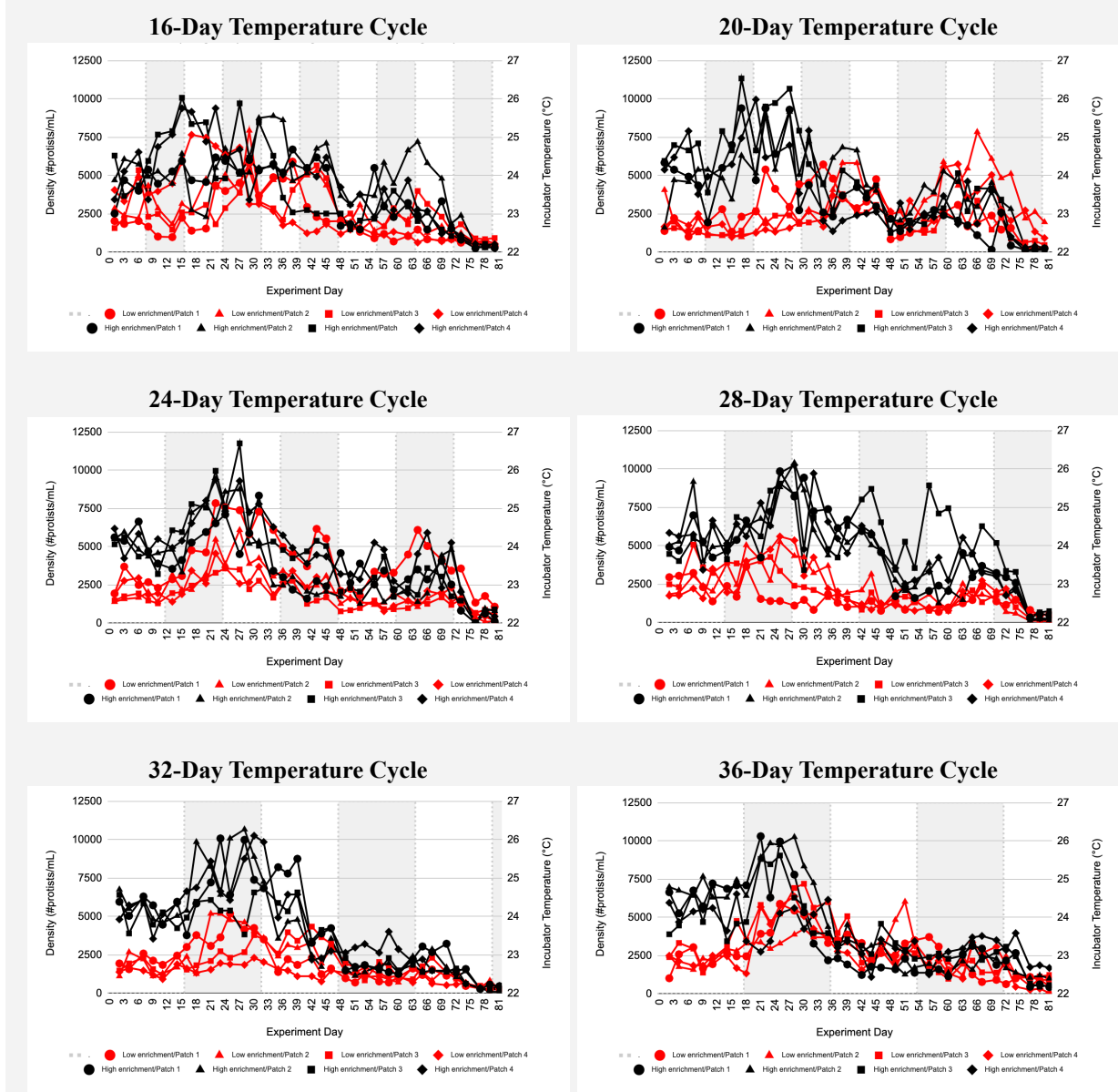


Figure 3.3: Predation-free control time series of *T. pyriformis* density grouped by temperature cycle in low and high enrichment. Shaded time indicates when jars are at 27°C.

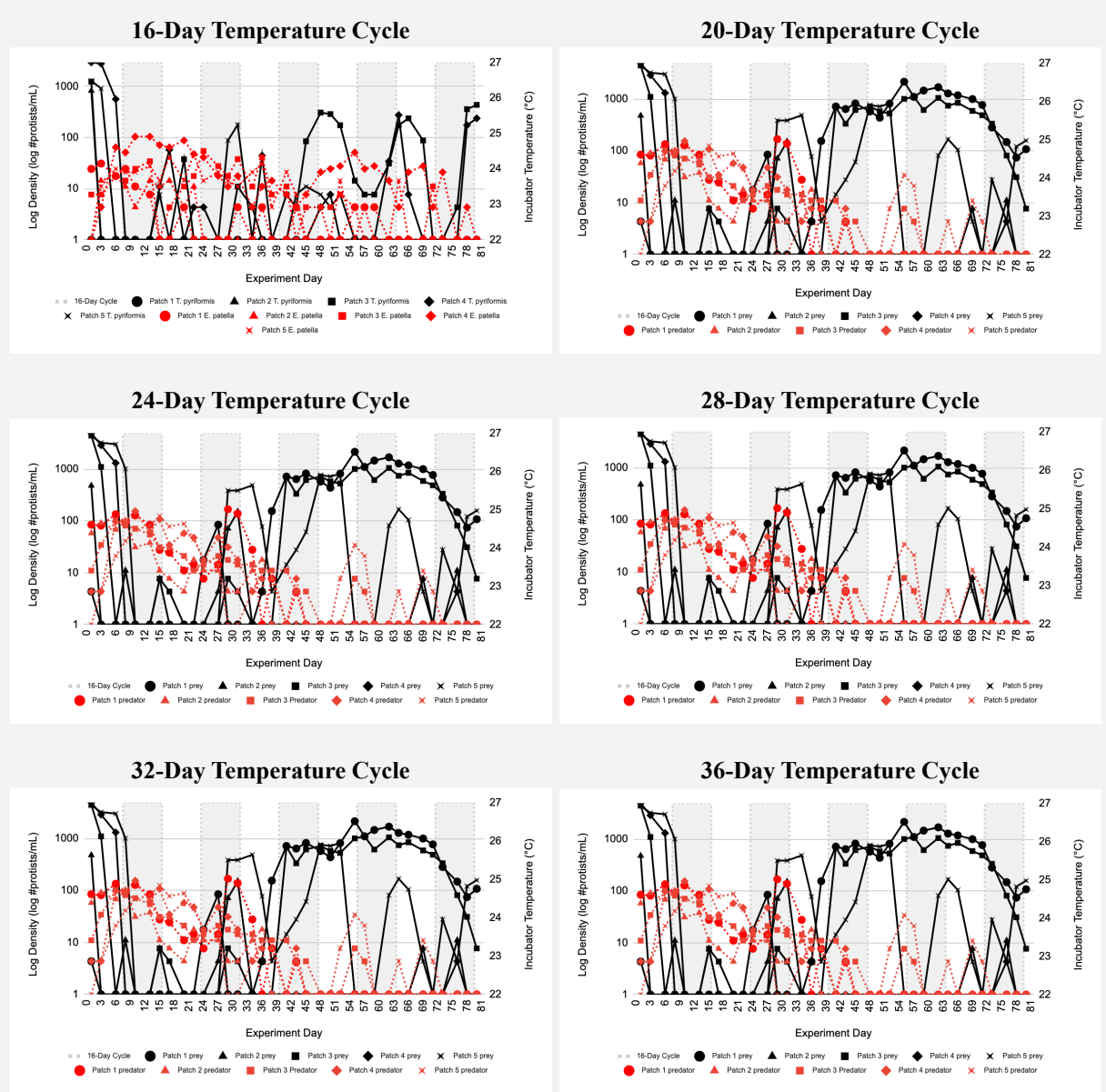
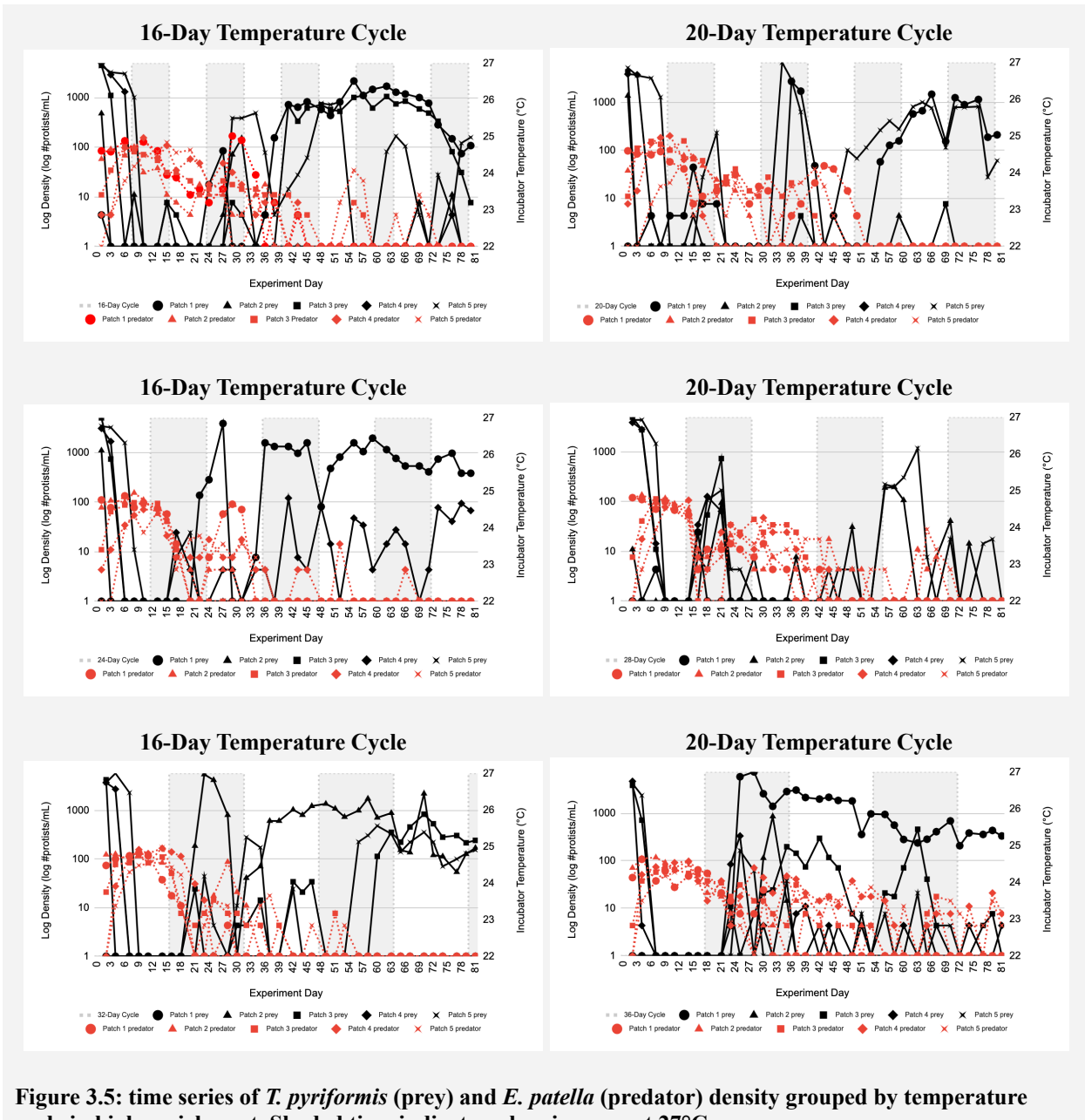


Figure 3.4: Time series of *T. pyriformis* (prey) and *E. patella* (predator) density grouped by temperature cycle in low enrichment. Shaded time indicates when jars are at 27°C.



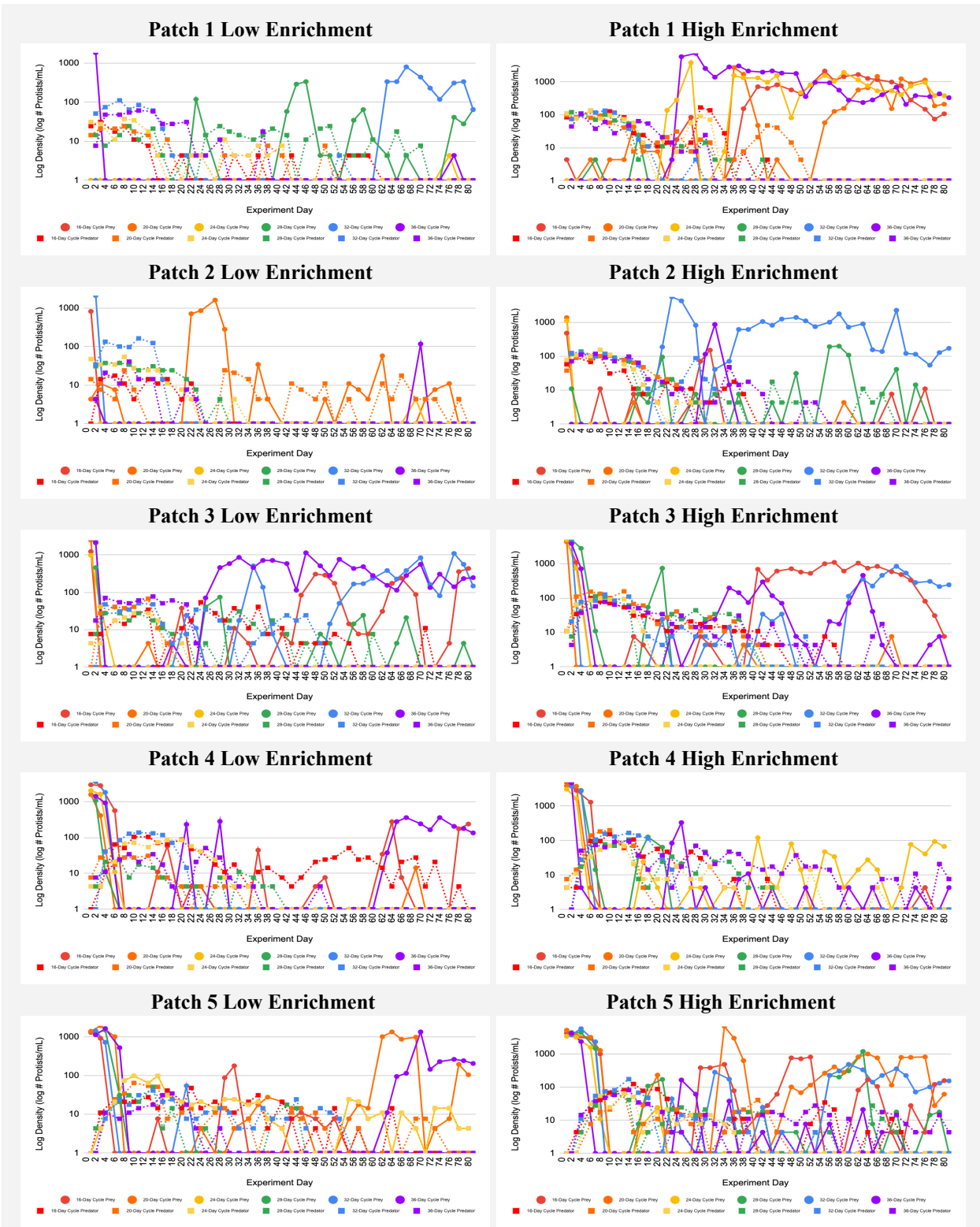


Figure 3.6: time series of *T. pyriformis* (prey) and *E. patella* (predator) density grouped by patch.

Wavelet Analysis

Wavelet analysis was conducted to detect any significant instances of cycling via power spectra of the time series of protist density, and in all, there were very few jars that exhibited any instances of cycles over the duration of the experiment, and none of the instances of cycles persisted for long periods of time over the experiment. First looking at the wavelet power spectra of the 16 day temperature cycle at low enrichment (Figure 3.7), there were only a few instances where some jars exhibited a small degree of cycling. For *T. pyriformis*, the first and second patch densities dropped to extinction. In the fifth patch for *T. pyriformis*, the power spectrum shows a significant instance of cycling with a period of approximately 16 to 20 days throughout the middle of the time series, but this cycling does not persist throughout the experiment. This same significant cycling period is also apparent towards the latter-half of the time series for the third and fourth patches of *T. pyriformis*. Interestingly, the cycle periods that persisted within *T. pyriformis* closely matched the 16-day temperature cycle treatment period imposed, and it is also close to half the natural predator-prey cycle period of approximately 28 days (Fox et al. 2011, Hopson & Fox 2018, Laan & Fox 2019). For *E. patella* at low enrichment, there are no patches that drop to extinction, and similar instances of approximately 16 to 20 day cycle periods appeared in the first patch, however this appearance of cycling does not persist as long in the time series as it does for patches of *T. pyriformis*. All remaining patches of *E. patella* appeared to fluctuate randomly through time with some random significant power spikes that don't appear to translate to instances of cycles.

Looking next at high enrichment, there appeared to be overall fewer instances of potential cycles for the 16-day temperature cycle treatment than there was for low enrichment (Figure 3.8). For both *T. pyriformis* and *E. patella*, the only instance of some cycles were found in the

fifth patches where cycles with a period of approximately 16 days appeared after the first 20-30 days of the time series and persisted through towards the end of the sampling period. All other patches of *T. pyriformis* either grew to carrying capacity in accordance with a depleted *E. patella* population (first and third patches) or fell to low densities (second and fourth patches). The first four patches of *E. patella* all gradually depleted to low densities, and even to extinction in the cases where *T. pyriformis* grew uninhibited by predation through time (first and third patches). Interestingly, while it was expected that there would be fewer instances of cycles at low enrichment compared to high enrichment, the opposite has taken effect for the case of jars in the 16-day temperature cycle treatment. While the high enrichment treatment was expected to produce higher amplitude cycles that persisted longer through time, it may be the case that the high enrichment treatment led to more volatile high amplitude cycles that create steep increases in density that then crash to extinction.

For the 20-day temperature cycle treatment at low enrichment (Figure 3.9), the first, third and fourth patches of *T. pyriformis* either remained extinct for the duration of the experiment, or remained at low density and only occasionally and randomly spiking in density over time. For these same patches, the densities of *E. patella* randomly fluctuated as they gradually decreased until it reached a density close to zero. However, in the second and fifth patches, the power spectra highlighted some instances where populations could be cycling at periods that closely match the natural predator-prey cycle period (Fox et al. 2011, Hopson & Fox 2018, Laan & Fox 2019). These instances of population cycles vary between the patches, and neither patch has cycles that persist for the duration of the experiment. Yet the highlighted significance within the power spectra are closely matched between *E. patella* and *T. pyriformis* within the same patches, indicating the potential for correlated cycling between predator and prey. While there does

appear to be some instances of significance within the power spectra, it is difficult to determine if this explains a significant occurrence of cycles as predicted in the jars since these potential cycles do not persist for very long within the time series.

In Figure 3.10, the first and fifth patches of the 20-day temperature cycle treatment at high enrichment display unique patterns for *T. pyriformis* over time. There are initially no instances of cycling for either patch for *T. pyriformis*, but then both patches experience one full cycle at approximately 28 days one month into the experiment right before they then grow to carrying capacity, where *E. patella* then went extinct and *T. pyriformis* were allowed to grow uninhibited by their predator. While the power spectra indicated a highlighted significance for *T. pyriformis*, the same was not true for *E. patella* in the same patches, where the predator fluctuated through time until it declined to extinction. The first four patches all had *T. pyriformis* that declined to low densities that would occasionally peak slightly above the sampling threshold, and *E. patella* densities that gradually declined to low density.

Next, looking at the power spectra for the 24-day temperature cycle treatment at low enrichment (Figure 3.11), there were no significant instances of cycling for *T. pyriformis*, but some instances of significance for the first and fifth patches of *E. patella*. The first four patches had *T. pyriformis* densities dropping below the detectable sampling threshold for the duration of the experiment, with the first and second patches briefly spiking in density towards the end of the time series. The fifth patch of *T. pyriformis* randomly fluctuated over the duration of the experiment. The first patch of *E. patella* appeared to initially cycle close to the natural predator-prey period of approximately 28 days (Fox et al. 2011, Hopson & Fox 2018, Laan & Fox 2019) before it abruptly stopped cycling and remained at low density for the duration of the time series. The fifth patch of *E. patella* appeared to randomly fluctuate up to half way through

the experiment, where the power spectra then highlighted cycle periods close to the natural predator-prey cycle length and half of the natural predator-prey cycle period length (Fox et al. 2011, Hopson & Fox 2018, Laan & Fox 2019). This highlighted power spectrum for *E. patella* does not appear to coincide with the dynamics of *T. pyriformis*, and it is difficult to determine if these areas of significance describe cyclic patterns of interest.

At high enrichment for the 24-day temperature cycle treatment (Figure 3.12), there are no instances of significance in the power spectra for both *T. pyriformis* and *E. patella*. The second, third, and fifth patches of *T. pyriformis*, as well as the first, second, third, and fifth patches of *E. patella* decrease to below the sampling threshold for the duration of the experiment. The first patch of *T. pyriformis* grows to carrying capacity, indicating an extinction of *E. patella* in the same patch. In the fourth patch at high enrichment, both *T. pyriformis* and *E. patella* randomly fluctuate over the duration of the time series. Similarly to the 16 day temperature cycle treatment, there are more instances of cycling that appear at low enrichment than at high enrichment, potentially due to cyclic volatility leading to very low densities in both predator and prey that are unable to recover.

Next, looking at the power spectra for the 28-day temperature cycle treatment at low enrichment (Figure 3.13), significant fluctuations with a period close to the natural predator-prey cycle period (Fox et al. 2011, Hopson & Fox 2018, Laan & Fox 2019) persist for a short time mid-way through the first patch of *T. pyriformis*. This cyclic pattern does not translate to the predator, where the first patch of *E. patella* fluctuates randomly over time. In the third patch, both *T. pyriformis* and *E. patella* display an initial yet short-lived significant power spectra at a period of approximately 30 days, once again close to the natural predator-prey cycle period (Fox et al. 2011, Hopson & Fox 2018, Laan & Fox 2019). Halfway through the experiment, the

potential cycles are lost and the protists both fluctuate randomly over time. The second, fourth, and fifth patches for both *T. pyriformis* and *E. patella* populations decline to low densities, with *E. patella* declining in density at a slower rate than *T. pyriformis*.

At high enrichment (Figure 3.14), *T. pyriformis* in the first, third, and fourth patches peak once or twice at some early point in the time series and remain at low density over the remainder of the experiment. The first and fourth patches of *E. patella* slowly decrease to low density, which coincides with the lack of prey available for *E. patella* in these respective patches. However, the third patch of *E. patella* appears to display some initial cycling at a period that closely matches the natural predator-prey cycle period (Fox et al. 2011, Hopson & Fox 2018, Laan & Fox 2019), and the trough in the density of *E. patella* coincides with the spike in *T. pyriformis* density for the same patch. However, half way through the experiment, the cycles are lost and both predator and prey remain at low density for the remainder of the time series. The second patch of *T. pyriformis* displays random fluctuations over time, and a larger significant peak close to the end of the time series at a period of approximately 16 days, however this highlighted significance in the power spectra does not persist for long, and therefore it is difficult to conclude if this constitutes a significant instance of cycling. In the fifth patch, both *T. pyriformis* and *E. patella* display a wide range of highlighted significance in their respective power spectra. For *T. pyriformis*, it appears that the density is potentially cycling at a longer than normal period, initially, while then displaying a single cycle close to the natural predator-prey cycle period (Fox et al. 2011, Hopson & Fox 2018, Laan & Fox 2019) towards the end of the time series. The density of *E. patella* in this same patch randomly fluctuates until half way through the time series where it then experiences two distinct peaks in density that provide a wide range of power spectrum significance that is difficult to decipher. A longer time series

would be beneficial for understanding these dynamics more clearly to determine whether or not this patch is experiencing persisting cycles with significantly longer periods compared to the period length of the natural predator-prey cycle (Fox et al. 2011, Hopson & Fox 2018, Laan & Fox 2019).

For the 32-day temperature cycle treatment at low enrichment (Figure 3.15), there were no significant instances of cycles in either *T. pyriformis* or *E. patella*. The first patch of *T. pyriformis* remains at low density for most of the time series until it suddenly grows to carrying capacity, which coincides with *E. patella* density declining to extinction in the first patch. The second and fourth patches of both *T. pyriformis* and *E. patella* experienced declines in density and never recovered at any point during the experiment. The third patch displayed random fluctuations in density for both protists, while the fifth patch displayed similar random fluctuations for *E. patella* while *T. pyriformis* spiked in density 20 days into the experiment and then returned to low density and never recovered.

In Figure 3.16, the patches at high enrichment for the 32-day temperature cycle treatment displayed similar limited instances of cycles, except for the fifth patch. In the fifth patch, the power spectrum for *T. pyriformis* highlights some significant cycling with a period that matches close to the natural predator-prey cycle of the protists (Fox et al. 2011, Hopson & Fox 2018, Laan & Fox 2019). This instance of cycling does not persist throughout the time series, as *E. patella* displayed dampening fluctuations that led to extinction, which allowed *T. pyriformis* to grow to carrying capacity at the end of the time series. In all other patches, the protists either fluctuated randomly through time (second and third patches of *T. pyriformis*) or decreased to low density (first, second, third, and fourth patches of *E. patella*). The first patch of *T. pyriformis*

likely went extinct early in the experiment, and remained at low density for the duration of the time series.

Finally, looking at the power spectra for the 36-day temperature cycle treatment at low enrichment (Figure 3.17), there once again are no instances of cycles. *T. pyriformis* density either decreased and persisted at low density with occasional random spikes in density (first and second patches), or persisted at low density until *E. patella* went extinct and grew to carrying capacity (third, fourth, and fifth patches). *E. patella* exhibited similar dynamics across all five patches, fluctuating in a slow decline to low density, and to extinction in some cases (third, fourth, and fifth patches).

At high enrichment (Figure 3.18), there were once again very limited instances of cycles. The first patch displayed extinction of *E. patella*, and the quick rise of *T. pyriformis* to carrying capacity. The second and third patches displayed *E. patella* slowly decreasing to low density, with *T. pyriformis* randomly spiking in density in the second patch, and *T. pyriformis* randomly fluctuating with changing periods in the third patch. In the fourth and fifth patches, *T. pyriformis* appeared to begin cycling as it significantly peaked around 20 days into the experiment, however this cyclic pattern quickly dampened and *T. pyriformis* continued fluctuating randomly through time. The fourth patch of *E. patella* underwent random fluctuations through time while the fifth patch of *E. patella* displayed the strongest evidence for population cycles as it maintained a cycle period of approximately 30 days for the first 55 to 60 days of the experiment.

While there were some small glimpses of population cycles in the microcosm jars, none of the dynamics persisted long enough to be able to definitively describe them as predicted predator-prey cycles. Additionally, there were more instances of extinction in the microcosm jars than there were instances of cycling. In all, 22 jars (36.7%) experienced extinction of *T.*

pyriformis, and 32 jars (53.3%) experienced extinction of *E. patella* by the end of the experiment. Further analysis in this chapter analyzing instances of spatial synchrony are challenged with this absence of population cycles and large degree of extinction. Population cycles are a key component of the hypothesis being tested to describe how population cycles might be entrained, and ultimately synchronized. The following results attempt to decipher any potential instances of spatial synchrony, as well as any temperature cycle effects or enrichment level effects that may be interpreted from this non-cyclic predator-prey system.

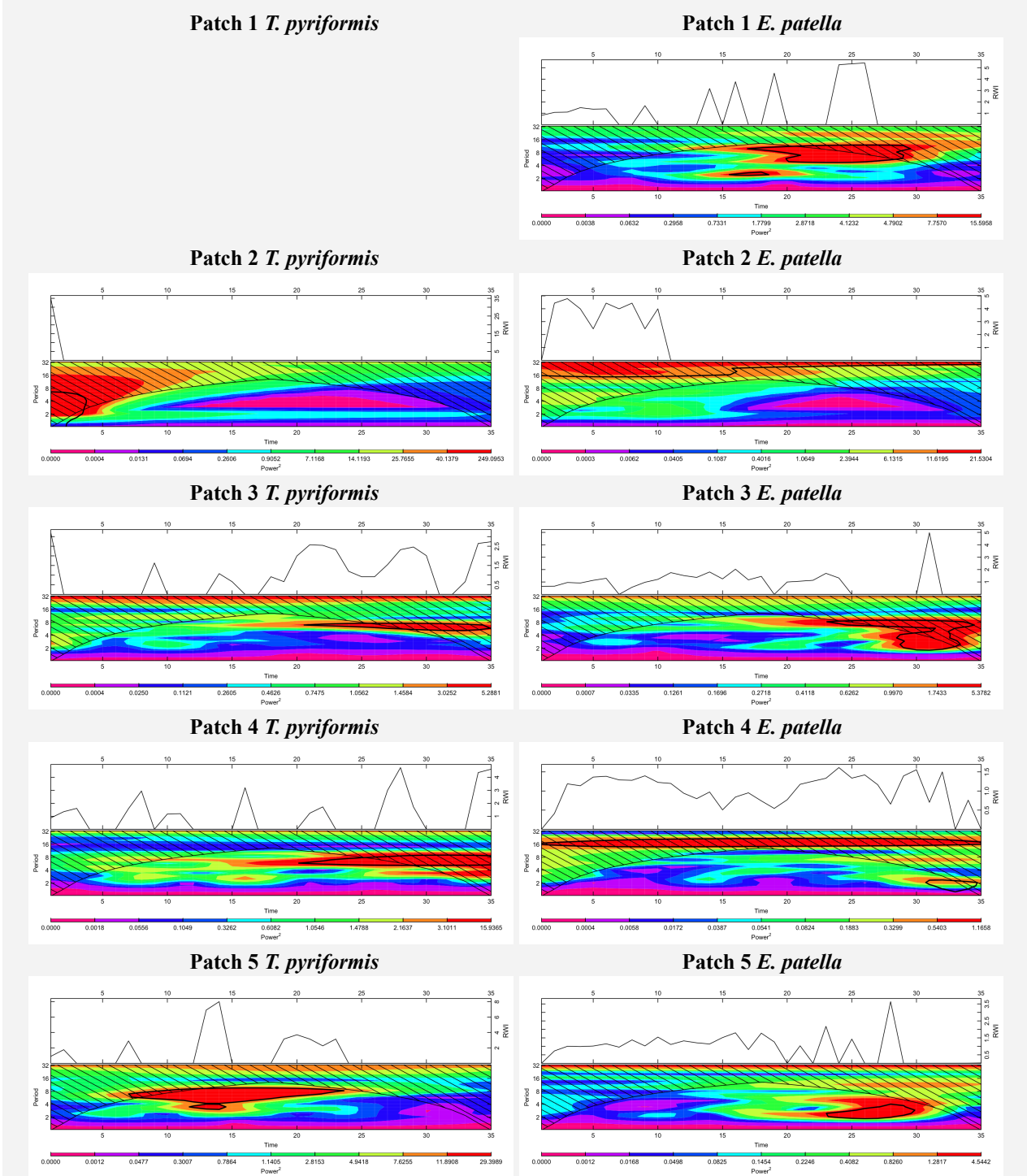


Figure 3.7: Low enrichment 16-Day temperature cycle wavelet power spectra for patches of *T. pyriformis* and *E. patella*. Patch 1 *T. pyriformis* abundance was zero for the duration of the experiment and a power spectrum could not be produced. Time represents the sample number taken (1 through 35) and actual cycle period is $2 \times$ period on y-axis. Significant power spectra outlined with black contour.

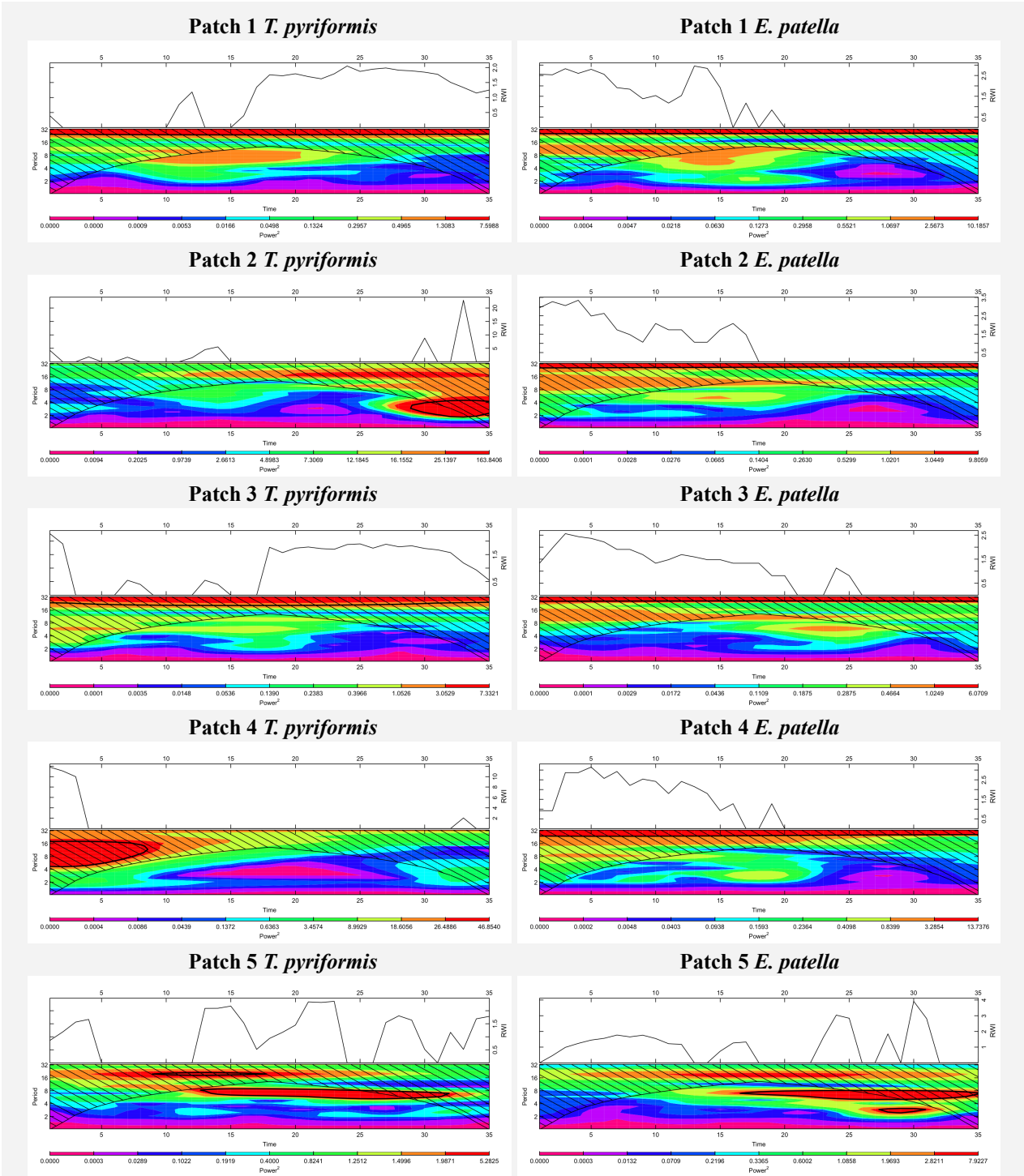


Figure 3.8: High enrichment 16-Day temperature cycle wavelet power spectra for patches of *T. pyriformis* and *E. patella*. Time represents the sample number taken (1 through 35) and actual cycle period is $2 \times$ period on y-axis. Significant power spectra outlined with black contour.

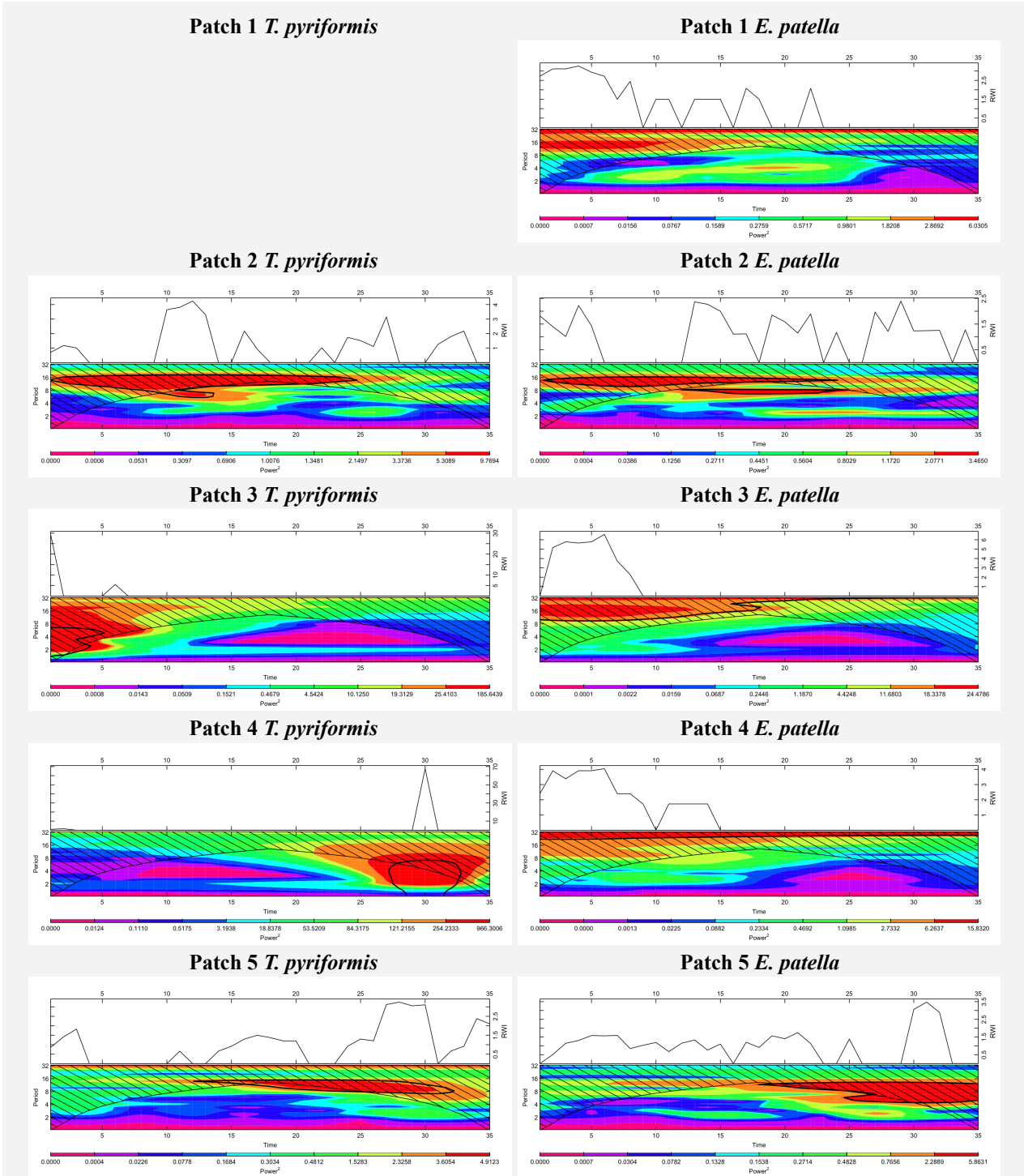


Figure 3.9: Low enrichment 20-Day temperature cycle wavelet power spectra for patches of *T. pyriformis* and *E. patella*. Patch 1 *T. pyriformis* abundance was zero for the duration of the experiment and a power spectrum could not be produced. Time represents the sample number taken (1 through 35) and actual cycle period is 2×period on y-axis. Significant power spectra outlined with black contour.

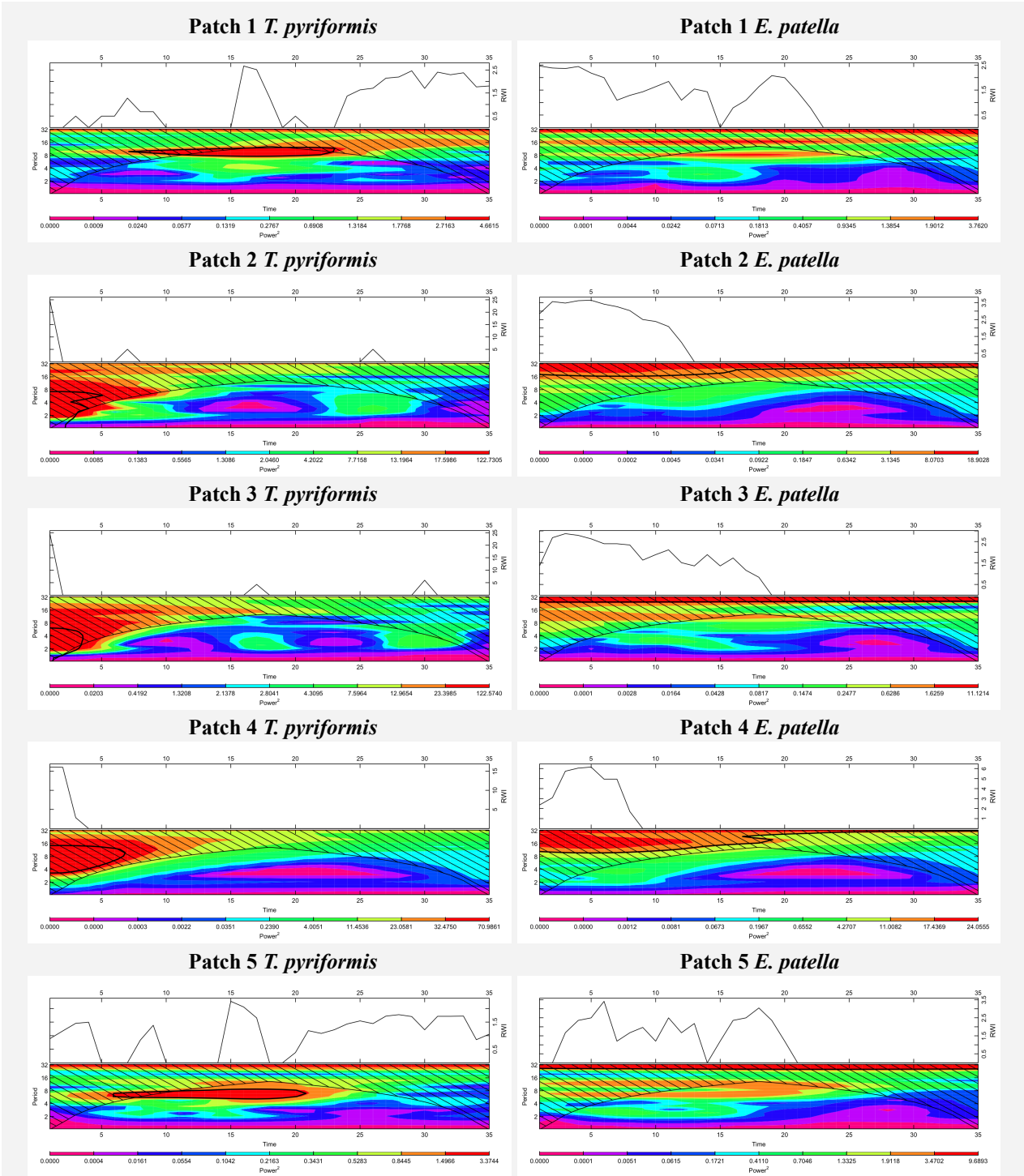


Figure 3.10: High enrichment 20-Day temperature cycle wavelet power spectra for patches of *T. pyriformis* and *E. patella*. Time represents the sample number taken (1 through 35) and actual cycle period is $2 \times$ period on y-axis. Significant power spectra outlined with black contour.

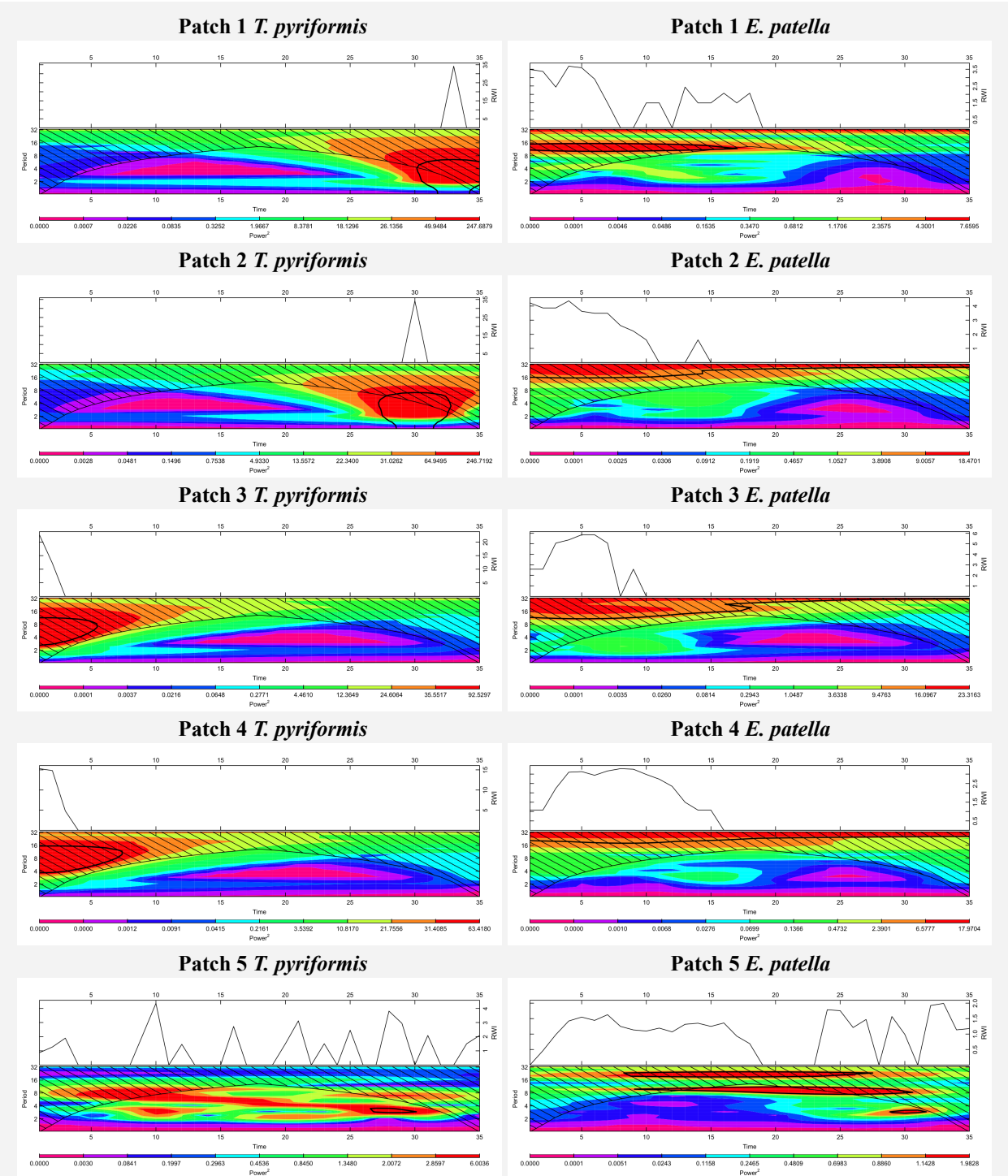


Figure 3.11: Low enrichment 24-Day temperature cycle wavelet power spectra for patches of *T. pyriformis* and *E. patella*. Time represents the sample number taken (1 through 35) and actual cycle period is $2 \times$ period on y-axis. Significant power spectra outlined with black contour.

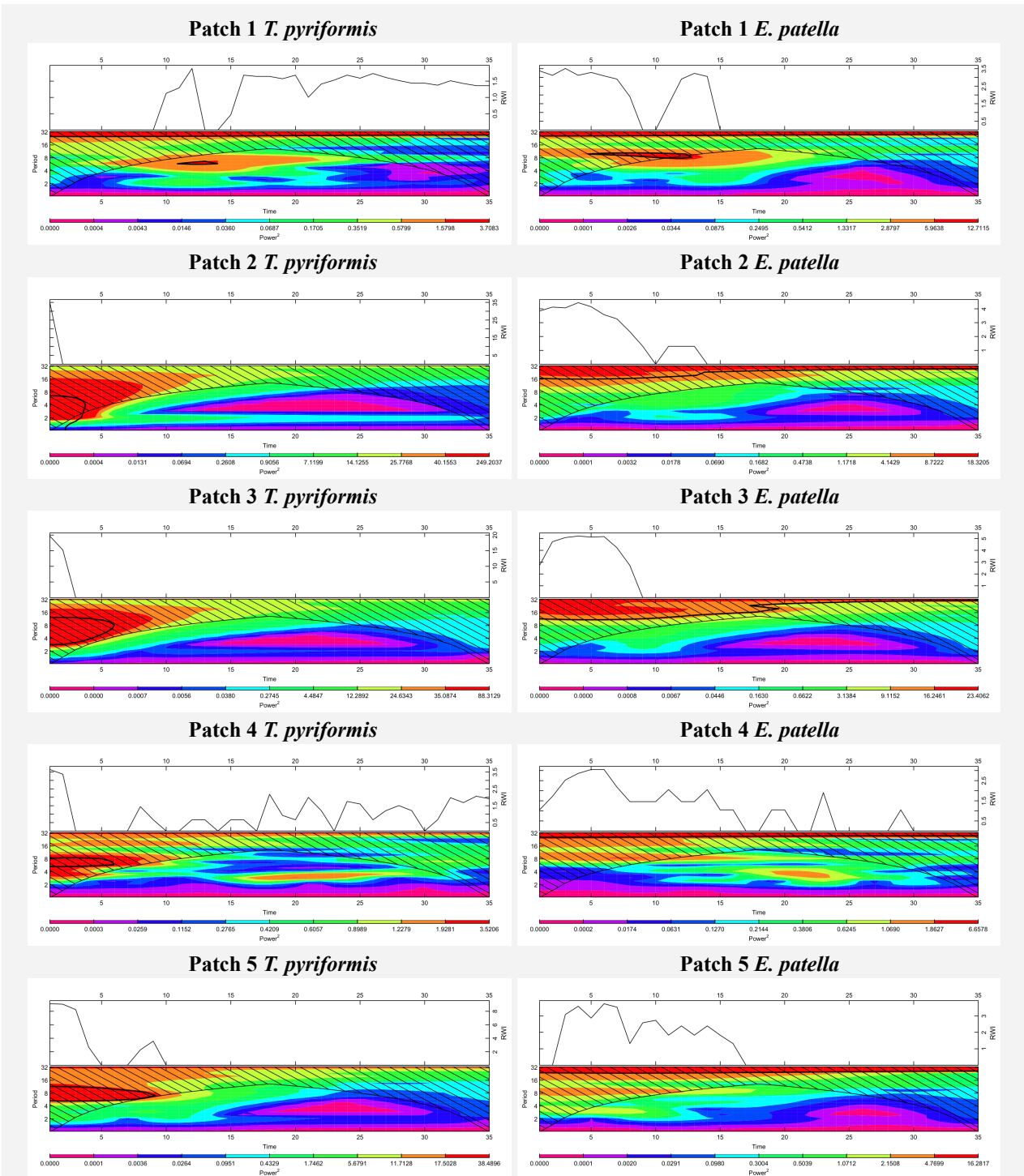


Figure 3.12: High enrichment 24-Day temperature cycle wavelet power spectra for patches of *T. pyriformis* and *E. patella*. Time represents the sample number taken (1 through 35) and actual cycle period is $2 \times$ period on y-axis. Significant power spectra outlined with black contour.

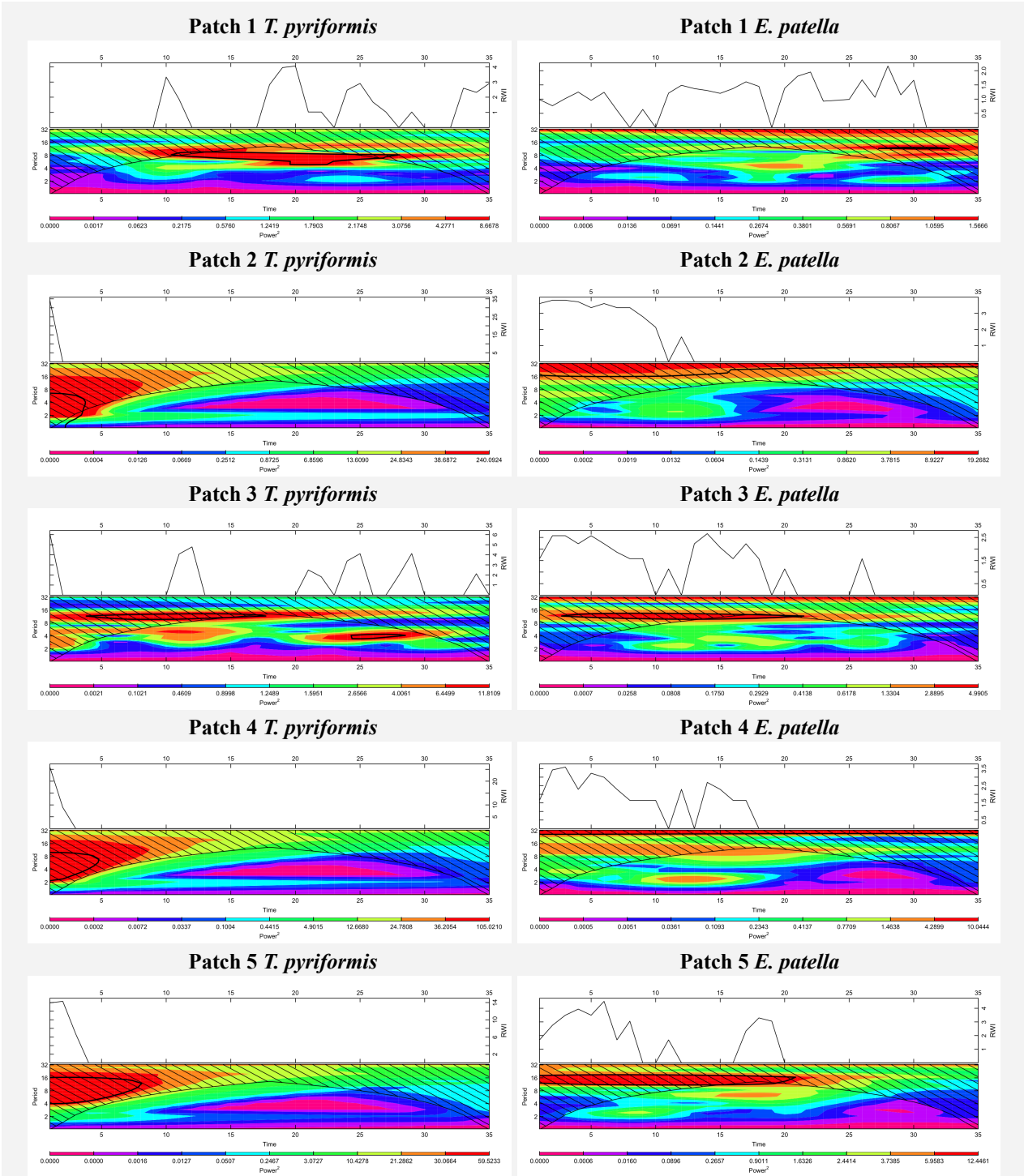


Figure 3.13: Low enrichment 28-Day temperature cycle wavelet power spectra for patches of *T. pyriformis* and *E. patella*. Time represents the sample number taken (1 through 35) and actual cycle period is $2 \times$ period on y-axis. Significant power spectra outlined with black contour.

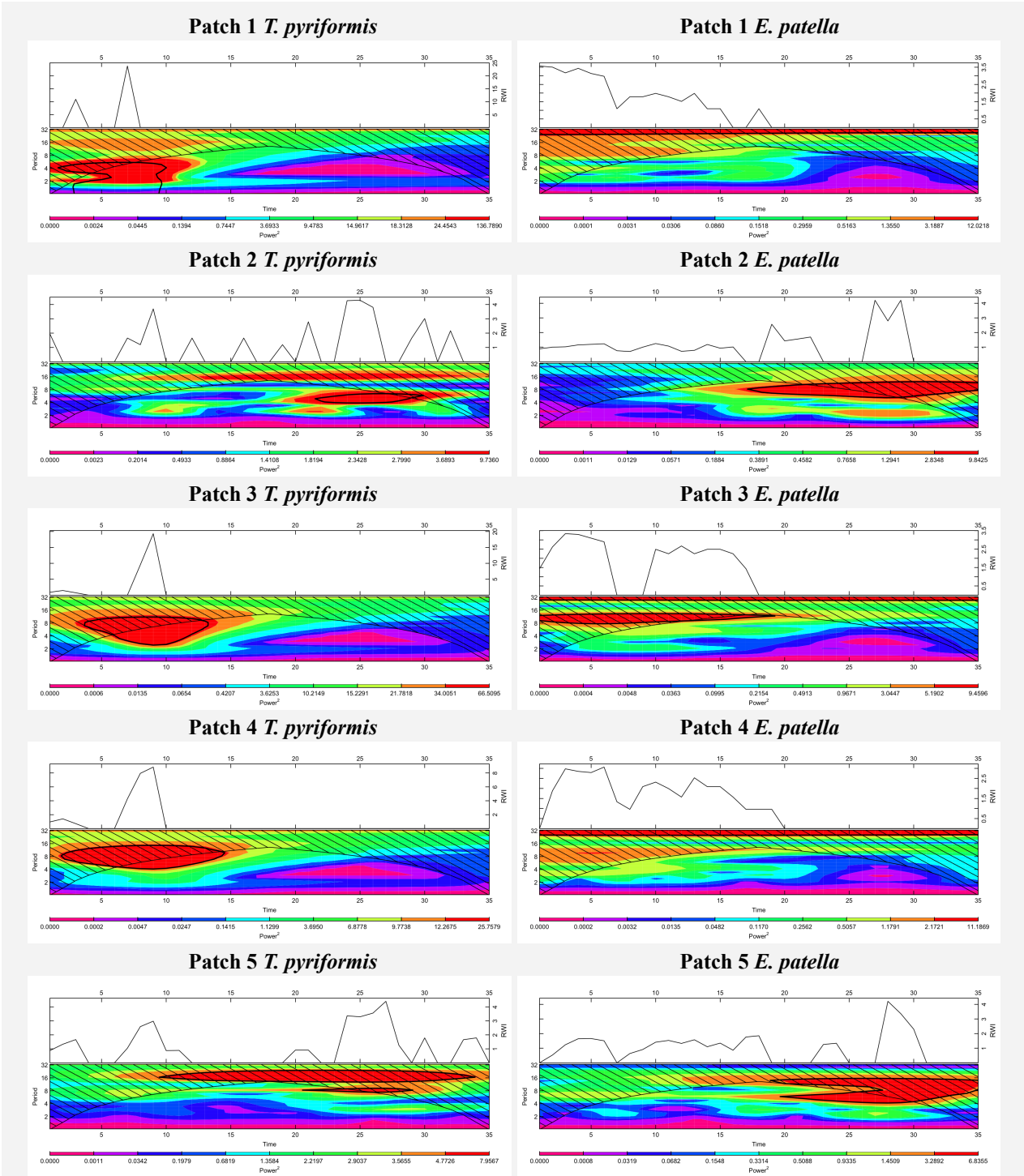


Figure 3.14: High enrichment 28-Day temperature cycle wavelet power spectra for patches of *T. pyriformis* and *E. patella*. Time represents the sample number taken (1 through 35) and actual cycle period is $2 \times$ period on y-axis. Significant power spectra outlined with black contour.

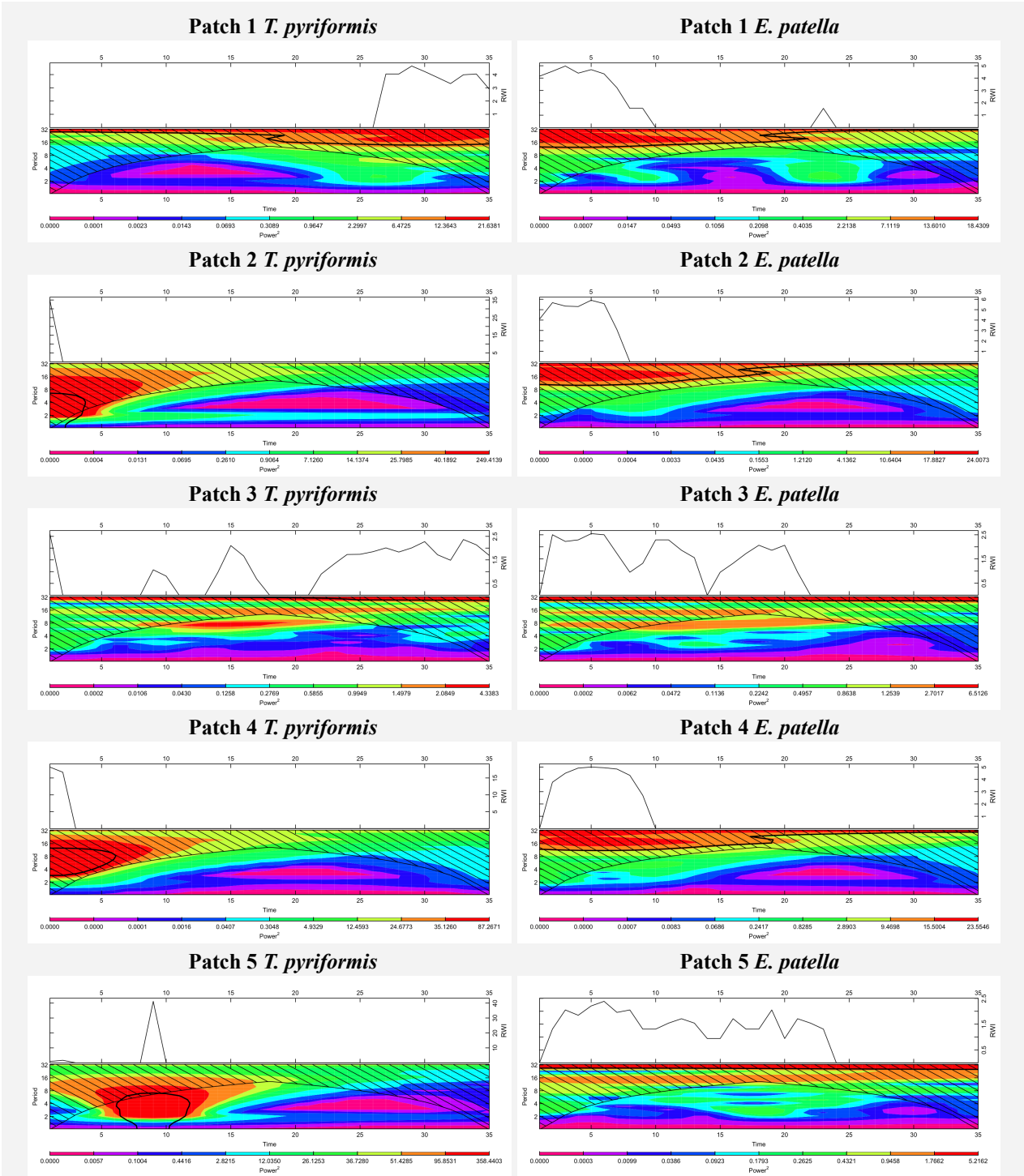


Figure 3.15: Low enrichment 32-Day temperature cycle wavelet power spectra for patches of *T. pyriformis* and *E. patella*. Time represents the sample number taken (1 through 35) and actual cycle period is $2 \times$ period on y-axis. Significant power spectra outlined with black contour.

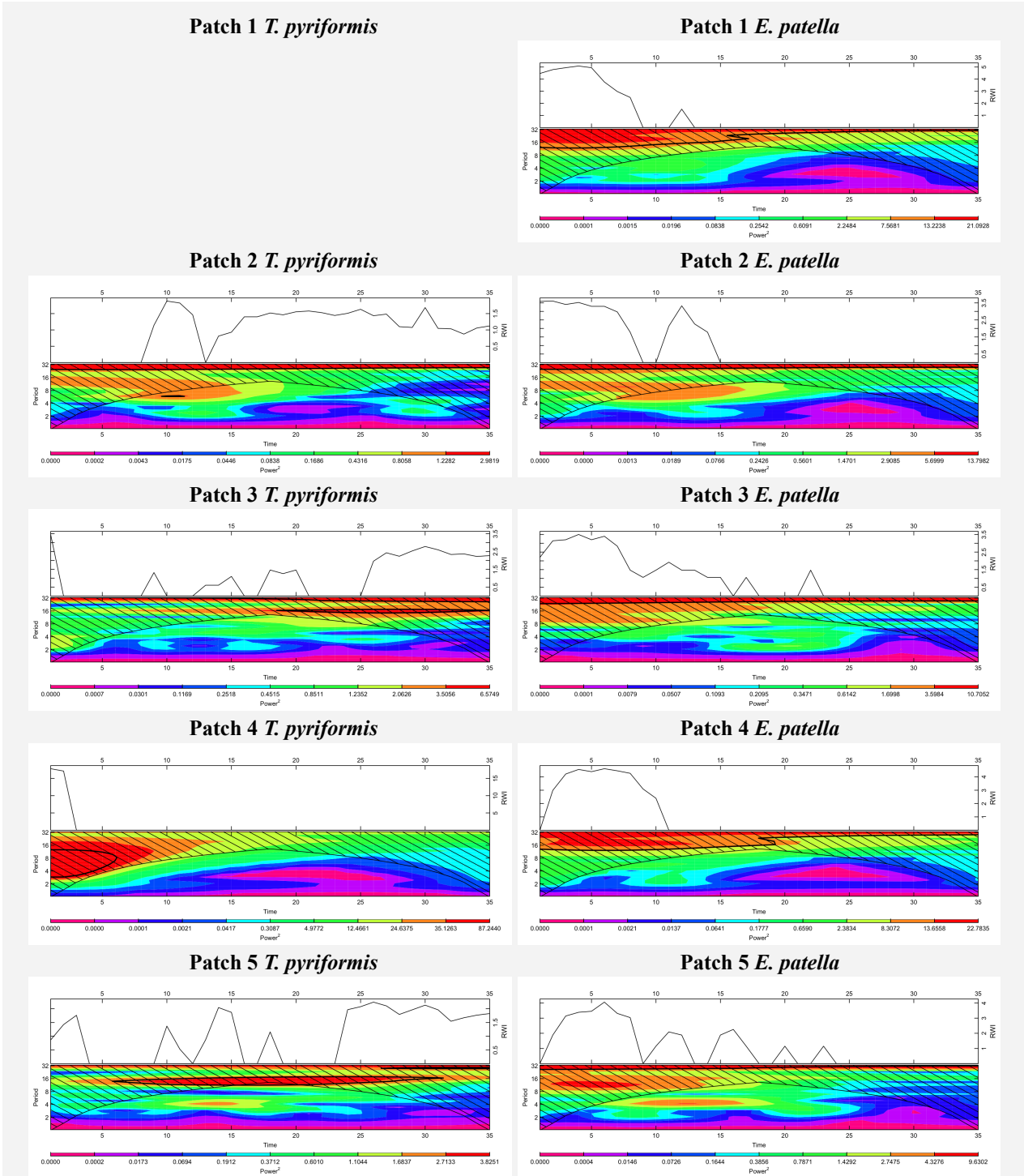


Figure 3.16: High enrichment 32-Day temperature cycle wavelet power spectra for patches of *T. pyriformis* and *E. patella*. Patch 1 *T. pyriformis* abundance was zero for the duration of the experiment and a power spectrum could not be produced. Time represents the sample number taken (1 through 35) and actual cycle period is 2×period on y-axis.

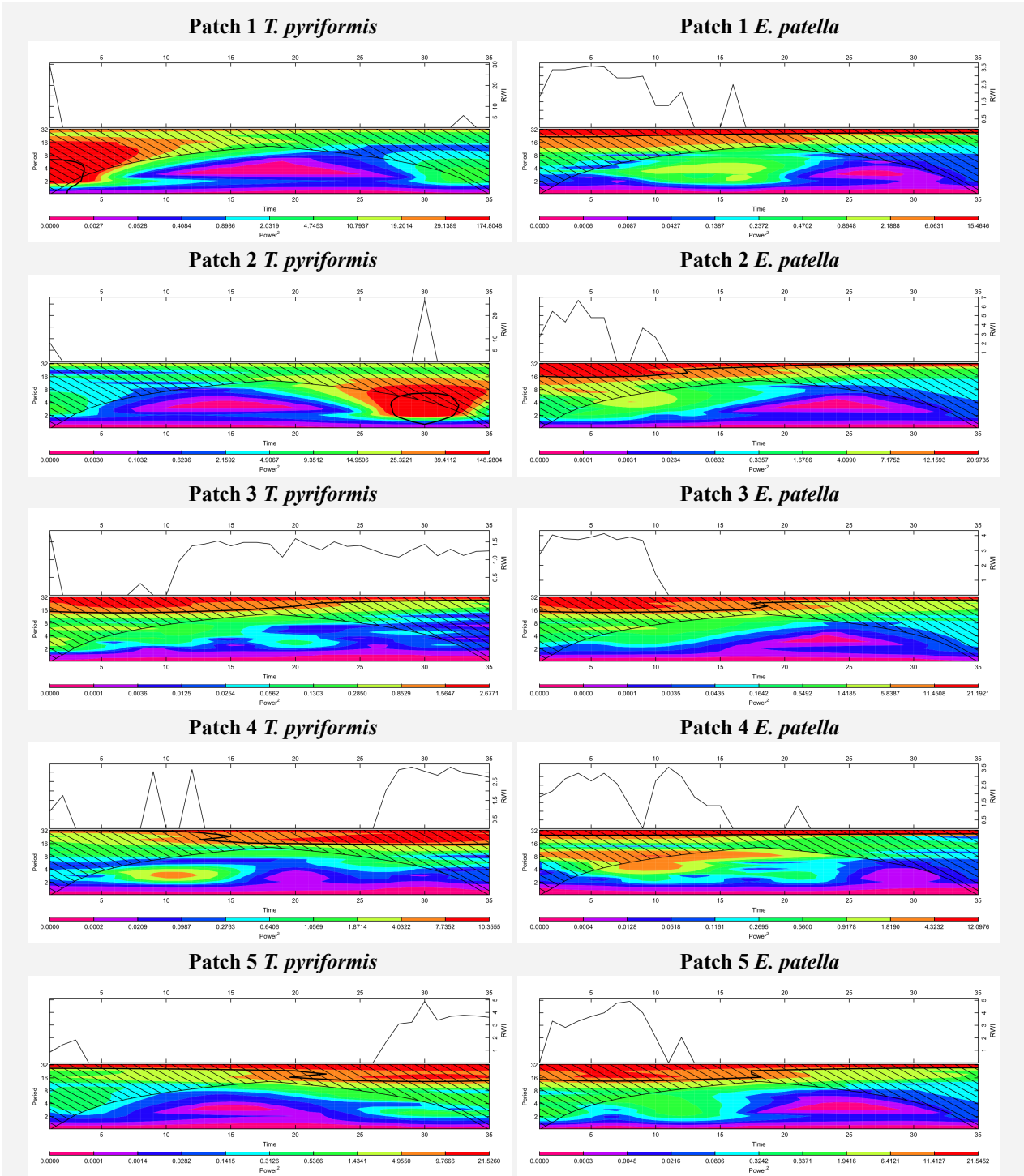


Figure 3.17: Low enrichment 36-Day temperature cycle wavelet power spectra for patches of *T. pyriformis* and *E. patella*. Time represents the sample number taken (1 through 35) and actual cycle period is $2 \times$ period on y-axis. Significant power spectra outlined with black contour.

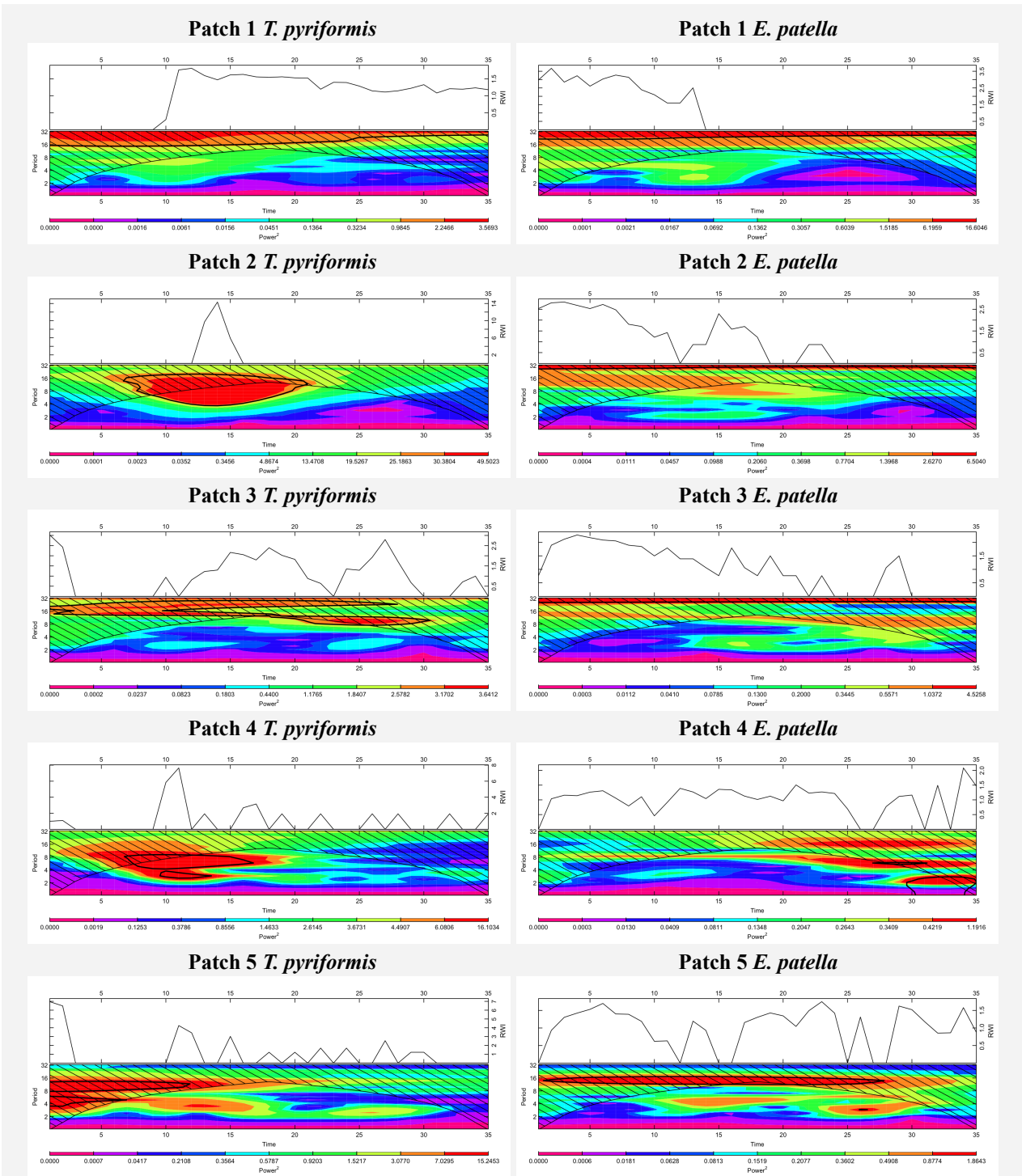


Figure 3.18: High enrichment 36-Day temperature cycle wavelet power spectra for patches of *T. pyriformis* and *E. patella*. Time represents the sample number taken (1 through 35) and actual cycle period is 2×period on y-axis. Significant power spectra outlined with black contour.

Time Series Cross Correlation and Permutation

Starting with the visual analysis of cross correlation values between jars, it was expected that jar patches spaced closer in time would be more positively correlated than jar patches spaced further in time. There should also be higher positive correlation between jars within the same temperature cycle treatment. Additionally, it was expected that jars in the 28-day temperature cycle treatment will be more positively correlated, and this correlation will decrease at both longer and shorter temperature cycle period lengths. Therefore, in the correlogram matrices produced, it is expected that there will be high correlation between jar patch numbers, along the diagonal for within-treatment temperature cycle correlation, as well as a high correlation hot-spot centered around the 28-day temperature cycle treatment.

When observing *T. pyriformis* cross correlation values (Figure 3.19), there was no strong effect for either of these predictions that was immediately apparent. There were a large number of non-significant cross correlations, and the majority of the significant cross correlations were positive. This was likely due to the fact that many jars followed the same pattern where *T. pyriformis* declined to low density and remained at low density for the majority of the time series, only seldomly returning to high density and oftentimes returning at random. There was no strong correlation pattern observed within-treatment for the temperature cycles, and only some instances of higher positive correlation between jar patches spaced closer in time compared to patches jar patches spaced further in time. There did appear to be higher positive correlation concentrated central to the correlogram, which indicates higher correlation amongst jars closer to the 28-day temperature cycle treatment. Jars in the longest and shortest temperature cycle period treatments were less positively correlated than jars in the mid-range of temperature cycle period treatments, which aligns with what was expected. There were also some instances of significant

negative correlation, and most of the instances of this were associated with jars where *E. patella* went extinct and *T. pyriformis* grew to carrying capacity and remained at high density for a large portion of the time series. In these instances, higher negative correlation values can be associated with high enrichment jars that provide more resources for *T. pyriformis* to grow to a higher carrying capacity compared to a lower carrying capacity at low enrichment.

When observing *E. patella* cross correlation values (Figure 3.20), there were much fewer non-significant cross correlation values, and all correlation values were positive. Two jars in particular, the second patch of low enrichment/20-day temperature cycle treatments and the first patch of low enrichment/28-day temperature cycle treatments, were mostly non-significant when compared to other jars. These two jars did not fall to low density or go extinct by the end of the time series and their dynamics were fluctuating in a particularly random and non-cyclic manner. Overall, *E. patella* was highly correlated across all patches, temperature cycles, and enrichment levels and there are no observable patterns that can be distinguished. Since the majority of *E. patella* across all treatments followed the same pattern of initial growth followed by slow decline to low density or extinction, the majority of the jars were highly correlated. The small degree of patterns in population dynamics that was observed in *T. pyriformis* was not matched as expected by *E. patella*.

Looking next at the results from the permutation tests run on the cross correlation values of the treatments (Table 3.4), the results of this analysis were a bit confounding. The permutation tests were run to determine if the cross correlation values for jars in the enrichment treatment, the temperature cycle treatment, or a combination of both treatments were significantly different than if they were randomly permuted across the given treatments. For *T. pyriformis*, only crosses between the enrichment level treatments had a significant ordering of cross correlation values.

This indicated that cross correlation values for low enrichment are significantly different from cross correlation values at high enrichment. Looking back to Figure 3.19, it appeared that *T. pyriformis* cross correlations between temperature cycle treatments indicated higher correlation when crossed with temperature cycles close to the natural predator-prey cycle of 28-days (Fox et al. 2011, Hopson & Fox 2018, Laan & Fox 2019). However, based on the results from the permutation test for temperature cycle crosses, this pattern was not considered significant.

The truly puzzling results appear for *E. patella* in Table 3.4 where permutation tests for crosses between temperature cycles, crosses between enrichment levels, and crosses between both temperature cycles and enrichment levels all provided significant results. Based on the large extent of positive correlation across all crosses in Figure 3.20, it was expected that all permutation tests would have the opposite outcome of no significance. It is possible that the couple of jars mentioned above (second patch low enrichment/20-day temperature cycle and first patch low enrichment/28-day temperature cycle) that did not follow the same overall dynamics as all other jars could potentially be confounding the overall results of these permutation tests.

Boxplots of the cross correlation values (Figures 3.21 and 3.22) with respect to treatment crosses were created to assist with understanding the results of the permutation tests conducted (Table 3.4). For *T. pyriformis* (Figure 3.21), all distributions of cross correlation values for all treatment crosses are widely distributed and overlap to a large extent. Crosses between temperature cycles all had cross correlation value medians above zero, and all cross correlation value distributions scaled across zero. The cross correlation distributions for *T. pyriformis* were overall symmetrical and had a large extent of overlap with one another. There were only two temperature cycle crosses that had significant outliers, including the 16-day temperature cycle crossed with the 32-day temperature cycle, and the 16-day temperature cycle crossed with the

36-day temperature cycle which also had the most narrow distribution. The large extent of overlap between cross correlation value distributions matched with the non-significant permutation test result (Table 3.4).

T. pyriformis crosses between enrichment levels all had cross correlation value medians above zero, and all cross correlation value distributions scaled across zero (Figure 3.21). It appeared that cross correlation value medians scaled negatively with increasing enrichment, which aligns with the significant permutation test results (Table 3.4). In this case, it appears that jars at low enrichment are significantly more positively correlated than jars at high enrichment. *T. pyriformis* had more jars that fell to extinction or grew to carrying capacity at high enrichment, which would create fewer positively correlated dynamics as opposed to *T. pyriformis* at low enrichment which had more stable lower density dynamics overall.

Crosses between enrichment levels and temperature cycles for *T. pyriformis* all had cross correlation value medians above zero, and cross correlation value distributions scale across zero except for the 16-day temperature cycle/high enrichment treatments crossed with the 16-day temperature cycle/high enrichment treatments, and 36-day temperature cycle/low enrichment treatments crossed with themselves that have distributions scaling above zero (Figure 3.21). Both of these treatment crosses also notably had the smallest distribution ranges. The cross correlation distributions for *T. pyriformis* were overall symmetrical and had a large extent of overlap with one another. The large extent of overlap between cross correlation value distributions matches with the non-significant permutation test result (Table 3.4). There were ten temperature cycle and enrichment level crosses that had significant outliers, the majority of which included the 36-day temperature cycle/high enrichment treatment cross. This treatment cross had jars that had

specific instances of random fluctuations in *T. pyriformis* at higher densities for the full length of the time series compared to other temperature cycle treatments.

For *E. patella* (Figure 3.22), crosses between temperature cycles all had cross correlation value medians above zero, and all cross correlation value distributions scaled above zero. There were many more outliers compared to *T. pyriformis* crosses, and the majority of the outliers were found in crosses with the 20-day temperature cycle treatment. It appears that shorter period temperature cycle treatments had overall wider cross correlation value distributions than longer period temperature cycle treatments.

E. patella crosses between enrichment levels all had cross correlation value medians above zero, and all cross correlation value distributions scaled above zero except for the low enrichment treatment crossed with itself which scaled just across zero (Figure 3.22). Interestingly, the pattern in enrichment level cross correlation values for *E. patella* appears to be the opposite of what was found in *T. pyriformis*, where jars at high enrichment are significantly more positively correlated than jars at low enrichment. *E. patella* had more jars that fell to extinction at low enrichment, which would create fewer positively correlated dynamics as opposed to *E. patella* at high enrichment which had more fluctuating dynamics overall.

Crosses between enrichment level and temperature cycles for *E. patella* all had cross correlation value medians above zero (Figure 3.22). Cross correlation value distributions all scale above zero, except for a few. The 16-day temperature cycle/low enrichment treatment crossed with both the 20-day temperature cycle/low enrichment and the 28-day temperature cycle/high enrichment treatments, as well as the 20-day temperature cycle/low enrichment treatment crossed with both the 28-day temperature cycle/low enrichment and the 36-day temperature cycle/high enrichment treatments, and the 16-day temperature cycle/low enrichment crossed with the

28-day temperature cycle/high enrichment treatments which all scaled just across zero. Many distributions have outliers, but most notably the majority of outliers were found in distributions of crosses with the 20-day temperature cycle treatment. It appears that treatments with longer temperature cycle periods and treatments with higher enrichment have narrower cross correlation value distributions. There also appears to be overall lower correlation values for 16-day temperature cycle/low enrichment crosses. These differences in cross correlation distributions could account for the significant results from the permutation tests conducted (Table 3.4). In addition, since the range of densities reached by *E. patella* are much lower than the large range of densities reached by *T. pyriformis*, the observed significant results from the permutation tests could be due to this narrowed difference in distribution range.

In all, with the absence of cycles, it becomes extremely difficult to discern whether the significant cross correlations found are indicative of spatial synchrony. The results from the cross correlation analysis and permutation tests in this case are somewhat unreliable, and it cannot be said with certainty if there were true instances of spatial synchrony occurring between any of the jars. The results going forward will analyze whether or not the specific temperature cycle and enrichment treatments had any particular effects on the dynamics of *T. pyriformis* and *E. patella* in absence of looking for spatial synchrony.

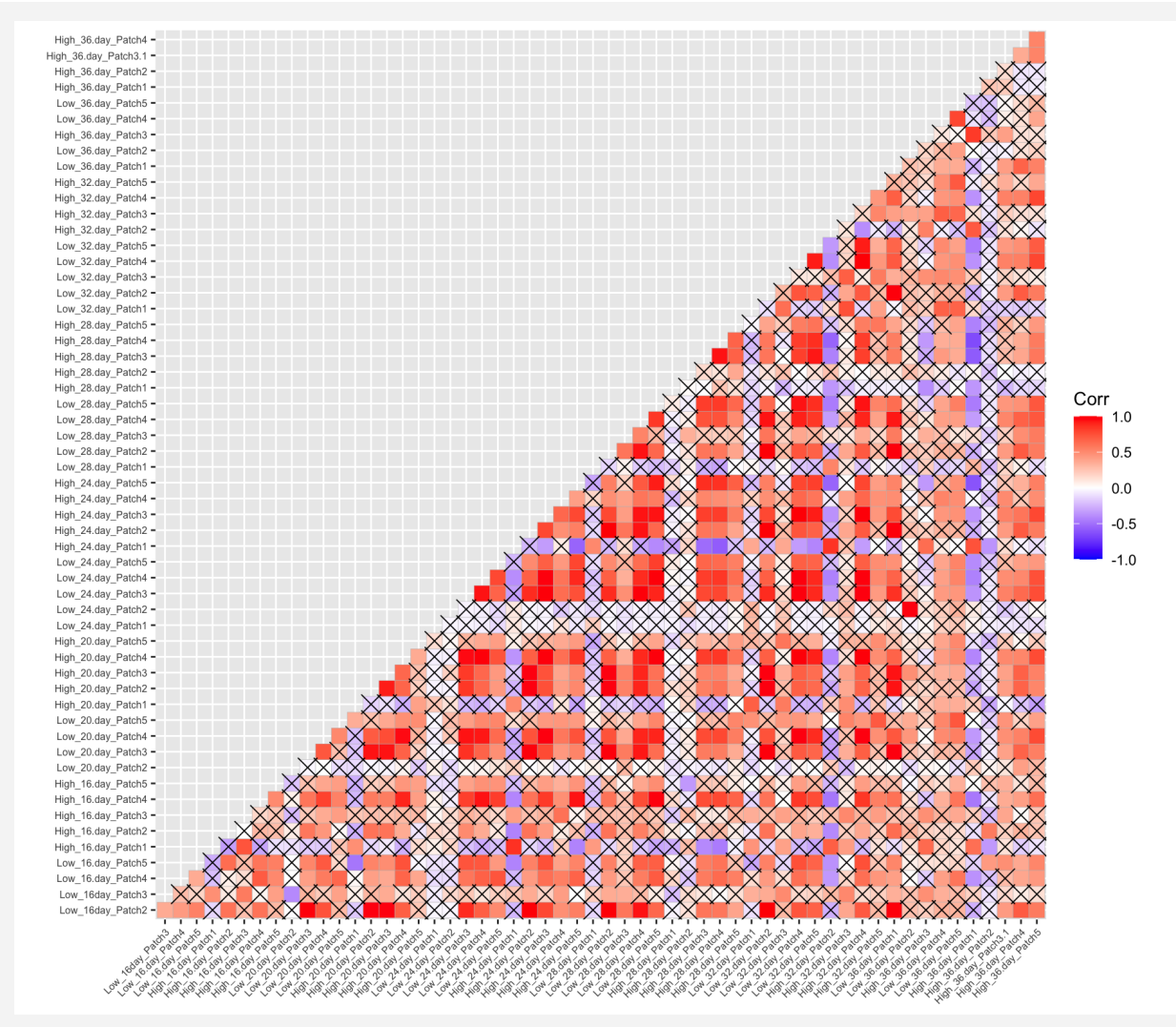


Figure 3.19: Correlogram for cross correlation values of *T. pyriformis* density time series by enrichment (low/high), temperature cycle (16, 20, 24, 28, 32, and 36 day), and patch replicate. Non-significant cross correlation values are marked with X.

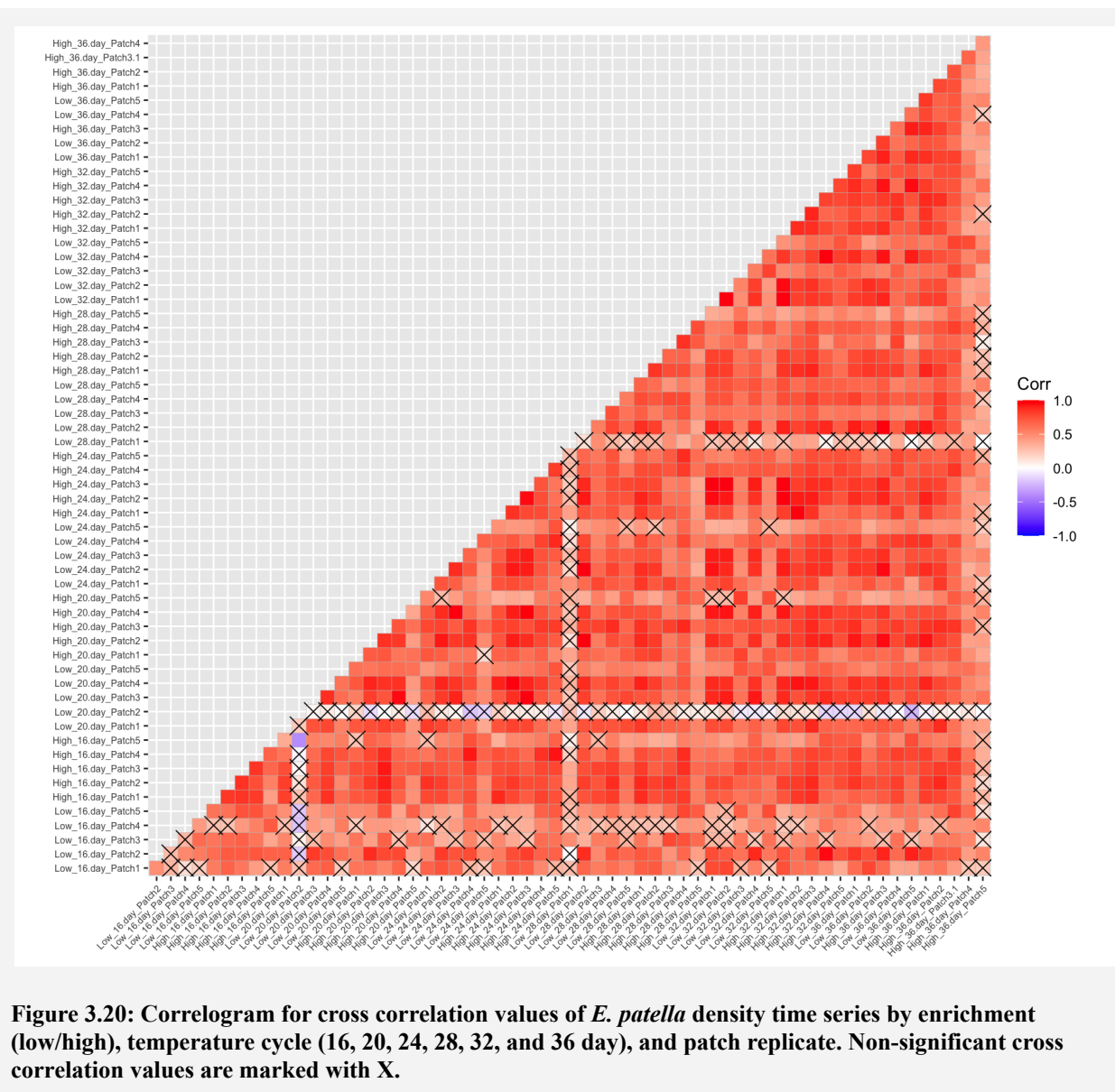
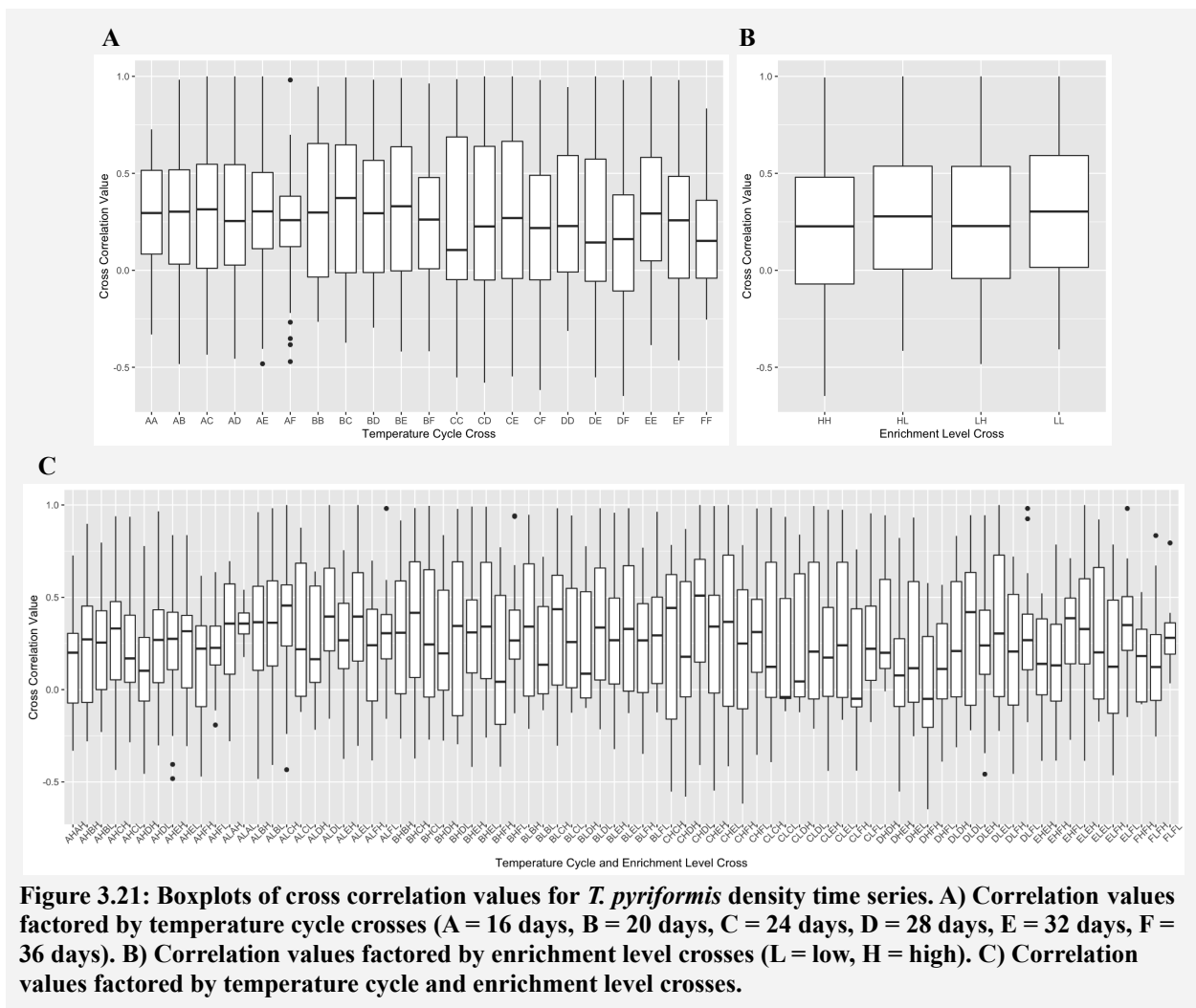


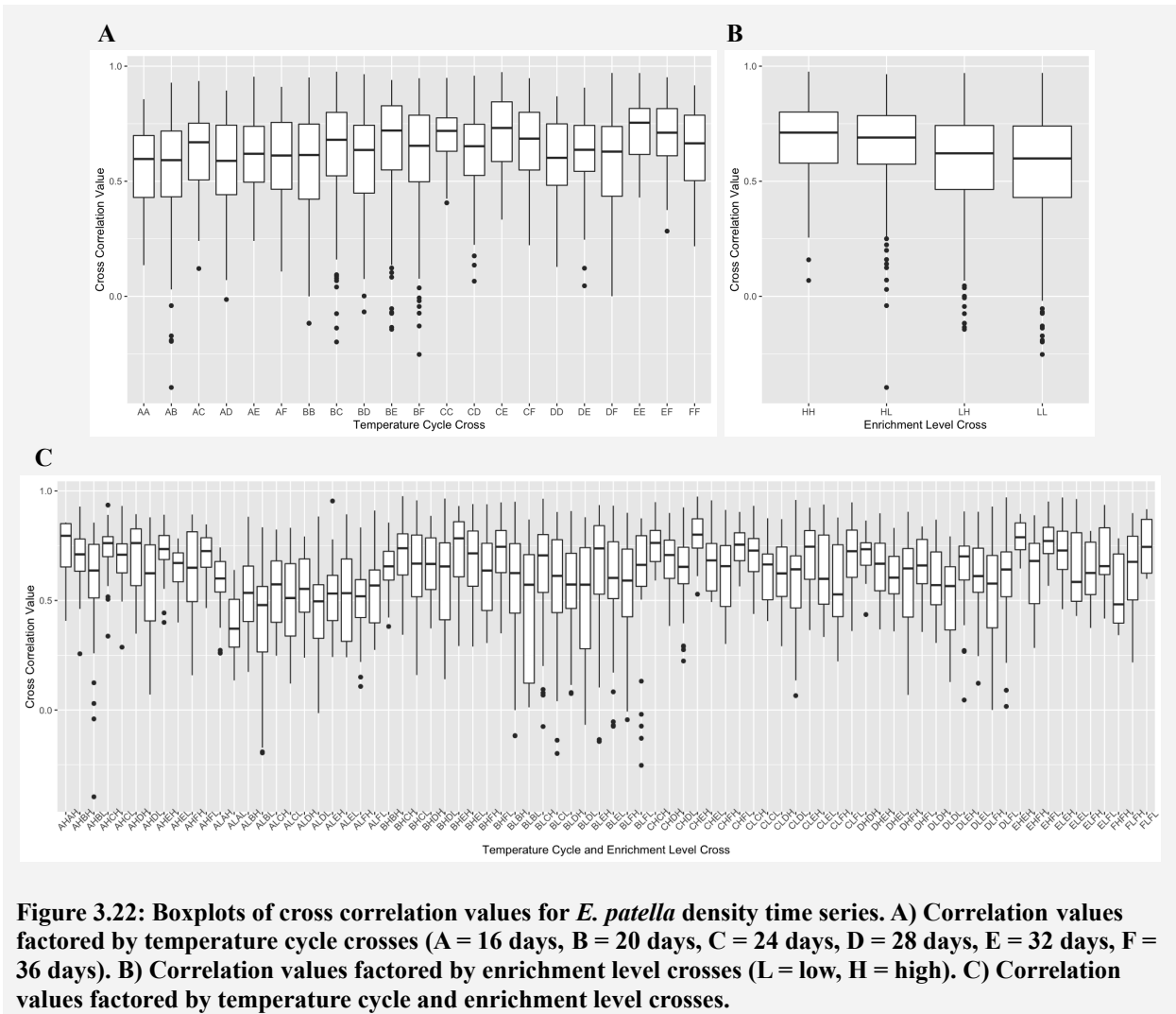
Figure 3.20: Correlogram for cross correlation values of *E. patella* density time series by enrichment (low/high), temperature cycle (16, 20, 24, 28, 32, and 36 day), and patch replicate. Non-significant cross correlation values are marked with X.

Table 3.4: Approximative K-sample Fisher-Pitman permutation tests of cross correlation values.

Species	Crosses	Time Series Correlation Permutation Test	
		χ^2	p-value
<i>Tetrahymena pyriformis</i>	Temperature Cycle	24.529	0.2188
	Enrichment Level	25.003	2e-05 *
	Temperature Cycle & Enrichment Level	85.371	0.2374
<i>Euploites patella</i>	Temperature Cycle	88.085	< 1e-05 *
	Enrichment Level	89.226	< 1e-05 *
	Temperature Cycle & Enrichment Level	273.64	< 1e-05 *

NOTE: * significant p-value ($\alpha < 0.05$)



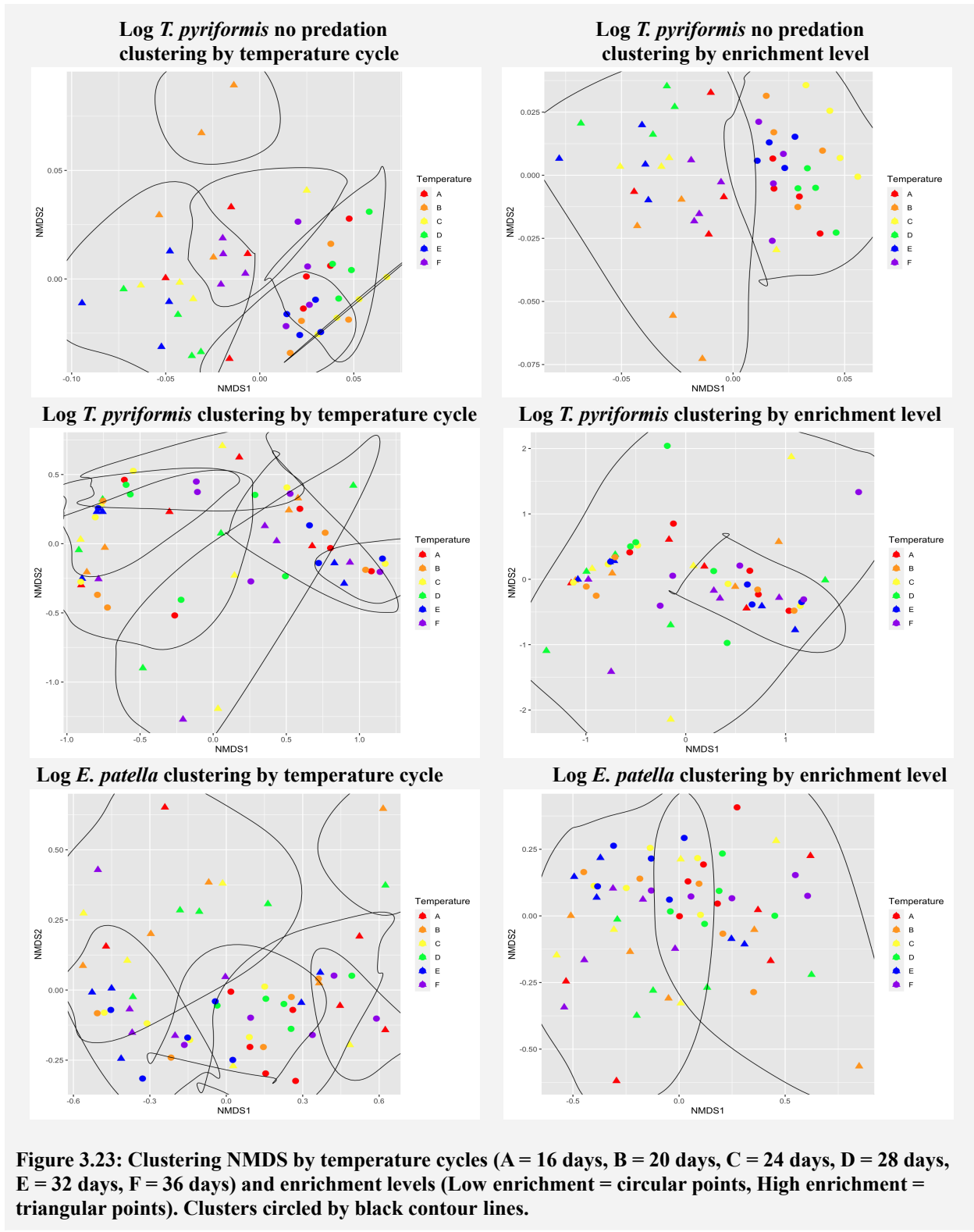


Clustering Analysis

To follow up with additional analysis to better determine treatment level effects, k-means clustering analysis was used to assess how well jar patches fit within their respective treatments. The control jars with absent *E. patella* were also included for this analysis to interpret treatment effects both with and without predation.

First looking at clustering based on temperature cycles (k means set at 6 to replicate the 6 temperature cycle treatments), all assigned treatment levels were randomly scattered between the six assigned clusters, and the clusters overlapped a fair amount (Figure 3.23). This was true for *T. pyriformis* under no predation, *T. pyriformis* under predation, and for *E. patella*. Population dynamics could not be accurately clustered based on temperature cycles, and therefore the dynamics that were seen in *E. patella* and in *T. pyriformis* with and without predation are not a direct result of the specific temperature cycles that they were subjected to.

Next, looking at clustering based on enrichment levels (k means set at 2 to replicate the low and high enrichment level treatments), the results were essentially the same for jars where predation was present, but predation-free *T. pyriformis* was perfectly clustered between both enrichment levels (Figure 3.23). All other assigned treatment levels were randomly scattered between the two assigned clusters, and clusters appeared to overlap (Figure 3.23). Population dynamics in jars where *E. patella* is present cannot be accurately clustered based on enrichment level, and therefore the dynamics that were seen in *E. patella* and in *T. pyriformis* are not a direct result of the specific temperature cycles that they were subjected to. The high correlation amongst jars, lack of cycling dynamics, and high number of extinction all are potentially masking any treatment effects, inhibiting the clustering of jars based on the temperature cycle or enrichment level treatments.



PERMANOVA

For the last stage of my analysis to determine treatment level effects, I wanted to see if the jar patches could be statistically forced into their respective treatments based on the time series dynamics of the individual microcosm jars. This was done using PERMANOVA, where protist density is permuted across treatment (either enrichment level, temperature cycle, or both) and the day within the time series that it was sampled. First looking at *T. pyriformis* control with *E. patella* absent (Table 3.5), the results indicate that protist densities grouped by temperature cycle treatments and sampling days, by enrichment level treatments and sampling days, as well as both treatments and sampling days are all significantly different than if they were randomly permuted across treatments and sampling days. Post-hoc multilevel pairwise comparisons were conducted on the temperature cycle treatment and both the temperature cycle/enrichment level treatments. This post-hoc pairwise comparison on the enrichment level treatment was excluded since there were only two enrichment levels to compare (low and high enrichment) and therefore there is only one possible pairwise comparison to be made. It can be concluded that *T. pyriformis* densities differ significantly between the low enrichment and high enrichment treatments, which is as was expected since *T. pyriformis* at high enrichment have more available resources and populations can grow to significantly higher densities than at low enrichment where the carrying capacity of the population is more limited.

Out of 15 post-hoc multilevel pairwise comparisons, there was only one significant comparison for the temperature cycle treatment and sampling days (Table 3.6). The densities of *T. pyriformis* in the 24-day temperature cycle treatment were significantly different than densities in the 36-day temperature cycle treatment. When looking at both temperature cycle and enrichment level treatments across sampling days (Table 3.7), 50 out of the 66 possible

multilevel pairwise comparisons were significant. 40 out of the 50 significant comparisons were across high and low enrichment levels. The remaining significant within-enrichment comparisons were mostly within high enrichment, with only one significant comparison being within low enrichment. The comparisons between temperature cycles were fairly symmetrical across all temperature cycles being compared. There were only 5 significant within-temperature cycle comparisons, which included all temperature cycle period lengths except for the 24-day temperature cycle. Based on these results, it appears that enrichment has an overall more impactful effect on the density of *T. pyriformis* compared to temperature cycle, which has no overarching significant effect on its own.

Next looking at *T. pyriformis* under predation of *E. patella* (Table 3.8), the results indicate that protist densities grouped by temperature cycle treatments and sampling days, by enrichment level treatments and sampling days, as well as both treatments and sampling days are all not significantly different than if they were randomly permuted across treatments and sampling days. Therefore, there is no significant difference between enrichment level treatments as well as temperature cycle treatments. Post-hoc pairwise comparisons were not conducted for any treatment levels in this case. Interestingly, these results entirely contradict the results for *T. pyriformis* with predation absent. This suggests that predation has a strong effect on *T. pyriformis* density, and impacts how enrichment and temperature cycles affect *T. pyriformis* density. It could also be the case that we see no significant treatment effects on *T. pyriformis* when *E. patella* is present since predation depletes *T. pyriformis* to very low densities that often fall below the sampling threshold. Any treatment level effects become difficult to detect when *T. pyriformis* densities remain too low for sampling for large portions of the time series.

Finally looking at *E. patella* (Table 3.9), the results indicate that densities grouped by enrichment level treatments and sampling days, and both enrichment level and temperature cycle treatments and sampling days were significantly different than if they were randomly permuted across treatments and sampling days. Densities grouped by temperature cycle and sampling days were not significantly different than if they were randomly permuted across temperature cycles and sampling days. The post-hoc pairwise comparison for the enrichment level treatment was excluded once again since there were only two enrichment levels to compare (low and high enrichment), but *E. patella* densities do differ significantly between the low enrichment and high enrichment treatments.

Only 12 out of 66 possible post-hoc multilevel pairwise comparisons for temperature cycle and enrichment level treatment crosses for *E. patella* were significant (Table 3.10). Nine out of the 12 comparisons were across high and low enrichment levels, with the remaining three comparisons being within high enrichment. This may be due to the fact that there were more extinctions of *E. patella* at high enrichment than at low enrichment. Half of the significant pairwise comparisons included the 28-day temperature cycle treatment, and the 36-day temperature cycle treatment had the second highest number of significant pairwise comparisons. Both the 28-day and 36-day temperature cycle treatments also had the only two significant within-temperature cycle comparisons. Both the 28-day and 36-day temperature cycle treatments had the most persistent fluctuations of *E. patella* that maintained densities to the end of the time series, rather than slowly declining over time. As with *T. pyriformis*, it appears that enrichment has a stronger effect on the density of *T. pyriformis* compared to temperature cycle, which has no overarching significant effect on its own.

Table 3.5: PERMANOVA results for *T. pyriformis* under no predation.

A) <i>T. pyriformis</i> log density grouped by temperature cycle and sample days						
	DF	Sums of Squares	Mean Squares	F Model	R ²	p-value
Sample days by temperature cycle	5	19.818	3.9636	1.647	0.16393	0.025*
Residuals	42	101.072	24.065		0.83607	
Total	47	120.890			1	

B) <i>T. pyriformis</i> log density grouped by enrichment level and sample days						
	DF	Sums of Squares	Mean Squares	F Model	R ²	p-value
Sample days by temperature cycle	1	34.021	34.021	18.015	0.28142	0.001*
Residuals	46	86.869	1.888		0.71858	
Total	47	120.890			1	

C) <i>T. pyriformis</i> log density grouped by temperature cycle/enrichment level and sample days						
	DF	Sums of Squares	Mean Squares	F Model	R ²	p-value
Sample days by temperature cycle	11	76.236	6.9305	5.5874	0.63062	0.001*
Residuals	36	44.654	1.2404		0.36938	
Total	47	120.890			1	

*Significant result, post-hoc test required

Table 3.6 Post-hoc pairwise comparisons for *T. pyriformis* under no predation by temperature cycle and sample days. Only significant results included.

Pairwise Comparison	DF	Sums of Squares	F Model	R2	p-value
24-Day vs. 36-Day	1	7.649	2.910	0.172	0.050

NOTE: Total 15 pairwise comparisons.

Table 3.7 Post-hoc pairwise comparisons for *T. pyriformis* under no predation by enrichment level, temperature cycle and sample days. Only significant results.

Pairwise Comparison	DF	Sums of Squares	F Model	R2	p-value
16-Day/High vs. 16-Day/Low	1	4.864	3.977	0.399	0.020
16-Day/High vs. 20-Day/Low	1	9.131	6.934	0.536	0.037
16-Day/High vs. 24-Day/High	1	11.556	9.798	0.620	0.026
16-Day/High vs. 24-Day/Low	1	5.759	4.212	0.412	0.033
16-Day/High vs. 28-Day/Low	1	9.573	8.068	0.574	0.028
16-Day/High vs. 32-Day/Low	1	10.672	10.873	0.644	0.030
16-Day/High vs. 36-Day/High	1	2.690	2.915	0.327	0.029
16-Day/High vs. 36-Day/Low	1	4.544	4.122	0.407	0.028
16-Day/Low vs. 20-Day/High	1	5.353	3.568	0.373	0.041
16-Day/Low vs. 24-Day/High	1	16.522	11.418	0.656	0.021
16-Day/Low vs. 28-Day/High	1	6.803	5.952	0.498	0.030
16-Day/Low vs. 28-Day/Low	1	3.525	2.423	0.288	0.036
16-Day/Low vs. 32-Day/High	1	3.991	3.629	0.377	0.025
16-Day/Low vs. 36-Day/High	1	3.970	3.336	0.357	0.029
20-Day/High vs. 20-Day/Low	1	10.615	6.659	0.526	0.033
20-Day/High vs. 24-Day/High	1	8.772	6.022	0.501	0.031
20-Day/High vs. 24-Day/Low	1	5.289	3.217	0.349	0.055
20-Day/High vs. 28-Day/Low	1	7.460	5.097	0.459	0.029
20-Day/High vs. 32-Day/Low	1	9.296	7.386	0.552	0.025
20-Day/High vs. 36-Day/High	1	3.519	2.933	0.328	0.029
20-Day/High vs. 36-Day/Low	1	5.223	3.786	0.387	0.031
20-Day/Low vs. 24-Day/High	1	22.170	14.390	0.706	0.032
20-Day/Low vs. 28-Day/High	1	10.672	8.628	0.590	0.029
20-Day/Low vs. 28-Day/Low	1	7.271	4.698	0.439	0.028
20-Day/Low vs. 32-Day/High	1	11.087	9.289	0.608	0.030
20-Day/Low vs. 32-Day/Low	1	5.867	4.370	0.421	0.031

Pairwise Comparison	DF	Sums of Squares	F Model	R2	p-value
20-Day/Low vs. 36-Day/High	1	8.744	6.811	0.532	0.033
20-Day/Low vs. 36-Day/Low	1	4.368	2.984	0.332	0.018
24-Day/High vs. 28-Day/High	1	9.565	8.699	0.592	0.032
24-Day/High vs. 28-Day/Low	1	17.391	12.331	0.673	0.030
24-Day/High vs. 32-Day/High	1	10.949	10.366	0.633	0.035
24-Day/High vs. 32-Day/Low	1	19.758	16.391	0.732	0.032
24-Day/High vs. 36-Day/High	1	14.284	12.459	0.675	0.028
24-Day/High vs. 36-Day/Low	1	15.428	11.632	0.660	0.023
24-Day/Low vs. 28-Day/High	1	6.950	5.399	0.474	0.027
24-Day/Low vs. 32-Day/High	1	4.994	4.015	0.401	0.031
28-Day/High vs. 28-Day/Low	1	11.745	10.614	0.639	0.029
28-Day/High vs. 32-Day/High	1	2.471	3.284	0.354	0.024
28-Day/High vs. 32-Day/Low	1	13.437	14.904	0.713	0.027
28-Day/High vs. 36-Day/High	1	3.333	3.955	0.397	0.029
28-Day/High vs. 36-Day/Low	1	6.323	6.184	0.508	0.036
28-Day/Low vs. 32-Day/High	1	7.232	6.802	0.531	0.029
28-Day/Low vs. 36-Day/High	1	7.662	6.642	0.525	0.033
28-Day/Low vs. 36-Day/Low	1	4.376	3.282	0.354	0.034
32-Day/High vs. 32-Day/Low	1	8.358	9.737	0.619	0.027
32-Day/High vs. 36-Day/High	1	2.872	3.593	0.375	0.029
32-Day/High vs. 36-Day/Low	1	4.231	4.320	0.419	0.030
32-Day/Low vs. 36-Day/High	1	9.864	10.400	0.634	0.023
32-Day/Low vs. 36-Day/Low	1	3.194	2.831	0.321	0.031
36-Day/High vs. 36-Day/Low	1	4.144	3.875	0.392	0.031

NOTE: Total 66 pairwise comparisons.

Table 3.8 PERMANOVA results for *T. pyriformis*.

D) <i>T. pyriformis</i> log density grouped by temperature cycle and sample days						
	DF	Sums of Squares	Mean Squares	F Model	R ²	p-value
Sample days by temperature cycle	5	202.49	40.497	1.1416	0.10065	0.308
Residuals	51	1809.19	35.474		0.89935	
Total	56	2011.68			1	

E) <i>T. pyriformis</i> log density grouped by enrichment level and sample days						
	DF	Sums of Squares	Mean Squares	F Model	R ²	p-value
Sample days by temperature cycle	1	78.64	78.641	2.2375	0.03909	0.073
Residuals	55	1933.04	35.146		0.96091	
Total	56	2011.68			1	

F) <i>T. pyriformis</i> log density grouped by temperature cycle/enrichment level and sample days						
	DF	Sums of Squares	Mean Squares	F Model	R ²	p-value
Sample days by temperature cycle	11	403.07	36.643	1.0251	0.20037	0.436
Residuals	45	1608.61	35.747		0.79963	
Total	56	2011.68			1	

*Significant result, post-hoc test required

Table 3.9: PERMANOVA results for *E. patella* under no predation.

A) <i>E. patella</i> log density grouped by temperature cycle and sample days						
	DF	Sums of Squares	Mean Squares	F Model	R ²	p-value
Sample days by temperature cycle	5	48.50	9.6994	1.3538	0.11139	0.079
Residuals	54	386.89	7.1647		0.88861	
Total	59	435.39			1	

B) <i>E. patella</i> log density grouped by enrichment level and sample days						
	DF	Sums of Squares	Mean Squares	F Model	R ²	p-value
Sample days by temperature cycle	1	26.50	26.5049	3.7597	0.06088	0.003*
Residuals	58	408.89	7.0497		0.93912	
Total	59	435.39			1	

C) <i>E. patella</i> log density grouped by temperature cycle/enrichment level and sample days						
	DF	Sums of Squares	Mean Squares	F Model	R ²	p-value
Sample days by temperature cycle	11	114.70	10.427	1.5607	0.26344	0.007*
Residuals	48	320.69	6.681		0.73656	
Total	59	435.39			1	

*Significant result - post-hoc test required

Table 3.10 Post-hoc pairwise comparisons for *E. patella* by enrichment level, temperature cycle and sample days, only significant results.

Pairwise Comparison	DF	Sums of Squares	F Model	R2	p-value
16-Day/High vs 20-Day/Low	1	19.612	3.249	0.289	0.016
16-Day/High vs 28-Day/Low	1	14.967	2.469	0.236	0.010
16-Day/High vs 36-Day/Low	1	16.291	3.328	0.294	0.018
20-Day/Low vs 28-Day/High	1	14.754	2.517	0.239	0.014
20-Day/Low vs 32-Day/High	1	13.005	2.325	0.225	0.006
24-Day/High vs 36-Day/High	1	16.534	2.385	0.230	0.038
28-Day/Low vs 28-Day/High	1	12.064	2.049	0.204	0.048
28-Day/Low vs 32-Day/High	1	11.901	2.118	0.209	0.034
28-Day/High vs 32-Day/High	1	15.300	2.952	0.270	0.009
28-Day/High vs 36-Day/Low	1	17.230	3.649	0.313	0.025
32-Day/High vs 36-Day/High	1	17.555	2.557	0.242	0.044
36-Day/Low vs 36-Day/High	1	21.912	3.422	0.230	0.007

NOTE: Total 66 pairwise comparisons.

3.4 Discussion

The overall outcome from this microcosm experiment yielded no significant cycling, and subsequently, no spatial synchrony between any of the jars. While there visually appeared to be some initial synchrony when first sampling, it did not persist and all jars lost this brief instance of potential synchrony when the jars were exposed to 27°C and *T. pyriformis* density first declined. After this initial decline in *T. pyriformis* in all jars, there was not enough of a sufficient recovery of predator-prey cycles that could allow for cyclic entrainment into synchrony by the imposed temperature cycles. Instead, many jars had either *T. pyriformis*, *E. patella*, or both that went extinct before the end of the experiment. However, there were overall more predator extinctions than prey extinctions.

In a previous study by Fussmann et al. (2014), severe consumer extinctions in warmed microcosms were explained by warming-induced population oscillator destabilization. It is very likely that this same warming-induced destabilization took place in the microcosm jars of this study. While warming temperatures are able to stabilize predator-prey dynamics, beyond a certain threshold level, warming can cause predator extinction due to starvation (Fussmann et al. 2014). It may be the case that the initial steep decline in *T. pyriformis* created harsh enough conditions for *E. patella* that they began to starve and eventually declined to extinction. The pilot experiment in Appendix C attempted to establish a safe temperature threshold for *E. patella* in this experiment. However, it may be the case that the pilot experiment should have been run with a wider temperature range to determine if temperatures cooler than 27°C would have still produced the desired cyclic predator-prey dynamics without creating so much thermal stress that drove so many jars to extinction.

Another major limitation to the experiment was the small temperature differential in the temperature cycles. The treatment-level analyses showed that the different temperature cycle periods had no significant effect on the population dynamics in the jars. Due to COVID-19, I was very limited with the parameters I could set with the incubators I built. If I had the ability to reduce temperatures below room temperature, there could have been much larger amplitudes created in the temperature cycles imposed on the jars. These larger amplitudes may have produced the necessary coupling strength for greater cycle entrainment, producing more apparent and persistent instances of spatial synchrony between the jars. Additionally, the ability to set colder temperatures would have allowed me to reduce the upper threshold of the temperature cycles to further limit the risk for warming-induced extinctions.

Another factor that was not initially considered in the study was temperature-dependent viscosity of the media. Beveridge et al. (2010) previously found that viscosity had a significant effect on the growth rates and carrying capacity of protist consumers, as well as the average density of the top predator. Higher viscosity at warmer temperatures were correlated with reduced swimming speeds, reduced feeding in consumers, and reduced prey encounter rates (Beveridge et al. 2010). This could have also been a factor in the warming-related extinctions that were observed.

There were many other unexpected patterns seen throughout the jars, especially in the control jars where *T. pyriformis* grew in absence of predation. The convergence of the high and low enrichment levels following a rise in *T. pyriformis* density at the first increase in temperature in Figure 3.3 was not expected. While it is normal for populations grown in microcosms to slowly decline with age, the high enrichment *T. pyriformis* unexpectedly declined to similar densities to the low enrichment *T. pyriformis* despite having more media resources available for

greater population growth. One potential reason for this convergence between enrichment levels could be due to the fact that one wheat seed was placed in both high and low enrichment jars. The wheat seed acts as a carbon and nutrients source for bacteria (Laan & Fox 2019) and it may be possible that a second wheat seed was required for high enrichment jars to promote higher densities in bacteria in the high enrichment treatment. However, this convergence between enrichment levels does not appear to have had a substantial effect since the clustering analysis and PERMANOVA were able to significantly distinguish between both enrichment treatments amongst the dynamics displayed in the jars. However this was not the case in jars where *E. patella* was introduced, and adding a second wheat seed to high enrichment jars might have helped with differentiating the high and low enrichment treatments when predation is present. Though, it is difficult to say with certainty whether or not adding a second wheat seed would be useful, and replication of this experiment with adjusted methods would be beneficial.

Despite the ambitious start to this experiment in the midst of a global pandemic, the results were unable to determine whether protist predator-prey cycles can be entrained by cyclic temperature cycles to produce spatial synchrony.

CHAPTER 4: Conclusions and Future Directions

4.1 Can cyclic environmental fluctuations synchronize population cycles?

The short answer to this question is theoretically, yes. However, the only conclusive results I was able to obtain were from model simulations, and I was not able to replicate the results from the model simulations in a natural protist predator-prey system. So this question is only half answered since I was only able to observe synchrony in a theoretical model, but not in a real-life system.

Based on the model from Chapter 2, we can say that spatial synchrony is in fact driven by high amplitude cyclic environmental fluctuations that closely match the period of the populations that are being synchronized. Synchrony does occur when population cycles become entrained to cyclic environmental fluctuations, and the populations are then entrained to one another and phase-lock into synchrony. Synchrony does not occur when environmental oscillations deviate from the natural predator-prey cycle of the population as the cycles become too mismatched to be adequately entrained. Also, high amplitude environmental cycles produce higher instances of spatial synchrony by increasing the strength of entrainment.

One of the predictions I sought to answer could not be answered by the model that was built, and the experiment did not yield any meaningful results to be able to answer this prediction either. It was predicted that synchrony will not occur when resource enrichment is low and produces low-amplitude population cycles that are too weak to be entrained.

The goal of this experiment was to determine whether population cycles and cyclic environmental fluctuations have a significant impact on the occurrence and persistence of spatial synchrony. Through the model, it was revealed that there does appear to exist a synchronization

threshold range where environmental oscillations have the ability to entrain two populations into phase-lock and produce spatial synchrony. This range is still not clearly defined, and it has yet to be determined how this synchronization range might change depending on the given parameters that populations might follow.

4.2 Future Directions

My hope is that this study will provide insight into where further knowledge of spatial synchrony is required. The COVID-19 global pandemic produced many hurdles that I attempted to overcome, and this study would benefit from further attention now that the quarantine measures are nearing an end. If this study were repeated, I suggest that improvements be made to the model to illustrate how cycling different parameters, including more than two patches, cycling multiple parameters, and using different cycle periods, amplitudes, and phases could impact the occurrence and persistence of synchrony between patches. I also suggest altering the model parameters to account for simulated low and high enrichment treatments. For the experiment, I suggest repeating the same methods, but using a greater temperature differential with cooler temperatures for the temperature cycle treatment. I suggest utilizing many more replicates with the help of a research assistant to produce more instances of predator-prey cycles and fewer instances of extinctions. I also suggest adding a second wheat seed to the high enrichment treatment to ensure that enrichment levels remain distinct from one another.

On a larger scale, there are areas of this study that can be used to steer other research in the future. Instead of limiting this analysis to microcosms, it would be beneficial to study this same topic in larger-scale organisms experiencing natural environmental cycles such as cyclic temperatures and precipitation. While it may be difficult to perform an experiment at a large

enough scale for most natural populations, there is lots of research being done on small mammals and birds that could prove to be useful systems to study. Additionally, past studies of synchrony could be reviewed in conjunction with historical weather data to search for any potential historical instances of cycle entrainment from cyclic weather patterns. Understanding the implications that environmental cycles have on natural populations can potentially inform how synchronous populations will behave when faced with the implications of large-scale changes in the environment such as climate change, which is important for the preservation of synchronous populations that could experience dangerous synchronous declines in abundance. I hope that this experiment will provide more significant information and insights that helps research move towards a better understanding of the unique phenomenon of spatial synchrony in population dynamics in relation to cyclic environmental fluctuations.

REFERENCES

- Allstadt, A. J., A. M. Liebhold, D. M. Johnson, R. E. Davis, and K. J. Haynes. 2015. Temporal variation in the synchrony of weather and its consequences for spatiotemporal population dynamics. *Ecology* **96**(11):2935-2946.
- Anderson, M. J. 2017. Permutational Multivariate Analysis of Variance (PERMANOVA). *Wile StatsRef: Statistics Reference Online*. <https://doi.org/10.1002/9781118445112.stat07841>
- Bache, S. M., and H. Wickham. 2020. magrittr: A Forward-Pipe Operator for R. R package version 2.0.1. <https://CRAN.R-project.org/package=magrittr>
- Becks, L., and H. Arndt. 2013. Different types of synchrony in chaotic and cyclic communities. *Nature* **4**:1359.
- Benton, T. G., M. Solan, J. M. J. Travis, S. M. Sait. 2007. Microcosm experiments can inform global ecological problems. *Trends in Ecology & Evolution* **22**(10):516-521.
- Beveridge, O. S., O. L. Petchey, and S. Humphries. 2010. Direct and indirect effects of temperature on the population dynamics and ecosystem functioning of aquatic microbial ecosystems. *Journal of Animal Ecology* **79**:1324-1331.
- Bjornstad, O. 2001. Cycles and synchrony: two historical ‘experiments’ and one experience. *Journal of Animal Ecology* **69**(5):869-873.
- Brommer, J. E., H. Pietiainen, K. Ahola, P. Karell, T. Karstiinen, and H. Kolunen. 2010. The return of the vole cycle in southern Finland refutes the generality of the loss of cycles through ‘climatic forcing’. *Global Change Biology* **16**(2):577-586.
- Bunn A., M. Korpela, F. Biondi, F. Campelo, P. Mérian, F. Qeadan, and C. Zang. 2020. dplR: Dendrochronology Program Library in R. R package version 1.7.1.

<https://CRAN.R-project.org/package=dplR>

- Buntgen, U., D. Frank, A. Liebhold, D. Johnson, M. Carrer, C. Urbinati, M. Grabner, K. Nicolussi, T. Levanic, and J. Esper. 2009. Three centuries of insect outbreaks across the European Alps. *New Phytologist* **182**(4):929-941.
- Buonaccorsi, J. P., J. S. Elkinton, S. R. Evans, and A. M. Liebhold. Measuring and testing for spatial synchrony. 2001. *Ecology* **82**(6):1668-1679.
- Curan L. M., and C. O. Webb. 2000. Experimental tests of the spatiotemporal scale of seed predation in mast-fruiting Dipterocarpaceae. *Ecological Monographs* **70**:129-148.
- DeRose, J. R., and J. N. Long. 2012. Factors Influencing the Spatial and Temporal Dynamics of Engelmann Spruce Mortality during a Spruce Beetle Outbreak on the Markagunt Plateau, Utah. *Forest Science* **58**(1):1-14.
- Duncan, A. B., A. Gonzalez, and O. Kaltz. 2015. Dispersal, environmental forcing, and parasites combine to affect metapopulation synchrony and stability. *Ecology* **96**(1):284-290.
- Earn, D. J. D., S. A. Levin, and P. R. Rohani. 2000. Coherence and Conservation. *Science* **290**(5495):1360-1364.
- Fedy, B. C., and K. E. Doherty. 2011. Population cycles are highly correlated over long time series and large spatial scales in two unrelated species: greater sage-grouse and cottontail rabbits. *Oecologia* **165**:915-924.
- Fox, J. W., D. A. Vasseur, S. Hausch, and J. Roberts. 2011. Phase locking, the Moran effect and distance decay of synchrony: experimental tests in a model system. *Ecology Letters* **14**:163-168.
- Fox, J. W., G. Legault, D. A. Vasseur, and J. A. Einarson. 2013. Nonlinear Effect of Dispersal Rate on Spatial Synchrony of Predator-Prey Cycles. *PLoS ONE* **8**(11):e79527.

Harrell F. E. Jr. 2020. Hmisc: Harrell Miscellaneous. R package version 4.4-2.

<https://CRAN.R-project.org/package=Hmisc>

Fussmann K. E., F. Schwarzmuller, U. Brose, A. Jousset, and B. C. Rall. 2014. *Nature Climate Change* **4**:206-210.

Hastings, A. 2019. Long-term predator-prey cycles finally achieved in the lab. *Nature* **577**:172-173.

Haydon, D. T., and P. E. Greenwood. 2000. Spatial Coupling in Cyclic Population Dynamics; Models and Data. *Theoretical Population Biology* **58**(3):239-254.

Haynes, K. J., A. M. Liebhold, and D. M. Johnson. 2009. Spatial analysis of harmonic oscillation of gypsy moth outbreak intensity. *Oecologia* **159**:249-256.

Haynes, K. J., A. M. Liebhold, O. N. Bjornstad, A. J. Allstadt, and R. S. Morin. 2017. Geographic variation in forest composition and precipitation predict the synchrony of forest insect outbreaks. *Oikos* **127**(4):634-642.

Hopson, J., and J. W. Fox. 2018. Occasional long distance dispersal increases spatial synchrony of population cycles. *Journal of Animal Ecology* **88**(1):154-163.

Hothorn, T., K. Hornik, M. A. van de Wiel, and A. Zeileis. (2006). A Lego system for conditional inference. *The American Statistician* **60**(3):257-263.

Ims, R. A., N. G. Yoccoz, and S. B. Hagen. 2004. Do sub-Arctic winter moth populations in coastal birch forest exhibit spatially synchronous dynamics? *Journal of Animal Ecology* **73**(6):1129-1136.

Ims, R. A., J. A. Henden, and S. T. Killengreen. 2008. Collapsing population cycles. *Trends in Ecology & Evolution* **23**(2):79-86.

Jones J., P. J. Doran, R. T. Holmes. 2003. Climate and food synchronize regional forest bird

abundances. *Ecology* **84**:3024-3022.

Kahilainen, A., S. V. Nouhuys, T. Schulz, and M. Saastamoinen. 2018. Metapopulation dynamics in a changing climate: Increasing spatial synchrony in weather conditions drives metapopulation synchrony of a butterfly inhabiting a fragmented landscape. *Global Change Biology* **24**(9):4316-4329.

Kassambara, A. 2019. *ggcorrplot*: Visualization of a Correlation Matrix using 'ggplot2'. R package version 0.1.3. <https://CRAN.R-project.org/package=ggcorrplot>

Koenig W. D. 2001. Synchrony and periodicity of eruptions by boreal birds. *Condor* **103**:725-735.

Koenig, D., and A. M. Liebhold. 2005. Effects of periodical cicada emergences on abundance and synchrony of avian populations. *Ecology* **86**(7):1873-1882.

Korpimaki, E., P. R. Brown, J. Jacob, and R. P. Pech. 2004. The Puzzles of Population Cycles and Outbreaks of Small Mammals Solved? *BioScience* **54**(12):1071-1079.

Kvasnes, M. A. J., H. C. Pedersen, T. Storaas, and E. B. Nilsen. 2014. Large-scale climate variability and rodent abundance modulates recruitment rates in Willow Ptarmigan (*Lagopus lagopus*). *Journal of Ornithology* **155**:891-903.

Laan, E., and J. W. Fox. 2019. An experimental test of the effects of dispersal and the paradox of enrichment on metapopulation persistence. *Oikos* **129**(1):49-58.

Liebhold, A., W. D. Koenig, and O. N. Bjornstad. 2004. Spatial Synchrony in Population Dynamics. *Annual Reviews* **35**:467-490.

Liebhold, A. M., M. Holyoak, N. Mouquet, P. Amarasekare, J. M. Chase, M. F. Hoopes, R. D. Holt, J. B. Shurin, R. Law, D. Tilman, M. Loreau, and A. Gonzalez. 2004. The

metacommunity concept: a framework for multi-scale community ecology. *Ecology Letters* **7**:601-613.

Arbizu, P. M. 2017. pairwiseAdonis: Pairwise Multilevel Comparison using Adonis. R package version 0.0.1. <https://CRAN.R-project.org/package=pairwiseAdonis>

Oksanen, J., F. G. Blanchet, M. Friendly, R. Kindt, P. Legendre, D. McGlinn, P. R. Minchin, R. B. O'Hara, G. L. Simpson, P. Solymos, M. Henry, H. Stevens, E. Szoeics, and H. Wagner. 2020. vegan: Community Ecology Package. R package version 2.5-7. <https://CRAN.R-project.org/package=vegan>

Paradis, E., S. R. Baillie, W. J. Sutherland, and R. D. Gregory. 2000. Spatial synchrony in populations of birds: Effects of habitat, population trend, and spatial scale. *Ecology* **81**(8):2112-2125.

Post, E., and M. C. Forchhammer. 2002. Synchronization of animal population dynamics by large-scale climate. *Nature* **420**:168-171.

Pikovsky, A., M. Rosenblum, and J. Kurths. 2001. Synchronization: A Universal Concept in Nonlinear Sciences. Cambridge University Press.
<https://doi.org/10.1017/CBO9780511755743>

Pomara, L. Y., and B. Zuckerberg. 2017. Climate variability drives population cycling and synchrony. *Diversity and Distributions* **23**(4):421-434.

R Core Team. 2020. R: A language and environment for statistical computing. R Foundation for Statistical Computing, Vienna, Austria. URL: <https://www.R-project.org/>.

Raimondo, S., A. M. Liebhold, J. S. Strazanac, and L. Butler. 2004. Population synchrony within and among Lepidoptera species in relation to weather, phylogeny, and larval phenology. *Ecological Entomology* **29**(1):96-105.

- Rosenzweig, M. L., and R. H. MacArthur. Graphical Representation and Stability Conditions of Predator-Prey Interactions. *The American Naturalist* **97**(895):209-223.
- Row, J. R., and B. C. Fedy. 2017. Spatial and temporal variation in the range-wide dynamics of greater sage-grouse. *Oecologia* **185**(4):687-698.
- Satake, A., O. Bjornstad, and S. Kobra. 2004. Masting and trophic cascades: interplay between Rowan trees, apple fruit moth, and their parasitoid in Southern Norway. *Oikos* **104**:540-550.
- Schauber, E. M., D. Kelly, P. Turchin, C. Simon, and W. G. Lee. 2002. Masting by 18 New Zealand plant species: the role of temperature as a synchronizing cue. *Ecology* **83**:1214-1225.
- Slater, J. V. 1954. Temperature Tolerance in Tetrahymena. *The American Society of Naturalists* **88**:840.
- Soetaert, K., T. Petzoldt, R. Woodrow Setzer. 2010. Solving Differential Equations in R: Package deSolve. *Journal of Statistical Software* **33**(9):1-25.
- Thought Emporium. 2018. Building a Heatblock and Incubator. *YouTube*. URL: https://www.youtube.com/watch?v=Zm378x6zJYc&ab_channel=TheThoughtEmporium
- Van Panuis, W. G., M. Choisy, X. Xiong, N. S. Chok, P. Akarasewi, S. Iamsirithaworn, S. K. Lam, C. K. Chong, F. C. Lam, B. Phommasak, P. Vongphrachanh, K. Bouaphanh, H. Rekol, N. T. Hien, P. Q. Thai, T. N. Duong, J. H. Chuang, Y. L. Liu, L. C. Ng, Y. Shi, E. A. Tayag, V. G. Roque Jr., L. L. L. Suy, R. G. Jarman, R. V. Gibbons, J. M. S. Velasco, I. K. Yoon, D. S. Burke, and D. A. T. Cummings. 2015. Region-wide synchrony and traveling waves of dengue across eight countries in Southeast Asia. *PNAS* **112**(42):13069-13074.

- Vasseur, D. A., and J. W. Fox. 2007. Environmental fluctuations can stabilize food web dynamics by increasing synchrony. *Ecology Letters* **10**(11): 1066-1074.
- Vasseur, D. A., and J. W. Fox. 2009. Phase-locking and environmental fluctuations generate synchrony in a predator-prey community. *Nature* **460**:1007-1010.
- Wickham, H. 2007. Reshaping Data with the reshape Package. *Journal of Statistical Software* **21**(12):1-20.
- Wickham, H. 2016. *ggplot2: Elegant Graphics for Data Analysis*. Springer-Verlag New York.
- Wickham, H., M. Averick, J. Bryan, W. Chang, L. D'Agostino McGowan, R. François, G. Grolemund, A. Hayes, L. Henry, J. Hester, M. Kuhn, T. Lin Pedersen, E. Miller, S. M. Bache, K. Müller, J. Ooms, D. Robinson, D. P. Seidel, V. Spinu, K. Takahashi, D. Vaughan, C. Wilke, K. Woo, and H. Yutani. 2019. Welcome to the tidyverse. *Journal of Open Source Software* **4**(43):1686. <https://doi.org/10.21105/joss.01686>
- Wickham, H., J. Hester, and W. Chang. 2020. devtools: Tools to Make Developing R Packages Easier. R package version 2.3.2. <https://CRAN.R-project.org/package=devtools>
- Walter, J. A., L. W. Sheppard, T. L. Anderson, J. H. Kastens, O. N. Bjornstadd, A. M. Liebhold, and D. C. Reuman. 2017. The geography of spatial synchrony. *Ecology Letters* **20**(7):801-814.
- Williams, D. W., and A. M. Liebhold. 2000. Spatial synchrony of spruce budworm outbreaks in eastern North America. *Ecology* **81**(10):2753-2766.

APPENDIX A: Spatial Synchrony and Population Cycles Literature Review

Table A: Literature review summary. Includes the title, author(s), journal and date published, as well as the study system. Spatial synchrony was linked to population cycles, either directly, indirectly, or not at all.

Title	Author	Journal	Date	Study System	Cycling and Synchrony
Spatial and temporal patterns of small-rodent population dynamics at a regional scale	Steen et al.	Ecology	1996	Bank vole	Cycles and synchrony present, but not directly linked
The Spatial Dimension in Population Fluctuations	Ranta et al.	Science	1997	Canadian lynx	Cycles and synchrony present, but not directly linked
Synchronous dynamics and rates of extinction in spatially structured populations	Heino et al.	Proceedings of the Royal Society B	1997	Model	No cycles but a mention of population fluctuations with synchrony
Synchrony in outbreaks of forest Lepidoptera: A possible example of the Moran effect	Myers	Ecology	1998	Lepidoptera	Cycles and synchrony present, but not directly linked
Population variability in space and time: the dynamics of synchronous population fluctuation	Ranta et al.	Oikos	1998	Model	Cycles and synchrony are directly linked
Synchronicity, chaos and population cycles: spatial coherence in an uncertain world	Lloyd & May	Trends in Ecology & Evolution	1999	Canadian lynx	Cycles and synchrony are directly linked
Spatially autocorrelated disturbances and patterns in population synchrony	Ranta et al.	Proceedings of the Royal Society B	1999	Model	No cycles but a mention of population fluctuations with synchrony
Spatial population dynamics: analyzing patterns and processes of population synchrony	Bjornstad et al.	Trends in Ecology & Evolution	1999	Review	Cycles and synchrony are directly linked
Spatial autocorrelation of ecological phenomena	Koenig	Trends in Ecology & Evolution	1999	Review	No cycles but a mention of population cycles with synchrony
Spatial synchrony in populations of birds: effects of habitat, population trend, and spatial scale	Paradis et al.	Ecology	2000	British birds	Synchrony present without cycles

Title	Author	Journal	Date	Study System	Cycling and Synchrony
Spatial synchrony of spruce budworm outbreaks in Eastern North America	Williams & Liebhold	Ecology	2000	Spruce budworm	Cycles and synchrony present, but not directly linked
Dispersal, Environmental Correlation, and Spatial Synchrony in Population Dynamics	Kendall et al.	The American Naturalist	2000	Model	Cycles and synchrony are directly linked
Spatial asynchrony and demographic traveling waves during red grouse population cycles	Moss et al.	Ecology	2000	Red grouse	Cycles and synchrony present, but not directly linked
Effects of Patch Number and Dispersal Patterns on Population Dynamics and Synchrony	Ylikarjula et al.	Journal of Theoretical Biology	2000	Model	No cycles but a mention of population fluctuations with synchrony
Weather and synchrony in 10-year population cycles of rock ptarmigan and red grouse in Scotland	Watson et al.		2000	Rock ptarmigan and red grouse	Cycles and synchrony are directly linked
Spatial synchronization of vole population dynamics by predatory birds	Ims & Andreassen	Nature	2000	Voles	Synchrony present, but cycles not measured
Cycles and synchrony: two historical ‘experiments’ and one experience	Bjornstad	Journal of Animal Ecology	2001	Measles, whooping cough, rodents	Cycles and synchrony are directly linked
Phase coupling and synchrony in the spatiotemporal dynamics of muskrat and mink populations across Canada	Haydon et al.	PNAS	2001	Muskrat and mink	Cycles and synchrony are directly linked
Historical trends, seasonality and spatial synchrony in green sea turtle egg production	Chaloupka	Biological Conservation	2001	Green sea turtle	Cycles and synchrony present, but not directly linked
Population synchrony and environmental variation: an experimental demonstration	Benton et al.	Ecology Letters	2001	Soil mite	Cycles and synchrony present, but not directly linked
Travelling waves and spatial hierarchies in measles epidemics	Grenfell et al.	Nature	2001	Measles	Cycles and synchrony present, but not directly linked
Synchrony, scale and temporal dynamics of rock partridge (<i>Alectoris graeca saxatilis</i>) populations in the Dolomites	Cattadori et al.	Journal of Animal Ecology	2001	Rock partridge	Cycles and synchrony present, but not directly linked

Title	Author	Journal	Date	Study System	Cycling and Synchrony
Measuring and testing for spatial synchrony	Buonaccorsi et al.	Ecology	2001	Model	No cycles but a mention of population fluctuations with synchrony
Spatial synchrony in field vole <i>Microtus agrestis</i> abundance in a coniferous forest in northern England: the role of vole-eating raptors	Petty et al.	Journal of Applied Ecology	2002	Vole-eating raptors	Cycles and synchrony present, but not directly linked
Global patterns of environmental synchrony and the Moran effect	Koenig	Ecography	2002	Weather model	No cycles but a mention of population fluctuations with synchrony
Synchrony in lemming and vole populations in the Canadian Arctic	Krebs et al.	Canadian Journal of Zoology	2002	Lemmings and voles	Cycles and synchrony present, but not directly linked
Migration and spatiotemporal variation in population dynamics in a heterogeneous environment	Engen et al.	Ecology	2002	Model	Cycles and synchrony present, but not directly linked
Spatial synchrony in forest insect outbreaks: Roles of regional stochasticity and dispersal	Peltonen et al.	Ecology	2002	Spruce budworm, western spruce budworm, larch bud moth, forest tent caterpillar, mountain pine beetle, and gypsy moth	Cycles and synchrony present, but not directly linked
Synchrony and second-order spatial correlation in host-parasitoid systems	Bjornstad & Bascompte	Journal of Animal Ecology	2002	Parasites	Cycles and synchrony are directly linked
Spatial synchrony of population changes in rocky shore communities in Shetland	Burrows et al.	Marine Ecology Progress Series	2002	Shetland communities	Cycles and synchrony present, but not directly linked
Detection of imperfect population synchrony in an uncertain world	Cazelles & Stone		2003	Model	Cycles and synchrony present, but not directly linked
Voles, lemmings and caribou - population cycles revisited?	Gunn	Rangifer	2003	Caribou	Cycles and synchrony present, but not directly linked

Title	Author	Journal	Date	Study System	Cycling and Synchrony
Experimental evolution of dispersal in spatiotemporally variable microcosms	Friedenberg	Ecology Letters	2003	Microcosms	No cycles but a mention of population fluctuations with synchrony
Synchrony in brown trout, <i>Salmo trutta</i> , population dynamics: a 'Moran effect' on early-life stages	Cattaneo et al.	Oikos	2003	Brown trout	No cycles but a mention of population fluctuations with synchrony
Do sub-Arctic winter moth populations in coastal birch forest exhibit spatially synchronous dynamics?	Ims et al.	Journal of Animal Ecology	2004	Arctic winter moth	Cycles and synchrony present, but not directly linked
Spatial Synchrony in Population Dynamics	Liebhold et al.	Annual Review of Ecology, Evolution, and Systematics	2004	Review	Cycles and synchrony are directly linked
The Puzzles of Population Cycles and Outbreaks of Small Mammals Solved?	Korpimaki et al.	Bio Science	2004	Small mammals (voles, lemmings, snowshoe hares)	Cycles and synchrony are directly linked
Spatiotemporal dynamics of epidemics: synchrony in metapopulation models	Lloyd & Jansen	Mathematical Biosciences	2004	Model	No cycles but a mention of population fluctuations with synchrony
Circumpolar variation in periodicity and synchrony among gypsy moth populations	Johnson et al.	Journal of Animal Ecology	2005	Gypsy moth	Cycles and synchrony present, but not directly linked
Spatiotemporal variation of the abundance of calcareous green macro algae in the Florida keys: a study of synchrony within a macroalgal functional-form group	Collado-Vides et al.	Journal of Phycology	2005	Calcareous green algae	Cycles and synchrony present, but not directly linked
Impact of predator pursuit and prey evasion on synchrony and spatial patterns in metapopulation	Li et al.	Ecological Modelling	2005	Model	Cycles and synchrony present, but not directly linked
Spatial synchrony in vole population fluctuations - a field experiment	Huitu et al.	Oikos	2005	Field voles	Cycles and synchrony are directly linked

Title	Author	Journal	Date	Study System	Cycling and Synchrony
Effects of periodical cicada emergences on abundance and synchrony of avian populations	Koenig & Liebhold	Ecology	2005	Cicada, cuckoos, red-bellied woodpeckers, blue jays, common grackles, brown-headed cowbirds, American crows, cuffed titmice, grey catbirds, brown thrashers, wood thrushes, northern mockingbirds, northern cardinals, house sparrows.	Cycles and synchrony present, but not directly linked
Parasites and climate synchronize red grouse populations	Cattadori et al.	Nature	2005	Parasites	Cycles and synchrony present, but not directly linked
Generalizations of the Moran Effect Explaining Spatial Synchrony in Population Fluctuations	Engen & Saether	The American Naturalist	2005	Model	Cycles and synchrony present, but not directly linked
Landscape level analysis of mountain pine beetle in British Columbia, Canada: spatiotemporal development and spatial synchrony within the present outbreak	Aukema et al.	Ecography	2006	Mountain pine beetle	No cycles, but a mention of population fluctuations with synchrony
Phase coupling and spatial synchrony of subpopulations of an endangered dune lizard	Chen et al.	Landscape Ecology	2006	Fringe-toed lizard	No cycles, but a mention of population fluctuations with synchrony
Geographically partitioned spatial synchrony among cyclic moth populations	Klemola et al.	Oikos	2006	<i>Epiprilla autumnata</i>	Cycles and synchrony present, but not directly linked
Environmental fluctuations can stabilize food web dynamics by increasing synchrony	Vasseur & Fox	Ecology Letters	2007	Model	Cycles and synchrony present, but not directly linked
Spatial synchrony in red grouse population dynamics	Kerlin et al.	Oikos	2007	Red grouse	Cycles and synchrony present, but not directly linked

Title	Author	Journal	Date	Study System	Cycling and Synchrony
Spatial synchrony in coral reef fish populations and the influence of climate	Cheal et al.	Ecology	2007	Reef fish	Cycles and synchrony present, but not directly linked
Climatically driven synchrony of gerbil populations allow large-scale plague outbreaks	Kausrud et al.	Proceedings of the Royal Society B	2007	Gerbils	Cycles and synchrony present, but not directly linked
Collapsing population cycles	Ims et al.	Trends in Ecology & Evolution	2008	Cases: Fennoscandian voles, grouse, larch budmoth, moths, lemmings.	Cycles and synchrony are directly linked
Influence of the Moran Effect on Spatiotemporal Synchrony in Common Carp Recruitment	Phelps et al.	Transactions of the American Fisheries Society	2008	Carp	No cycles but a mention of population fluctuations with synchrony
Phase-locking and environmental fluctuations generate synchrony in a predator-prey community	Vasseur & Fox	Nature	2009	Tetrahymena pyriformis and Euplates patella	Cycles and synchrony are directly linked
Three centuries of insect outbreaks across the European Alps	Buntgen et al.	New Phytologist	2009	Larch budmoth	Cycles and synchrony present, but not directly linked
Spatial analysis of harmonic oscillation of gypsy moth outbreak intensity	Haynes et al.	Oecologia	2009	Gypsy moth	Cycles and synchrony present, but not directly linked
Synchrony of spatial populations induced by coloured environmental noise and dispersal	Liu et al.	Biosystems	2009	Model	Cycles and synchrony are directly linked
Spatial-temporal analysis of species range expansion: the case of the mountain pine beetle, <i>Dendroctonus ponderosae</i>	Robertson et al.	Journal of Biogeography	2009	Mountain pine beetle	Cycles and synchrony are directly linked
Spatial synchrony propagates through a forest food web via consumer-resource interactions	Haynes et al.	Ecology	2009	Gypsy moth and white-footed mouse	Cycles and synchrony are directly linked
Circumpolar synchrony in big river bacterioplankton	Crump et al.	PNAS	2009	Bacterioplankton	Synchrony present, but cycles not measured

Title	Author	Journal	Date	Study System	Cycling and Synchrony
Dispersal and natural enemies interact to drive spatial synchrony and decrease stability in patchy populations	Vogwill et al.	Ecology Letters	2009	Model	Cycles and synchrony are directly linked
Spatial synchrony in microbial community dynamics: testing among-year and lake patterns	Rusak et al.	Verh. Internat. Verein. Limnol.	2009	Microbial communities	Synchrony present, but cycles not measured
The return of the vole cycle in southern Finland refutes the generality of the loss of cycles through ‘climatic forcing’	Brommer et al.	Global Change Biology	2010	Bank voles and field voles	Cycles and synchrony are directly linked
Synchrony of butterfly populations across species' geographic ranges	Powney et al.	Oikos	2010	Butterflies; meadow brown, gatekeeper, and ringlet	No cycles, but a mention of population fluctuations with synchrony
Ecological processes can synchronize marine population dynamics over continental scales	Gouhier et al.	PNAS	2010	Mussels	No cycles, but a mention of population fluctuations with synchrony
Spatial Synchrony in Intertidal Benthic Algal Biomass in Temperate Coastal and Estuarine Ecosystems	Van der Wal et al.	Ecosystems	2010	Microphytobenthos	Cycles and synchrony present, but not directly linked
Synchrony of population dynamics of two vineyard arthropods occurs at multiple spatial and temporal scales	Valpine et al.	Ecological Applications	2010	Agricultural arthropods	Cycles and synchrony present, but not directly linked
Spatial synchrony and temporal dynamics of juvenile red drum <i>Sciaenops ocellatus</i> populations in South Carolina, USA	Arnott et al.	Marine Ecology Progress Series	2010	Red drum	No cycles, but a mention of population fluctuations with synchrony
Synchrony and Stability of Food Webs in Metacommunities	Gouhier et al.	The American Naturalist	2010	Model	Cycles and synchrony present, but not directly linked
Spatial dynamics of Norwegian tetraonid populations	Kvasnes et al.	Ecol Res	2010	Tetraonid populations	No cycles, but a mention of population fluctuations with synchrony

Title	Author	Journal	Date	Study System	Cycling and Synchrony
Phase-locking, the Moran effect and distance decay of synchrony: experimental tests in a model system	Fox et al.	Ecology Letters	2011	<i>Tetrahymena pyriformis</i> and <i>Euploites patella</i>	Cycles and synchrony are directly linked
Synchrony in marine growth among Atlantic salmon (<i>Salmo solar</i>) populations	Jensen et al.	Canadian Journal of Fisheries and Aquatic Sciences	2011	Atlantic Salmon	No cycles, but a mention of population fluctuations with synchrony
Among-colony synchrony in the survival of Common Guillemots <i>Uria aalge</i> reflects shared wintering areas	Reynolds et al.	IBIS	2011	Common guillemots	Synchrony present, but cycles not measured
Population cycles are highly correlated over long time series and large spatial scales in two unrelated species: greater sage-grouse and cottontail rabbits	Fedy & Doherty	Oecologia	2011	Greater sage-grouse and cottontail rabbits.	Cycles and synchrony present, but not directly linked
Interspecies Synchrony in Salmonid Densities Associated with Large-Scale Bioclimatic Conditions in Central Idaho	Copeland & Meyer	Transactions of the American Fisheries Society	2011	Lotic salmonids	Cycles and synchrony present, but not directly linked
Temperature cues phenological synchrony in ant-mediated seed dispersal	Warren et al.	Global Change Biology	2011	Ants and plants	Synchrony present, but cycles not measured
Spatial synchrony of recruitment in mountain-dwelling woodland caribou	Hegel et al.	Population Ecology	2011	Caribou	No cycles, but a mention of population fluctuations with synchrony
Genetic, spatial, and temporal components of precise spawning synchrony in reef building corals of the <i>Monastraea annularis</i> species complex	Levitán et al.	Evolution	2011	<i>Monastraea annularis</i>	Cycles and synchrony present, but not directly linked
A dispersal-induced paradox: synchrony and stability in stochastic metapopulations	Abbott	Ecology Letters	2011	Model	Cycles and synchrony present, but not directly linked
Towards a measure of functional connectivity: local synchrony matches small scale movements in a woodland edge butterfly	Powney et al.	Landscape Ecology	2012	Ringlet butterfly	No cycles, but a mention of population fluctuations with synchrony

Title	Author	Journal	Date	Study System	Cycling and Synchrony
Factors Influencing the Spatial and Temporal Dynamics of Engelmann Spruce Mortality during a Spruce Beetle Outbreak on the Markagunt Plateau, Utah	DeRose & Long	Forest Science	2012	Spruce beetle	Cycles and synchrony present, but not directly linked
Reversal of multi century tree growth improvements and loss of synchrony at mountain tree lines point to changes in key drivers	Fajardo & McIntire	Functional Ecology	2012	Tree line	No cycles, but a mention of population fluctuations with synchrony
Local Variations in Spatial Synchrony of Influenza Epidemics	Stark et al.	PLOS ONE	2012	Influenza	Synchrony present, but cycles not measured
Spatiotemporal patterns of mountain pine beetle activity in the southern Rocky Mountains	Chapman et al. Ecology	Ecology	2012	Mountain pine beetle	Cycles and synchrony present, but not directly linked
Different types of synchrony in chaotic and cyclic communities	Becks & Arndt	Natural Communications	2013	<i>Tetrahymena pyriformis</i> and two bacteria <i>Pedobacter</i> species	Cycles and synchrony present, but not directly linked
Nonlinear Effect of Dispersal Rate on Spatial Synchrony of Predator-Prey Cycles	Fox et al.	PLOS ONE	2013	<i>Tetrahymena pyriformis</i> and <i>Euplates patella</i>	Cycles and synchrony present, but not directly linked
Predation inhibits the positive effect of dispersal on infraspecific and interspecific synchrony in pond meta communities	Howeth & Liebold	Ecology	2013	Zooplankton and bluegill sunfish	No cycles, but a mention of population fluctuations with synchrony
Decline of an arctic top predator: synchrony in colony size fluctuations, risk of extinction and the subpolar gyre	Descamps et al.	Oecologia	2013	Brunnich's guillemot	Cycles and synchrony present, but not directly linked
Population Fluctuations and Synchrony of Grassland Butterflies in Relation to Species Traits	Franzen et al.	PLOS ONE	2013	Butterflies	No cycles, but a mention of population fluctuations with synchrony
Population synchrony decreases with richness and increases with environmental fluctuations in an experimental metacommunity	Pandit et al.	Oecologia	2013	Aquatic invertebrates	Cycles and synchrony present, but not directly linked

Title	Author	Journal	Date	Study System	Cycling and Synchrony
Interspecific synchrony of seabird population growth rate and breeding success	Robinson et al.	Ecology and Evolution	2013	Seabirds	No cycles, but a mention of population fluctuations with synchrony
Large-scale spatial synchrony and cross-synchrony in acorn population by two California oaks	Koenic & Knops	Ecology	2013	California oaks	Cycles and synchrony present, but not directly linked
Spatiotemporal dynamics of dengue epidemics, Southern Vietnam	Cuong et al.	Emerging Infectious Diseases	2013	Dengue	Cycles and synchrony present, but not directly linked
Large-scale climate variability and rodent abundance modulates recruitment rates in Willow Ptarmigan (<i>Lagopus lagopus</i>)	Kvasnes et al.	Journal of Ornithology	2014	Willow ptarmigan	Cycles and synchrony present, but not directly linked
Warming induces synchrony and destabilizes experimental pond zooplankton metacommunities	Thompson et al.	Oikos	2014	Zooplankton and Ceridodaphnia	No cycles, but a mention of population fluctuations with synchrony
Patterns of zooplankton population synchrony in a tropical reservoir	Lodi et al.	Journal of Plankton Research	2014	Zooplankton assemblage (36 taxa)	No cycles, but a mention of population fluctuations with synchrony
Life-stage differences in spatial genetic structure in an irruptive forest insect: implications for dispersal and spatial synchrony	James et al.	Molecular Ecology	2014	Spruce budworm	Cycles and synchrony present, but not directly linked
Predicting bird phenology from space: satellite-derived vegetation green-up signal uncovers spatial variation in phenological synchrony between birds and their environment	Cole et al.	Ecology and Evolution	2015	Moth larvae, great tits, blue tits	Synchrony present, but cycles not measured
How robust is dispersal-induced spatial synchrony?	Zhang et al.	Chaos	2015	Model	Cycles and synchrony are directly linked
Region-wide synchrony and traveling waves of dengue across eight countries in Southeast Asia	Van Panhuis et al.	PNAS	2015	Dengue	Cycles and synchrony present, but not directly linked
Human disturbance affects the long-term spatial synchrony of freshwater invertebrate communities	Feio et al.	Environmental Pollution	2015	Invertebrates	Cycles and synchrony present, but not directly linked

Title	Author	Journal	Date	Study System	Cycling and Synchrony
Temporal variation in the synchrony of weather and its consequences for spatiotemporal population dynamics	Allstadt et al.	Ecology	2015	Gypsy moth	Cycles and synchrony are directly linked
Differences in spatial synchrony and interspecific concordance inform guide-level population trends for aerial insectivorous birds	Michel et al.	Ecography	2015	Chimney swift, purple martin, barn swallow, tree swallow, northern rough-winged swallow	No cycles, but a mention of population fluctuations with synchrony
Mean-field dispersion-induced spatial synchrony, oscillation and amplitude death, and temporal stability in an ecological model	Banerjee et al.	Physical Review E	2015	Model	Cycles and synchrony present, but not directly linked
Spatial and spatiotemporal variation in metapopulation structure affects population dynamics in a passively dispersing arthropod	Roissart et al.	Journal of Animal Ecology	2015	Spider mite	No cycles, but a mention of population fluctuations with synchrony
Dispersal, environmental forcing, and parasites combine to affect metapopulation synchrony and stability	Duncan et al.	Ecology	2015	Parasites	Synchrony present without cycles
Synchrony in Metapopulations with Sporadic Dispersal	Jeter & Belykh	International Journal of Bifurcation and Chaos	2015	Model	Cycles and synchrony present, but not directly linked
Spatial synchrony in population dynamics: The effects of demographic stochasticity and density regulation with a spatial scale	Engen & Saether	Mathematical Biosciences	2016	Model	No cycles, but a mention of population fluctuations with synchrony
Spatial synchrony of amphipods in giant kelp forests	Morton et al.	Marine Biology	2016	Giant kelp and amphipods	Synchrony present, but cycles not measured
Plant phenological synchrony increases under rapid within-spring warming	Wang et al.	Scientific Reports	2016	Local European plants	Cycles and synchrony present, but not directly linked

Title	Author	Journal	Date	Study System	Cycling and Synchrony
Recruitment synchrony of yellow perch (<i>Perca flavescens</i> , Percidae) in the Great Lakes region, 1966-2008	Honsey et al.	Fisheries Research	2016	Yellow perch	No cycles, but a mention of population fluctuations with synchrony
Climate change-related regime shifts have altered spatial synchrony of plankton dynamics in the North Sea	Defriez et al.	Global Change Biology	2016	Plankton	Cycles and synchrony present, but not directly linked
Integrating spatial synchrony/asynchrony of population distribution into stock assessment models: a spatial hierarchical Bayesian statistical catch-at-age approach	Jiao et al.	ICES Journal of Marine Science	2016	Atlantic weakfish	Synchrony present, but cycles not measured
Temporally increasing spatial synchrony of North American temperature and bird populations	Koenig & Liebhold	Nature Climate Change	2016	Wintering birds	Cycles and synchrony present, but not directly linked
Spatial synchrony of a threatened shorebird: Regional roles of climate, dispersal and management	Eberhard-Phillips et al.	Bird Conservation International	2016	Western snowy plover	Synchrony present, but cycles not measured
Inferring spatial structure from population genetics and spatial synchrony in demography of Baltic Sea: implications for management	Ostman et al.	Fish and Fisheries	2016	Fishery surveys	Cycles and synchrony present, but not directly linked
Climate variability drives population cycling and synchrony	Pomara & Zuckerberg	Diversity and Distributions	2017	Ruffed Grouse	Cycles and synchrony present, but not directly linked
Population extinctions can increase metapopulation persistence	Fox et al.	Nature Ecology & Evolution	2017	<i>Tetrahymena pyriformis</i> and <i>Euploites patella</i>	Cycles and synchrony are directly linked
Spatial and temporal variation in the range-wide cycling dynamics of greater sage-grouse	Row & Fedy	Oecologia	2017	Sage grouse	Cycles and synchrony are directly linked
A global geography of synchrony for terrestrial vegetation	Defriex & Reuman	Global Ecology and Biogeography	2017	Plants	Cycles and synchrony present, but not directly linked
Drivers of synchrony of acorn production in the valley oak (<i>Quercus lobata</i>) at two spatial scales	Koenig et al.		2017	Valley Oaks	Synchrony present, but cycles not measured

Title	Author	Journal	Date	Study System	Cycling and Synchrony
A global geography of synchrony for marine phytoplankton	Defriez & Reuman	Global Ecology and Biogeography	2017	Marine phytoplankton that contains chlorophyll a	Cycles and synchrony present, but not directly linked
Using geography to infer the importance of dispersal for the synchrony of freshwater plankton	Anderson et al.	Oikos	2017	Phytoplankton and zooplankton. <i>Bosmina longirostris</i> and <i>Daphnia lumholtzi</i>	No cycles, but a mention of population fluctuations with synchrony
The Moran effect and environmental vetoes: phenological synchrony and drought drive seed production in a Mediterranean oak	Bogdziewicz et al.	Proceedings of the Royal Society B	2017	Holm oaks	Cycles and synchrony present, but not directly linked
Macroscale patterns of synchrony identify complex relationships among spatial and temporal ecosystem drivers	Lottig et al.	Ecosphere	2017	Lake water surveys	Cycles and synchrony present, but not directly linked
Regional synchrony in full-scale activated sludge bioreactors due to deterministic microbial community assembly	Griffin & Wells	The ISME Journal	2017	Microbial ecosystems	Cycles and synchrony present, but not directly linked
Waves and synchrony in <i>Epippia autumnata</i> / <i>Operophtera brumata</i> outbreaks. II. Sunspot activity cannot explain cyclic outbreaks	Nilssen et al.	Journal of Animal Ecology	2017	<i>Epippia autumnata</i>	Cycles and synchrony present, but not directly linked
Synchrony in population counts predicts butterfly movement frequencies	Oliver et al.	Ecological Entomology	2017	Butterflies	Synchrony present, but cycles not measured
Geographic variation in forest composition and precipitation predict the synchrony of forest insect outbreaks	Haynes et al.	Oikos	2017	Gypsy moth	Cycles and synchrony present, but not directly linked
Bottom-up factors contribute to large-scale synchrony in spruce budworm	Bouchard et al.	Canadian Journal of Forest Research	2017	Spruce budworm	Cycles and synchrony present, but not directly linked
Occasional long distance dispersal increases spatial synchrony of population cycles	Hopson & Fox	Journal of Animal Ecology	2018	<i>Tetrahymena pyriformis</i> and <i>Euploites patella</i>	Cycles and synchrony present, but not directly linked

Title	Author	Journal	Date	Study System	Cycling and Synchrony
Synchrony - An emergent property of recreational fisheries	Kaemingk et al.	Journal of Applied Ecology	2018	Anglers	No cycles, but a mention of population fluctuations with synchrony
Rising synchrony controls western North American ecosystems	Black et al.	Global Change Biology	2018	Blue oak	Synchrony present, but cycles not measured
Metapopulation dynamics in a changing climate: Increasing spatial synchrony in weather conditions drives metapopulation synchrony of a butterfly inhabiting a fragmented landscape	Kahilainen et al.	Global Change Biology	2018	Flanville fritillary butterfly	Cycles and synchrony present, but not directly linked
A roadmap to disentangling ecogeographical patterns of spatial synchrony in dendrosciences	Shestakova et al.	Trees	2018	Forests	No cycles, but a mention of population fluctuations with synchrony
The effect of harvesting on the spatial synchrony of population fluctuations	Engen et al.	Theoretical Population Biology	2018	Harvest crops	No cycles, but a mention of population fluctuations with synchrony
Variation in aggregate descriptors of rocky shore communities: a test of synchrony across spatial scales	Arribas et al.	Marine Biology	2019	Mussels, macroinvertebrates, algae	Synchrony present, but cycles not measured
Climatic synchrony and increased outbreaks in allopatric populations of an invasive defoliator	Ward & Aukema	Biological Invasions	2019	Larch case bearer, eastern/western larch	No cycles, but a mention of population fluctuations with synchrony

APPENDIX B: Homemade Incubator Building Setup and Software

Heated incubators were built using a 100-quart cooler (Coleman Company Inc.) fitted with shelves for jars and heating elements. Shelves were built out of hard rubber floor mats (Storex Industries) cut to fit the cooler interior and were mounted using L-brackets screwed into the walls of the cooler. The interior of the cooler was lined with reflective aluminum tape to reflect and trap more heat inside the cooler. Two shelves were mounted, one lower shelf where the heating element sat, and an upper shelf where the jars sat. The heating element used was a large 25W terrarium heating pad (Exo Terra Conservation Networking). The heating pad was placed on its own shelf and jars were never placed directly on the heating pad to avoid overheating the glass jars. There were two waterproof temperature sensors (DS18B20s) inserted into drilled holes in the coolers. One sensor was placed in between the two shelves and measured the air temperature in the incubator. The other sensor was placed in a microcosm jar with water to measure water temperature which could better approximate the temperature in microcosm media. A third temperature sensor was placed in the room to measure air temperature outside the incubator to detect measurable differences in temperature inside and outside the incubator.

The temperature sensors were connected to an Arduino UNO with analog GPIO ports which were connected to an Llc 3191 5V relay. An Arduino program was written that reads the analog data from the temperature sensor pins in real-time and converts it to digital signals which are continually sent over the serial line interface to a computer. A python program was produced to run and print temperature readouts in the command line of a computer every 30 seconds, and one temperature was saved and printed to a .txt file every hour for later temperature checks.

While the heating pad had a built-in thermostat to maintain constant temperatures, additional temperature controls were put in place using the Arduino relay to ensure temperatures remained constant in case the built-in thermostat failed. The relay was programmed to ensure temperatures stay within a specific temperature range, 1°C above and below 27°C. When the temperature sensors in water reach 28°C, the Arduino relay will turn the heating pad off, and when the temperature sensors in water reach 29°C, the Arduino relay will turn the heating pad on.

The link to the Arduino program used can be found at;

<https://github.com/ColtonOsterlund/KaitlinMastersExperimentArduinoTempSensorData>

APPENDIX C: Microcosm Heat Tolerance Pilot Experiment

The purpose of this pilot experiment was to determine how long *T. pyriformis* and *E. patella* would persist at 29°C and 27°C, which helped to determine the best temperature to use for the temperature cycles in the experiment that would have an effect on the protists' dynamics without driving extinction in all the jars. The same jar setup procedures were followed as in the experimental methods, with jars being established trophically from the bottom-up. A low enrichment of 0.15 g PP/L was used instead of 0.1 g PP/L. Jars were sampled using the same methods as in the main experiment. The pilot experiment lasted for 19 days, which was enough time to determine how protists behaved at different temperatures and enrichment levels. A total of 56 jars were used. Jars were grouped by temperature, enrichment, and predation with four replicates in each group (Table B).

Figure B.1 and B.2 display the results from the pilot experiment. 27°C was chosen as the temperature for the temperature cycles as it resulted in much fewer extinctions than 29°C. It was decided to use a low enrichment of 0.1 g PP/L instead of 0.15 g PP/L to further reduce cycling in predator-prey dynamics.

Table B: Pilot experiment design

Temperature (°C)	Enrichment (g PP/L)	Predation	Number of Jars
22	0.15	Predator absent	4 jars
		Predator present	4 jars
	0.4	Predator absent	4 jars
		Predator present	4 jars
27	0.15	Predator absent	4 jars
		Predator present	4 jars
	0.4	Predator absent	4 jars
		Predator present	4 jars
29	0.15	Predator absent	4 jars
		Predator present	4 jars
	0.4	Predator absent	4 jars
		Predator present	4 jars

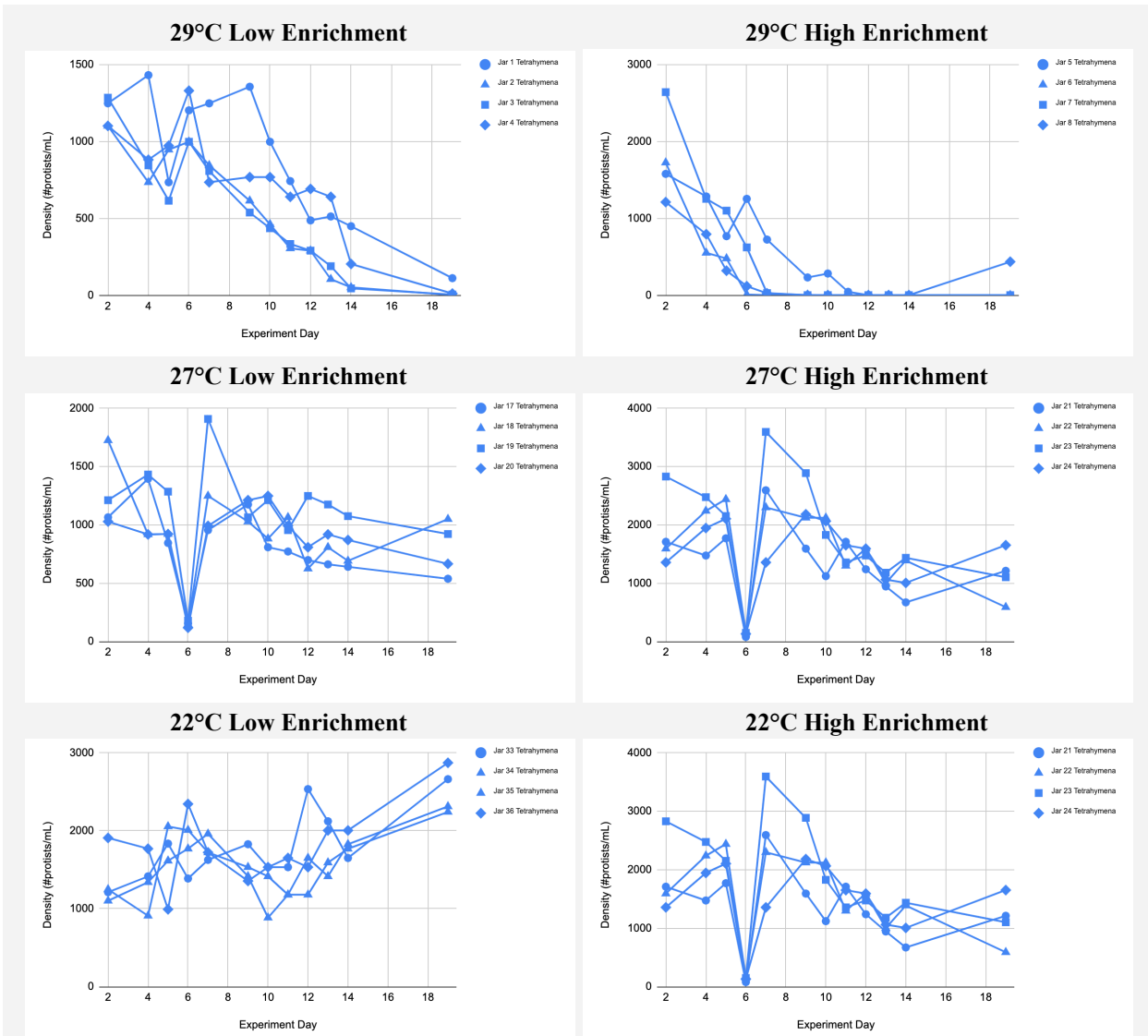


Figure B.1. Pilot experiment results with jars under no predation

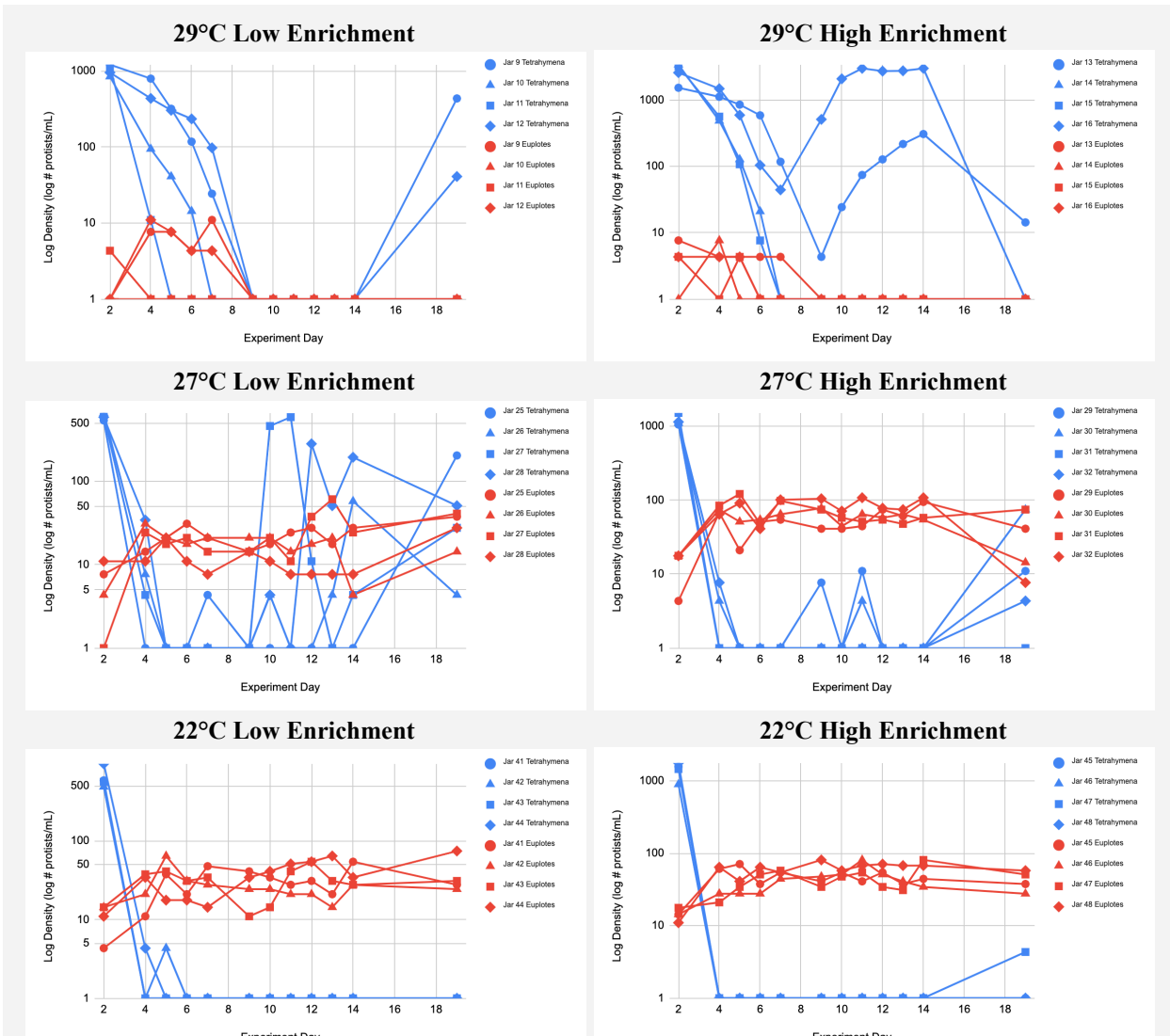


Figure B.2. Pilot experiment results with jars under predation.